LONGSHORE CURRENT AND SEDIMENT TRANSPORT

By
EDWARD BENNETT THORNTON

A DISSERTATION PRESENTED TO THE GRADUATE COUNCIL OF
THE UNIVERSITY OF FLORIDA
IN PARTIAL FULFILLMENT OF THE REQUIREMENTS FOR THE
DEGREE OF DOCTOR OF PHILOSOPHY

UNIVERSITY OF FLORIDA
1970

This work is dedicated to my wife, Sandra, to whom I owe the most.

ACKNOWLEDGMENTS

The author wishes to thank Drs. B. A. Christensen and R. G. Dean who provided invaluable guidance and inspiration during the course of this investigation. Dr. Dean was especially helpful in providing insight into the hydromechanics of the nearshore region, and Dr. Christensen was pacticularly helpful in providing assistance in the sediment transport aspects of this study. The author also wishes to thank Dr. Per Bruun who initiated the field study.

Thanks are due a great many people who assisted in the field measurements which were conducted under all weather conditions. The author wishes to thank Mrs. Mara Lea Hetherington who typed the manuscript.

Financial support for this study was supplied by the Department of Interior, Federal Water Pollution Control Administration, under contract with the Department of Coastal and Oceanographic Engineering, University of Florida.

TABLE OF CONTENTS

LIST OF TABLES

LIST OF FIGURES

LIST OF SYMBOLS

a = wave amplitude

B = proportionality factor associated with bed load transport

B_s = proportionality factor associated with bed load transport inside the surf zone

c = wave celerity

c_b = wave celerity at wave breaking

c_g = speed of wave energy propagation

c_o = wave celerity in deep water

C_f = Chézy's coefficient

d = mean sand grain size

$D = \bar{\eta} + h$, total depth of water

D_b = total depth of water at location of breaking waves

e_b = efficiency coefficient associated with bed load transport

e_s = efficiency coefficient associated with suspended load transport

E = energy density

E_o = energy density in deep water

f = friction factor

$f_h' = T_h/N_h$, dynamic friction factor associated with sediment transport

f_w = friction factor associated with wave motion

f_{wb} = friction factor associated with wave motion at breaking

F = energy density flux

g = acceleration due to gravity

h = depth below still water level

h_b = depth below still water level at wave breaking

h_o = depth below still water level in deep water

H = wave height

H_b = wave height at wave breaking

H_o = wave height in deep water

H_s = significant wave height

i = index corresponding to horizontal coordinate in the x-direction

j = index corresponding to horizontal coordinate in the y-direction

k = wave number

$K(\alpha)$ = ratio between set-up slope and beach slope

K_r = refraction coefficient

K_s = shoaling coefficient

L = wave length

L_o = wave length in deep water

m_h = mass of bed load sediments

m_s = mass of suspended sediments

$\tilde{M}_i = \bar{\bar{M}}_i + M_i$, total mass transport per unit width or total mean momentum per unit area

$\bar{\bar{M}}_i$ = mass transport per unit width associated with mean motion

M_i = mass transport per unit width associated with fluctuating motion

n = transmission coefficient

N_h = normal stress at the bed

N_s = normal stress at level of suspended sediment

p = pressure

P = power/unit area

P_h = power/unit area expended on the bed

P_s = power/unit area available for suspended sediment transport

q = net mass transport rate of sediment per unit width

q_h = bed load transport rate per unit width

q_s = suspended load transport rate per unit width

Q_s = total longshore sand transport rate

r = roughness parameter

R_i = total average resistance force

s = fraction of incoming energy flux available to the longshore current

S = proportionality factor associated with suspended load transport

S_s = proportionality factor associated with suspended load transport inside the surf zone

S_{ij} = excess momentum flux tensor (radiation stress tensor)

t = time

T = wave period

T_h = sediment shear stress

T_i = net horizontal force per unit area due to slope of free water surface

u_* = shear velocity

u_{hw} = water particle velocity due to wave motion at the bed

u_i = total water particle velocity

u_i' = fluctuating water particle velocity component

u_{mh} = maximum water particle velocity due to wave motion at the bed

u_{sh} = velocity of a sediment particle on the bed

u_w = water particle velocity due to wave motion

U = mean velocity component normal to the beach

$\tilde{U}_i = \overline{U}_i + U_i$, total mean transport velocity

$\overline{U}_i$ = mean transport velocity associated with mean motion

U_i = mean transport velocity associated with fluctuating motion

$\vec{v}$ = resultant velocity vector of combined wave and current motion

V = mean velocity component parallel to the beach

V_b = mean velocity component parallel to the beach at location of breaking waves

V_{sh} = mean velocity of bed load transport in the longshore direction

V_{ss} = mean velocity of suspended load transport in the longshore direction

w = vertical velocity component

w_s = fall velocity of sand grain

x = horizontal coordinate perpendicular to the beach

X_s = width of the surf zone

y = horizontal coordinate parallel to the beach

z = vertical coordinate

α = incident wave angle

α_b = incident wave angle at breaking

α_o = incident wave angle in deep water

β = bottom slope

δ_{ij} = kronecker delta

$\Delta\ell$ = unit length of the beach

ε = energy dissipation function

ε_f = energy dissipation due to bottom friction

ε_ϕ = energy dissipation due to percolation

ε_v = eddy viscosity

η = water surface elevation

$\bar{\eta}$ = mean water surface elevation

$\bar{\eta}_b$ = mean water surface elevation at breaking position

$\bar{\eta}_o$ = mean water surface elevation for zero angle of wave incidence

κ = ratio between breaking wave height and the depth of water at breaking

ℓ = rip current spacing

ℓ' = mixing length

ν = kinematic viscosity

ω = wave frequency

ϕ = velocity potential

Φ = permeability coefficient

ρ = density of fluid

ρ_s = density of sediments

σ = local wave frequency

τ = shear stress

τ_F = fluid shear stress

τ_h = shear stress at the bed

τ_{hw} = shear stress at the bed in the direction of wave motion

τ_{hy} = shear stress at the bed in the direction of mean motion

τ_s = inter-granular fluid shear stress

θ = phase lag

χ = phase function

ξ_n = water particle excursion due to wave motion at the bed

Subscripts

b = breaker line

h = bottom

o = deep water

s = sediment

ss = suspended sediment

w = wave

Abstract of Dissertation Presented to the Graduate Council
in Partial Fulfillment of the Requirements for the Degree of
Doctor of Philosophy

LONGSHORE CURRENT AND SEDIMENT TRANSPORT

By

Edward Bennett Thornton

March, 1970

Chairman: B. A. Christensen
Major Department: Civil Engineering

On the basis of a simplified model, an attempt is made to completely describe the littoral processes including both the longshore current and sand transport. The basic assumptions are that the conditions are steady, the bottom contours are straight and parallel but allow for an arbitrary bottom profile, the waves are adequately described by linear theory, and that spilling breakers exist across the surf zone. The equations of motion are employed to the second order in wave amplitude (first order in energy and momentum). Emphasis in the analysis is placed on formulating usable predictive equations for engineering practice. The wave-induced currents generated parallel to shore are investigated first. The littoral sand transport, which is dependent on the strength of the longshore current and the intensity of the wave action, is subsequently examined.

Conservation equations of mass, momentum, and energy, separated into the steady and unsteady components, are used to describe second order wave-induced phenomena of shoaling waves approaching at an angle

to the beach. An expression for the longshore current is developed, based on the alongshore component of excess momentum flux due to the presence of unsteady wave motion. This approach is parallel to but differs quantitatively from recent work by Bowen. The wave-induced currents are shown to be primarily confined to the area inside the breaker line, that is, the surf zone. The longshore current expression is investigated for varying bottom profiles to evaluate the physical significance of including different frictional resistance terms. Wave set-down and set-up have been included in the formulation. Comparison with experimental results from the laboratory and field show that if the assumed conditions are approximately fulfilled, the predicted results compare quite favorably.

The wave-induced sand transport alongshore is investigated from energy considerations in which the quantity of sand transported is expressed as a function of the energy utilized in bottom friction, viscous dissipation, and turbulence. Although an energy approach has been used before, this is the first application to predicting the distribution across the surf zone of the alongshore sand transport.

Sand transport data were collected in the field using unique bed load traps. Wave, tide, wind, and current information was collected simultaneously in order to check the derived predictive equations for longshore current and sediment transport. Although the absolute values of sand transport are not well predicted, quite reasonable predictions are obtained for the relative distribution of bed load transport both inside and outside the surf zone, and could be used as a qualitative predictive relationship for engineering applications.

CHAPTER I

INTRODUCTION

A. Introductory Note

Waves gather their energy from the wind at sea and then propagate until eventually reaching a shoreline. It is here that a wave, having perhaps obtained its energy from the wind over hundreds of miles and many hours, is dissipated over a very short distance in a matter of seconds. The area between where the waves first start to break and the beach is called the surf zone. The incessant dissipation of wave energy against the shoreline maintains the bottom sand and water within the surf zone in a constant state of motion, the processes of which are forever striving to reach a state of dynamic equilibrium.

Waves in the open ocean (outside storm areas) tend to be fairly regular and lend themselves to analytical description. As the waves move into shallower water, they undergo transformation due to shoaling and refraction, and their heights and wave lengths change. Theories, which have been developed to describe waves for various wave heights, periods, and depths, are reasonably valid up to conditions of near-breaking. The waves reach a maximum height at breaking. Upon breaking, they lose their ordered character, and can no longer be described analytically. Breaking waves are classified as spilling, plunging, or surging. The manner in which waves break determines the distribution of energy dissipation and the energy and momentum processes in the littoral zone.

Waves traveling toward the beach at an angle to the shore have a momentum flux component directed parallel to shore. This momentum flux can result in the generation of longshore currents. These currents have been found to be largely confined to the area inside the surf zone, with the wave-induced currents seaward of this zone being relatively weak.

Longshore currents are an agent for transporting material already "loosened" from the bottom by the more intense wave action. The longshore movement of sand, termed "littoral drift," is then the result of the combined action of sediment bed agitation by waves, acting primarily perpendicular to the beach, and transport by the longshore current. The littoral drift consists of suspended and bed load components. Inside the surf zone, where the turbulence is great due to breaking waves, both of these components are significant and vary across the width of the surf zone. Outside the surf zone, the turbulence and wave agitation are reduced, and the sand transport is principally in the form of bed load.

The distribution of longshore current and sediment transport across the surf zone is the subject of this report. Unfortunately, there is very little published data on this subject. Zenkovich [1] used fluorescent sand tracers and collected suspended sand samples across the surf zone to determine these distributions. Figure 1 shows the variation of the sand transport as related to the longshore current and bottom profile. During the test, the waves were relatively high, and the slope of the beach small so that spilling breakers prevailed. The waves spilled over the first bar, and then broke again on the inner bar. The longshore current distribution is fairly uniform within the surf zone. The sand

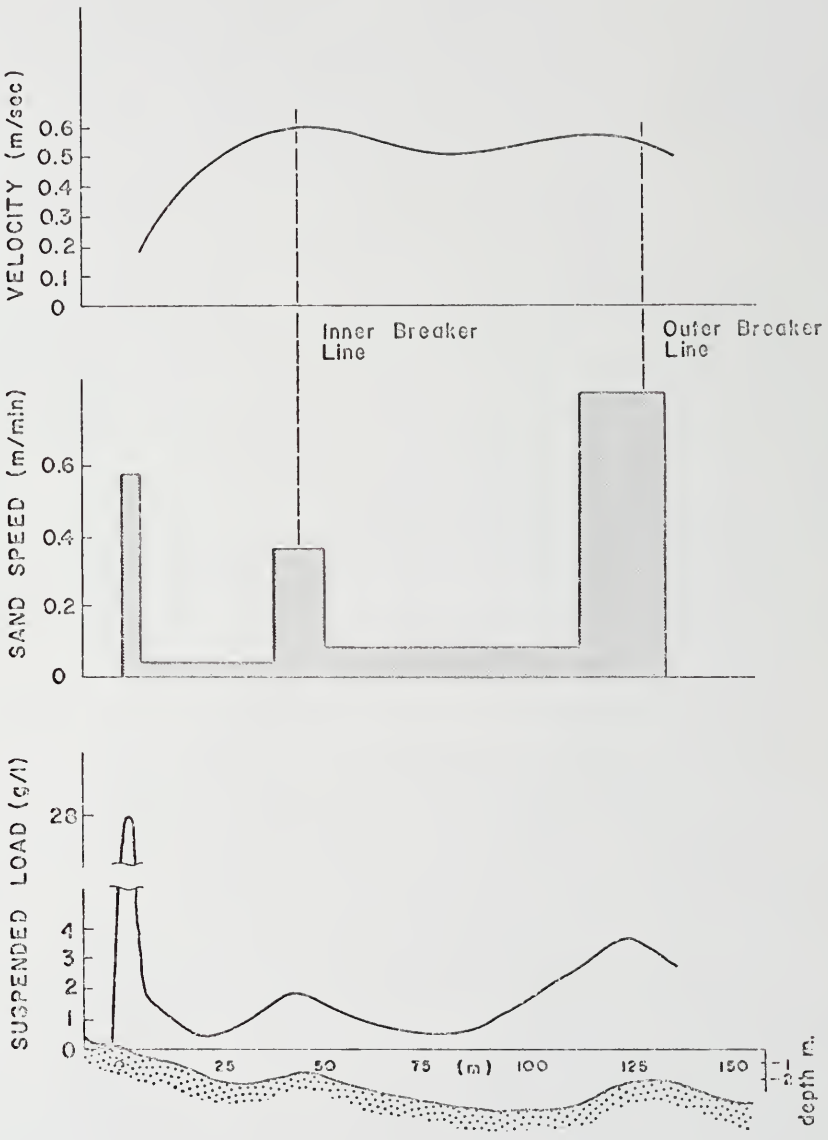

Figure 1. Distribution of Longshore Velocity and Sediment Transport across the Surf Zone (after Zenkovich [1])

transport is greatest over the bars where the energy dissipation is a maximum due to the breaking waves.

A knowledge of the variation and extent across the surf zone of the longshore current and sand transport is important in design considerations of structures placed in the littoral area. This kind of information is particularly important for groins or similar structures designed to impede sand movement. On the other hand, it is often desirable to have natural bypassing about jetties constructed for navigational purposes at inlets and harbors. The distribution of effluent, introduced onto beaches and into the littoral zone, is also influenced by the currents in the surf zone. There is a very real need for a more complete understanding of the littoral zone so that further improvements and preservation of our beaches can be based on more rational and concrete approaches.

This study logically breaks down into considering, first the waves and wave-induced currents separately and, then, the combined action on the sediments to determine the sand transport distribution. The following is a review of the literature pertinent to this study, both to serve the reader as a review of the past accomplishments and also to gain considerable insight into the problem at hand.

B. Historical Summary

1. Longshore Currents

a. Field experiments

During World War II, it became apparent there was an urgent need to better understand the surf zone and littoral environment in order to improve amphibious landings. This was the impetus for initiating a

thorough study of the mechanics of the surf zone which was later carried on after the war. Munk and Traylor [2] gathered data available at that time, conducted additional field experiments, and developed the first empirical formula relating the longshore current to the incident waves and bottom topography. They found that the longshore current was a function of the angle of wave incidence, the height of the breakers, the wave period, and the slope of the foreshore.

Shepard and colleagues at Scripps Institution of Oceanography continued this work after the war in a series of field measurements along a 100-mile stretch of the Southern California coast. From an accumulation of over 1,000 measurements emerged the first rather complete qualitative picture of the surf zone. The ideas expressed by Shepard [3] in the original summary of the data have changed very little to this day. The study showed that the most important parameter governing the longshore current is the angle of wave approach. It was also found that the strength of the current was related to the breaker height.

All the field experiments showed that the longshore current was largely confined to the surf zone and that a substantial velocity variation could exist across the surf zone. Shepard and Sayner [4] compiled the results of five years (comprising 800 days of measurements) taken at three locations along the 1,000-foot pier at Scripps Institution of Oceanography. The three measurement locations were at the end of the pier outside the surf zone, just outside the breakers, and inside the surf zone. They established that the currents inside and outside the surf zone were governed by the same mechanism, that is, they were correlated, and that the currents could be related to the wave height and direction. The currents varied considerably from offshore to the beach; the average

current velocity inside the surf zone was 1.0 foot per second compared to an average current just outside the breakers of about 0.2 foot per second.

Ingle [5] measured the distribution of longshore currents across the surf zone in conjunction with sand tracing experiments on a number of beaches along the California coast. All of these beaches, with the exception of one, were moderately steep. These tests showed that the maximum longshore current most often occurred midway between the breaker line and the swash zone.

The surf zone does not always present such a simple picture as first envisioned. On many occasions, there are strong currents of variable direction during times when large breakers approach almost normal to the coast. These currents are often associated with circulation cells and attendant rip currents which constitute a definable system. It has been found that these rip currents are least common along straight beaches with parallel contours and best developed in areas of irregular bottom topography.

Shepard and Inman [6] measured the areal variation of currents over a stretch of beach south of Scripps pier. They found that a rip current system was prevalent in this area and that the rips were controlled, to a large degree, by the wave convergence and divergence resulting from refraction of waves over the rather irregular bathymetry fronting the area. The areas of wave divergence were particularly evident over the two submarine canyons just offshore of the beach, and wave convergence occurred over submarine ridges. In areas of wave convergence, there was an influx of water across the surf zone, resulting

in an accumulation and a hydrostatic head causing a current away from the area of high breakers.

These currents flow toward areas of divergence and then turn seaward in the form of rip currents. This outflowing current then can turn again toward the point of onshore flow, thereby forming a complete circulation cell. The effect of wave convergence and divergence on the littoral circulation was found to be a maximum during times of long period waves which are more affected by the bottom topography.

Bowen [7] presented the results of an analytical investigation of the case of waves normally incident to the beach and substantiated some of the observed phenomena. He was able to show that regular variations in the wave height parallel to the beach could induce regular circulation patterns. He further showed that the gradients of wave heights could be possibly associated with edge waves or regular undulations in the bottom topography.

Sonu et al. [8] found a considerable variation in longshore currents during field experiments along the coast of North Carolina, and attributed this variation to the undulations in the bottom and the bar-trough system that prevailed. He concluded that the currents under stable conditions appeared to be generated by the momentum transfer from the plunging breakers over the bar and the mass transfer from the spilling breakers over the shoal. The hydrostatic head potential arising from the mass transfer into the surf zone is discharged seaward by rip currents.

Galvin and Savage [9] conducted field experiments at the same location and found that, during the four days of testing, a fairly

uniform current system prevailed with no evidence of a rip current system. This demonstrates that the littoral system is not constant and is governed by the conditions that prevail at the time of observations.

b. Laboratory studies

Much of the laboratory longshore current data have been found in conjunction with related littoral drift studies. Saville [10] measured longshore currents on a model sand beach having an initial slope of 1:10. The measurements were made after the bottom profile had achieved equilibrium. It was found that the maximum current always occurred along the nearshore bar where the waves break and was nearly uniform across the surf zone, decreasing slightly toward shore. The currents inside the surf zone were found to be approximately five times the current just outside the breakers which is in very close agreement with field measurements mentioned earlier.

Galvin and Eagleson [11] and Brebner and Kamphuis [12] performed very similar experiments on fixed plane beaches with a slope of 1:10. These studies showed that the maximum velocity is located between the still water line on the beach and the breaker position, usually closer to the still water line than to the breaker position. As the current flowed down the beach, the local maximum had a tendency to migrate toward the breaker position. It was also found that the currents were not uniform in the longshore direction. The currents increased downstream from an initial velocity at the retaining wall to a point beyond which a uniform distribution prevailed. The occurrence of rip-like currents was not observed in any of these laboratory experiments.

Two rather general types of littoral systems emerge--one, in which the longshore currents are fairly uniform in the longshore direction, and, the other, in which circulation cells and attendant rip currents predominate. These systems are depicted in Figures 2 and 3.

Where rip currents do not exist, there is a general return of water to the offshore to compensate for the shoreward mass transport of water by the incident waves. Longuet-Higgins [13] theoretically showed that for two-dimensional flow the incoming waves produce an onshore drift at the surface and bottom and an offshore flow at intermediate depths. This distribution was substantiated in the laboratory by Russell and Osorio [14] and in the field by Miller and Zeigler [15] whose measurements included waves breaking close to shore. Measurements taken at Fernandina Beach using an electromagnetic flowmeter further substantiate the occurrence of offshore and onshore flow simultaneously over depth. Thus, at one section perpendicular to the beach, transport can occur simultaneously onshore and offshore so that there is little net transport across the breakers.

A complete description of the surf zone requires considering a system that is three-dimensional and unsteady in time and space. The temporal variability appears to be small compared to the spatial variability (Sonu et al., op. cit.) and can be attributed partially to the nonstationarity and stochastic nature of the waves. The areal variation of longshore currents can often be related to the variations in the nearshore bathymetry and also to coastal structures. Jetties, groins, and other structures that protrude into the ocean interrupt the normal longshore current, and rip currents and large scale eddies are often located

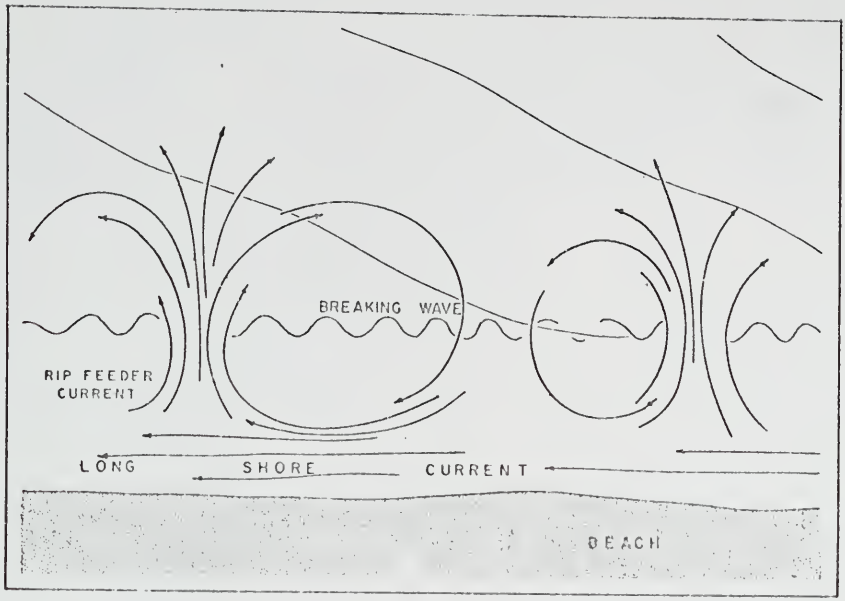

Figure 2. Rip Current System

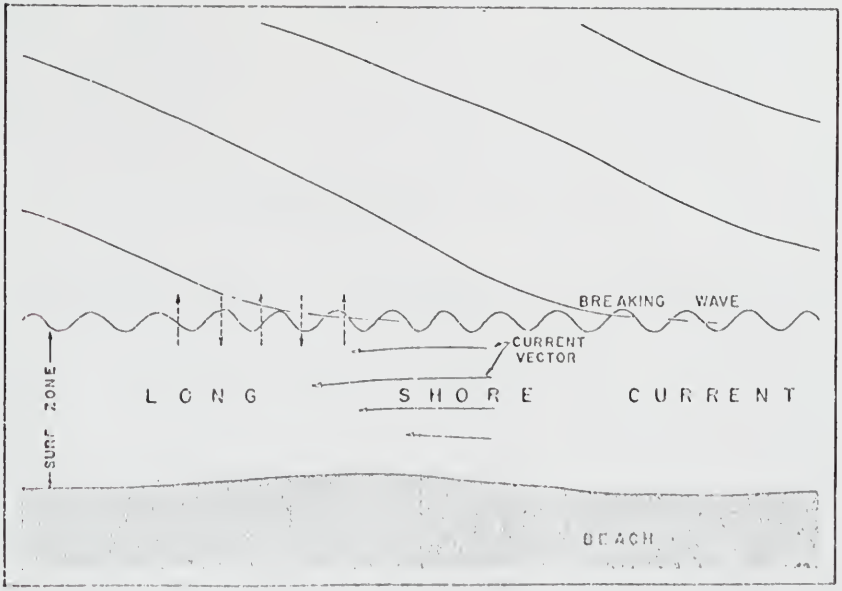

Figure 3. Uniform Longshore Current System

at the ends of such structures. Bowen (op. cit.) demonstrated that in the laboratory circulation cells can be induced by edge waves caused by gradients in the longshore breaker heights. The general complexity of the surf zone necessitates that simplifying assumptions be made in order to meaningfully describe particular phenonmenon.

c. Theory

Most of the longshore current formulas predict only the mean of the longshore current velocity. At present, there are at least fifteen such formulas, none of which satisfactorily predicts all conditions in nature. This is not too surprising in light of the rather drastic assumptions that are required to obtain an analytical formulation.

There are four basic approaches to the development of predictive equations for currents in the surf zone: (1) conservation of mass, (2) conservation of momentum, (3) conservation of energy, and (4) empirical correlation. A review of the more familiar equations is presented below, and Table I lists eleven of these formulas to facilitate comparison. Some of the equations have been expressed in slightly different forms than originally published in order that they all incorporate the same parameters; however, these changes deal only with the geometric relation for the breaking depth and slope of the beach and the relationship between the breaking depth and breaking wave height. The changes do not alter the currents predicted by the equations. Symbols, utilized in all equations, are listed in the preface.

Momentum considerations.--Putnam, Munk, and Traylor [16] used both the energy and momentum equations to derive the first rational equations for describing longshore currents. They considered the flux of mass and momentum into a control volume of differential length bounded by the

TABLE I. LONGSHORE CURRENT FORMULAS

Authors	Mean Longshore Current, V	Formulation	Eq. No.
Putnam-Munk-Traylor (1949)	$[6.97g \frac{s}{f} \tan\beta \, H_b^{\,2} \frac{\sin 2\alpha_b}{T}]^{1/3}$	Energy Conservation, Solitary waves	1.1
Eagleson (1965)	$[\frac{3}{8} g\kappa H_b \frac{\sin\beta \sin\alpha_b \sin 2\alpha_b}{f}]^{1/2}$	Momentum Conservation, Asymmetric-periodic waves	1.2
Putnam-Munk-Traylor (1949)	$\frac{A}{2}[(1 + \frac{4}{A} \; 2.28 g H_b \sin\alpha_b)^{1/2} - 1]$ $A = 20.88 \frac{\tan\beta}{fT} \cos\alpha_b H_b$	Momentum Conservation, Solitary waves	1.3
Galvin-Eagleson (1965)	$gT\tan\beta \sin 2\alpha_b$	Mass Conservation	1.4
Inman-Bagnold (1963)	$2.31 \frac{\kappa \ell \tan\beta}{T} \cos\alpha_b \sin\alpha_b$	Mass Conservation, Rip currents included	1.5
Bruun (1963)	$C_f [\frac{0.95}{\sqrt{g\kappa}} H_b^{3/2} \frac{\tan\beta \sin 2\alpha_b}{T}]^{1/2}$	Mass Conservation	1.6
Bruun (1963)	$2.31 \frac{\kappa \ell \tan\beta \cos\alpha_b}{T}$	Mass Conservation, Rip currents included	1.7
Inman-Quinn (1951)	$[(\frac{1}{4A^2} + 2.28 g H_b \sin\alpha_b)^{1/2} - \frac{1}{2A}]^2$ $A = 108.3 \frac{\tan\beta H_b \cos\alpha_b}{T}$	Empirical-based on momentum analysis	1.8
Brebner-Kamphius (1963)	$8.0 \sin^{1/3}\beta \frac{H_o^{2/3}}{T^{1/3}} [\sin 1.65\alpha_o + 0.1 \sin 3.30\alpha_o]$	Empirical-based on momentum analysis	1.9
Brebner-Kamphius (1963)	$14.0 \sin^{1/2}\beta \frac{H_o^{3/4}}{T^{1/2}} [\sin 1.65 \alpha_o + 0.1 \sin 3.30 \alpha_o]$	Empirical-based on energy analysis	1.10
Harrison (1968)	$0.241 H_b + 0.0318 T + 0.0374 \alpha_b + 0.0309 \tan\beta - 0.170$	Empirical-least square analysis	1.11

breaker line and the shore. The change in momentum flux across the breakers directed parallel to shore is balanced by the bottom shear stress. Solitary wave theory was used to calculate the momentum of the breaking waves. In this manner, they obtained an expression for the mean longshore velocity related to the angle of wave incidence α_b, breaking wave height H_b, bottom slope $\tan\beta$, wave period T, and friction factor f. Embodied in all of the momentum analyses is a friction factor that relates the velocity to the bed shear stress and represents an empirical coefficient. This equation was subsequently revised by Inman and Quinn [17] who found that a better fit to the data originally collected by Putnam et al., and additional field data collected by the authors, was obtained if the constant friction coefficient in the original equation was changed to be a function of the velocity.

Eagleson [18], using the same control volume approach, developed a mathematical model to represent the growth of a longshore current downstream of a barrier. In the associated laboratory experiments, it was found that a large percentage of the fluid composing plunging breakers (most common laboratory breaker type) is extracted from the surf zone. This fluid already has a longshore velocity to which is added the longshore component of the breaking wave. This argument provides a mechanism for growth of the longshore current downstream. The asymptotic solution to the differential equations showed that the system is stable and that the growth of the currents was bounded. These results agreed qualitatively with laboratory results and demonstrated that unless there are perturbations inducing gradients in the wave energy in the longshore direction, the current system tends to be uniform alongshore and stable for stationary wave conditions.

Bowen [19], in a very recent investigation, used a conservation of momentum approach to determine the longshore velocity distribution across the surf zone for the case of a plane beach. Reasonable results were obtained when compared to laboratory data. This is the same approach that will be used in this dissertation to develop equations describing the longshore current distributions for more general situations. A more complete discussion will be reserved for Chapter III.

Energy considerations.--Putnam et al. (op. cit.) also derived a mean longshore current equation from energy considerations alone. The derivation equates the changes in energy flux to the frictional energy losses parallel to the beach. A difficulty, with the resulting equation, is that it involves two undetermined constants, the friction factor f and the percentage of the wave energy available to the longshore current s, which makes the equation very difficult to apply.

Continuity considerations.--Bruun [20] and Inman and Bagnold [21] derived similar expressions using the continuity approach. These formulations are based on the fact that the incident waves introduce a mass flux of water into the surf zone which is then manifested as a spatial gradient in the longshore current. Both developments consider a plane beach of infinite length, implying that mass is uniformly introduced into the surf zone along the beach. The current will grow (since mass is continually being supplied to the surf zone), and, at intervals, it is necessary that there be outflow from the surf zone unless the current becomes unbounded. It is postulated that this outflow occurs in the form of rip currents which are evenly spaced along the coast. Thus, the equations contain an unknown parameter--the spacing of the rip currents. Unfortunately, few measurements have been made of rip current spacings

so that the use of these equations requires additional experimental data.

It should be noted that, due to the mass flux of waves, there is always transport of fluid into the surf zone and that, in all the physical models whether considering a mass, energy, or momentum approach, the mass flux must be accounted for in order to obtain a bounded solution. Thus, the assumption, that the mass transport is uniformly returned across the surf zone, is at least implied in all the developments which do not include concentrated return flow by rip currents.

Bruun (op. cit.) also considered the case where rip currents are absent, and the return flow is distributed uniformly over the vertical plane containing the breaker line. He reasoned that waves breaking at an angle to the beach contribute mass to the surf zone and locally raise the mean water level as the breaking wave crest propagates down the beach. This results in a slope of the water surface between crests which creates a longshore current. The longshore current is balanced by bottom shear stress related to the velocity through the Chézy formula. Galvin and Eagleson (op. cit.), reasoning from the continuity approach, equated a hypothetical mass flux across the breaker line proportional to the mass contained in the longshore current. Using both field and laboratory data, the two mass fluxes were correlated.

Empirical correlations.--Two types of empirical equations have been developed. The first type employs physical reasoning to determine the form and grouping of the important parameters which are then correlated with experimental data. Brebner and Kamphuis (op. cit.) used both the energy and momentum equations to obtain reasonable groupings by dimensional

analysis of the important parameters. Linear regression was then used to find the best fit for the longshore velocity to a large number of data that they had measured in the laboratory.

The second type of analysis employs multiple regression techniques. Sonu et al. (op. cit.) used this method to weight the various independent variables collected in their field studies. They found that the most important variable affecting the mean longshore current velocity was the angle of wave incidence, and the second most important, although much less, was the wind. These results are conflicting with those of a similar analysis reported by Harrison and Krumbein [22] who, using data collected at Virginia Beach, Virginia, found the most important variable to be the wave period which proved to be insignificant in Sonu's analysis. Sonu also performed a multiple quasi-nonlinear regression analysis which showed the most important variable affecting the mean longshore current velocity to be the wave height. In a later study, Harrison [23], using another set of data collected at Virginia Beach, found the incident wave angle to be the most important, followed by the wave period, height, and beach slope, respectively. Harrison points out that the use of such empirical equations is necessarily limited in application to "similar" situations; it is not possible to extrapolate to any particular case with confidence. The problem with using such techniques is that they are devoid of any physical basis and, as such, can give spurious correlation and conflicting results. The physics of the problem predict a nonlinear combination of the independent variables where linear multiple regression is inherently a linear combining or additive process.

Evaluation of theories.--Galvin [24] critically reviewed twelve mean longshore current theories and tested six of them that were

applicable to the "best of the published experimental data" from both the laboratory and field. In this way, he hoped to determine which equation most accurately represents the experimental measurements. Galvin concluded that there is still no completely satisfactory predictor of mean longshore currents.

Sonu et al. (op. cit.) conducted field experiments and found poor correlation when compared to six of the above equations. Their experiments did point out the importance of the nearshore topography on the current system, and how this may affect the outcome of such results. Shepard [4] earlier pointed out that another reason for lack of agreement between theory and field experiments could be the variation of current across the surf zone; each field data point is usually based on only a single location in the surf zone.

Many simplifying assumptions are necessary in developing the theories. Since exact expressions are not available, it is necessary, inside the surf zone, to select approximate expressions for the wave speed, wave shape, water particle velocity, partitioning of energy in the wave field, alongshore variation of waves and currents, and velocity and energy distributions across the surf zone. It is possible that improved theories for longshore currents will require a better understanding of the highly nonlinear waves in the vicinity of the surf zone. However, it would seem that an improvement in existing formulations could result by including the distribution of these quantities across the surf zone rather than considering only the mean values.

The importance of considering other factors, such as the wind, was demonstrated by Sonu's empirical correlations. He found the wind to be

the second most important variable in his set of field data. This shows the difficulty in comparing tests, particularly field data where information concerning the effects of bottom topography and winds often is not included. The extrapolation of data from one particular location to another without accounting for the importance of these effects can lead to invalid results.

All of the equations involve unknown coefficients to be determined experimentally. Generally, the friction factor in the momentum and energy equations is evaluated in the same manner as in open channel hydraulics. The validity of utilizing results from steady flow situations certainly needs to be investigated further and could hopefully result in a refinement.

Sonu points out that another possible improvement might derive from consideration of the dynamic processes of energy dissipation in the surf zone environment. The difficulty is that the flux of energy used in generating longshore currents is only a small fraction of the total available energy and, as such, represents a second order phenomenon (Galvin, op. cit.). On the other hand, it appears that the mass flux into the surf zone represents a primary feature of the surf zone so that conservation of mass might be a better basis for longshore current theories. One difficulty with using the continuity approach is that, although it allows a description of the mean current, no procedure has yet been developed, based on continuity considerations, which provides a prediction of the variation of the current across the surf zone.

2. Littoral Drift

a. Field experiments

Field experiments have played a very important role in the study of littoral processes. One of the difficulties encountered in sediment transport studies is that the similitude laws relating field to laboratory conditions have not been adequately established and verified. Thus, field studies are necessary for the understanding of littoral problems, either to supplement analytical or laboratory work, or as a means of solution by itself.

The measurement of littoral drift along a particular beach and the meaningful correlation with the wave environment is an extremely difficult task. Hence, only very limited data are available. The formula, most frequently used for determining total littoral drift, is attributed to Caldwell [25]. Dimensional arguments show that the rate of sediment transport can be related to the longshore component of wave power per unit beach length. Caldwell combined the results of field studies conducted in Anaheim, California, and those of Watts [26] at South Lake Worth, Florida, and proposed the following formula for the total longshore transport per unit time due to waves

$$Q_s = C[\rho g H_b^2 c_b \sin 2\alpha_b \Delta\ell]^{0.8} \tag{1.12}$$

where $\Delta\ell$ is a unit length of beach, and C is a constant of proportionality. This relationship has been tested against laboratory data by Savage [27] and shows reasonable correlation.

The earliest published information on the distribution of sand transport along the beach profile for prototype conditions was by the Beach Erosion Board [28]. The distribution of longshore current and suspended

sand, obtained from water samples, was measured from piers extending across the surf zone. These measurements showed that the greatest sand transport occurred at the breaker line, where the turbulence was a maximum, and decreased shoreward with another peak in the swash zone--another area of high turbulence. Seaward of the breakers, the sand transport decreased with increasing depth. There have been surprisingly few other field experiments of this type. Watts [29] conducted similar studies using a more elaborate continuous suspended sediment sampler. The results were qualitatively similar and showed that the amount of sand in suspension was related to the wave height, or energy, of the waves for a particular test. In these experiments, and some by Fukushima and Mizoguchi [30] using suspended samplers made of bamboo poles, the vertical distribution of suspended sediments was also measured. These data showed that the amount of suspended sediment in the swash zone and near the breaker line can be fairly evenly distributed over the vertical due to the high degree of turbulence throughout the water column. This is particularly true at the breaker line where a large vertical velocity component can be present in the case of plunging breakers. The greater portion of the transport in the surf zone is due to suspended load with the highest concentration near the bed; outside the surf zone, bed load is the predominate mode of transport.

Improvements in tracer techniques, particularly using either radioactive or fluorescent sand tracers, have increased the intensity of littoral drift studies in the field. A great number of studies have been conducted in recent years and have been summarized in a book by Ingle (op. cit.). Ingle also conducted a number of studies using fluorescent tracers on several Southern California beaches. The results of these

and some conducted by this researcher, and also earlier investigators, are all generally similar to that given in Figure 1 in describing the variation of sand transport across the surf zone. The fluorescent sand grains are found in greatest concentrations along points of high turbulence. In a bar-trough profile, the sand moves predominantly along the bar or in the swash zone. There is a minimum of tracer transport in the trough.

Tracer studies have been conducted using both the Eulerian and Lagrangian approaches. Most investigators have used the Lagrangian approach in which the tracer is introduced at a particular location, and the concentration distribution of the tracer is determined by obtaining bottom samples at various sample points. The concentration of tracers is then determined by counting the tracer grains in the sand samples. The Eulerian approach is to sample in time along a particular line across the surf zone, traversing the path of the tracers. A stable platform or other work facility is generally required in this method. This was the approach used by Zenkovitch, working from a tramway traversing the surf zone and by Bruun and Battjes [31], working from a pier. The experiments by Bruun were continued by this author.

The inherent difficulty of fluorescent tracer studies is that quantitative measurements require recovery of most of the tracer. Unfortunately, the recovery level is generally very low, amounting to only a few percent. This requires that accompanying measurements of the quantity of sand in suspension, or moving on the bed, also be determined. However, as a tool, or aid, for solving engineering problems in which qualitative information can be extremely important, fluorescent tracer techniques alone can be of great value.

b. Laboratory studies

A number of laboratory experiments have been conducted to determine the mechanisms causing sand transport in the surf zone. This discussion is limited to the three-dimensional studies simulating conditions in the prototype. Krumbein [32] conducted one of the first of these experiments and concluded that the mean littoral drift was a function of the deep water wave steepness, H_o/L_o. Subsequent studies by Saville (op. cit.) showed that a maximum transport occurred for a wave steepness of 0.025, and, for steepnesses greater or less than this value, the transport was less. This was further verified by Shay and Johnson [33] who also showed the transport to be a function of the wave angle. A maximum transport was found to occur for a deep water wave angle of 30 degrees.

Although these results imply that the transport is a function of wave steepness, the reason for this dependence has not been established. Galvin [34] conducted a series of experiments of breaking waves on laboratory beaches. He developed a classification for determining whether the waves develop into plunging or spilling breakers as related to wave steepness and the beach slope. These results, when compared to the littoral drift studies in the laboratory, indicate that maximum transport occurs for a plunging-type breaker and that the rate of transport may be more a function of the manner in which the waves break than the wave steepness.

The study by Saville and a subsequent study by Savage [35] also provide information concerning the distribution of littoral transport across the surf zone. A series of traps was used to traverse the downstream profile of a model beach so that both the total and distribution

across the surf zone could be determined. It was found that approximately 90 per cent of the transport occurred inside the surf zone. The distribution of transport across the surf zone was in qualitative agreement with field studies.

c. Theory

Although many predictive formulas have been proposed for the problem of sediment transport in alluvial channels, there have been relatively few attempts to explain the transport pheonomenon due to combined wave and current action. This is undoubtedly due to the limited success found using the predictive formulas for unidirectional flow and also because of the added complexity of dealing with oscillating flow.

A study of the mechanics of the forces acting on a sand grain under the combined action of waves and currents was made by Eagleson and Dean [36]. This study considered the combined gravity, friction, current and wave forces acting on an individual spherical particle on the bed. From this deterministic approach, accompanied by considerable laboratory studies, conditions for incipient motion were found. The forces on a suspended particle were also considered in the same study.

For a given sand grain size and density and beach slopes, there exists an equilibrium position, the so-called "null point," along the bottom profile where all the forces on the particle averaged over a wave cycle are balanced. Eagleson *et al*. [37] extended the study of the incipient motion condition mentioned above to better define the "null point" of a particular sand grain and were able to qualitatively explain sorting of sand along the profile according to size and weight characteristics. The forces acting on a sand grain can be elucidated, and

considerable insight gained into the nature of the problem from this deterministic approach to the sediment transport problem.

Difficulty is encountered in extrapolating from a single particle analysis based upon deterministic mechanics to the many particle analysis which in reality must be considered as a statistical mechanics problem. Kalkanis [38] used the same arguments as embodied in Einstein's approach to sediment transport in alluvial channels and extended it to the case of simple harmonic motion with a superimposed mean current. He assumed that the distribution of the turbulent water particle fluctuations are Gaussian over the wave period and, on this basis, derived a probabilistic model for the bed load movement. Laboratory experiments accompanied this study in an attempt to determine the necessary coefficients in Einstein's development. Unfortunately, the complexity of the formulation requires the determination of five parameters which must be based on considerably more data than have been examined to date.

Iwagaki and Sawaragi [39] developed a formula for predicting the total littoral transport rate applicable to long term average values. The basic assumption was that the average littoral transport is proportional to the shear velocity of the mean longshore current. The mean longshore current is determined by the Putnam, Munk, and Traylor energy formula for longshore currents (see Table 1). The formula, presented by Iwagaki and Sawaragi, in terms of measured quantities at the breaker line, is

$$Q_s = A \left[\frac{\tan\beta \sin 2\alpha_b}{T}\right]^{4/3} \frac{\cos\alpha_b}{d^{1/2}} H_b^{11/3} \qquad (1.13)$$

where A is a constant of proportionality, d is the mean grain size, and the other terms are as previously defined.

Le Méhauté and Brebner [40] proposed an equation for the total mean littoral transport rate based on physical reasoning guided by empirical information. The equation assumes the form

$$Q_s = c_b g H_b^2 \, T \sin \frac{7}{4} \alpha_b \tag{1.14}$$

The exponents and constants in this equation were selected to provide a best fit to the measured data.

A more straightforward approach is given by Bagnold [41]. This approach is based on considering the work required to move the sediments as related to the available energy of the waves and currents. He considers both the bed load and suspended sediment transport. Since this is essentially the method of analysis being employed in this dissertation, the formulation is presented completely in Chapter IV.

C. Purpose and Scope of the Investigation

The aim of the present research is to investigate the distribution of wave-induced longshore currents and sediment transport from offshore, across the surf zone, to the beach. Where possible, formulas are developed to predict quantitative information. A simplified physical model is considered which has wide application to nature. The basic assumptions are that steady-state conditions prevail and that the bottom contours are straight and parallel to the beach.

The study naturally breaks down into examining, first, the distribution of the shear stresses and longshore currents. Having obtained this information, it is then possible to describe the distribution of sediment transport.

Tools for the analysis are developed in Chapter II. A general set of conservation equations are set down, and the wave field, inside

In Chapter III, theoretical models for longshore current and shear stress distributions are developed governing the region from deep water onto the beach. A momentum approach is utilized in which the changes in momentum flux are balanced by frictional forces in the direction parallel to shore. The resolution of the shear stresses into wave and current components is demonstrated. The theoretical models for longshore currents are checked against existing field data.

Chapter IV utilizes the results of the predicted current and shear stress distributions to theoretically describe the variation of sediment transport across the surf zone.

Chapter V describes field experiments conducted which tend to substantiate the theoretical descriptions of the sediment transport distributions. The results of the field experiments and theory are compared and discussed.

CHAPTER II

CONSERVATION RELATIONSHIPS AND SPECIFICATION OF WAVE FIELD

A. Introduction

Past investigations have attempted to relate the mean longshore currents to wave-induced momentum, energy, or mass flux into the surf zone. The distribution of longshore currents can be similarly investigated by considering the changes in the momentum, energy, or mass flux across the surf zone. The present analysis utilizes the momentum principle to describe the variation of wave-induced longshore currents from deep water, across the surf zone, to the beach.

It is known that, due to the fluctuating water particle motion of the waves, there is a momentum flux component. If the waves have a direction component parallel to shore, a longshore current can be generated due to changes in the longshore momentum flux component of the shoaling waves. It is also known that there must be a displacement of the mean water surface elevation to balance the changes in the onshore momentum flux component of the shoaling waves.

In waves, the momentum flux is the sum of the pressure and the product of two velocities. It can be shown that the average momentum flux is nonlinear in wave height. In order to specify the excess momentum flux of the waves, it therefore becomes necessary to consider nonlinear, or higher order, effects of the wave motion. Since the waves are the mechanism responsible for the generation of the longshore

currents, much of the ensuing discussion is devoted to describing the waves.

The treatment of periodic gravity waves is generally developed by perturbation schemes built on the exact solution for the linearized equations of motion with specified boundary conditions. Difficulty, with this type of analysis, is encountered when considering higher order theory including a variation in the bottom boundary condition. For waves traveling in water of varying depth, two different approaches can be employed: the analytical method and the energy flux method. The analytical method involves solving the boundary value problem accounting for the slope of the bottom to the desired degree of approximation. This technique includes the slope, explicitly, in the perturbation expansion. The solution for the waves on a plane sloping bottom has been worked out to the second order by several authors. Mei et al. [42] have given a systematic approach for carrying the analysis to higher orders.

The analytical method is generally more consistent because it accounts for the bottom slope in the bottom boundary condition to the same order of approximation as is maintained in the free surface boundary conditions. The smallness of the bottom slope as well as the smallness of the amplitude is incorporated in the perturbation analysis. Although more attractive from an analytical point of view, this method has the inherent difficulty of requiring tedious computations for each particular case. Also, and more importantly for our needs, the more rigorous boundary value problem approach is not readily extended across the surf zone.

The energy method consists of solving the wave problem for a horizontal bottom and then extending these results to a sloping bottom by

means of energy flux considerations. Hence, for short distances, in the region outside the surf zone, it is assumed that waves on a sloping bottom can be considered the same as on a horizontal bottom. Then, adjacent increments of distance are connected together by means of the energy flux conservation equation. This results in a prediction of the wave height at any location outside the surf zone. Inside the surf zone, it will be assumed that the wave height is governed by the local water depth.

The method employed allows for the inclusion of dissipative effects, such as bottom friction, and the focusing of energy due to refraction by changes in bathymetry and currents. The accounting for these effects is often more important than the deformation of the water particle motion due to the bottom slope as given in the analytical procedure [43].

The validity of the energy method can be proven by comparison with the results of the exact analytical solution. To the first order of approximation in wave energy, for the case of small bottom slopes, identical results are obtained for the propagation of energy. This confirms the use of the energy flux equation to connect the solution for various depths for small bottom slopes, at least to the first order in wave energy. It is assumed that the method can then be extended to higher order nonlinear waves.

The treatment here is to use the energy method approach to describe the wave field to the first order in energy (second order in wave amplitude). This solution is then substituted into generalized conservation equations to extract the desired information.

B. Conservation Equations

A convenient starting point for this analysis is a statement of the general conservation equations of mass, momentum, and energy fluxes applicable to unsteady flow. The analysis is not concerned with the internal flow structure of the fluid; hence, the derivation can be simplified by integrating the conservation equations over depth. Conservation equations which have already been developed by Phillips [44] will be used and are presented below.

The conservation equations will be applied to wave motion, but they are equally applicable to general turbulent motion. The unsteady velocity field of the wave motion can be expressed in the same manner as in the treatment of turbulent motion as the sum of its mean and fluctuating parts

$$\vec{u} = (U_i(x,y,t) + u_i'(x,y,z,t),\ w(x,y,z,t)) \quad i = 1,2 \qquad (2.1)$$

where (1,2) refer to the horizontal coordinates (x,y), respectively, and z is the vertical coordinate. The tensor notation is used only for horizontal components of water particle motion. The mean current is assumed uniform over depth for simplicity. The pressure term can be stated similarly. These expressions can be substituted into the mass, momentum, and energy equations, and the mean and fluctuating contributions identified.

The conservation equations are to be averaged over depth and time (one can consider averaging over a few wave periods). For the case of waves superposed on a mean current, all the wave motion would be identified with the fluctuating quantity which, when integrated over the total depth, can contain a mean contribution due to the waves. The time averaging of the equations for a general development, being over a short

interval compared to the total time, does not preclude long term unsteadiness in the mean motion.

The utility of the conservation equations derived by Phillips is that the terms involving the mean and fluctuating quantities have been separated. This facilitates the understanding of the effect of the unsteady wave motion on the total flow phenomenon. They are a particularly useful aid in gaining physical insight into the complicated mechanisms taking place in the surf zone.

In addition to the "normally considered" conserved quantities of mass, momentum, and energy, a fourth condition is available to aid this analysis--conservation of phase, or more simply, conservation of waves. This condition, as applied to gravity waves, was first stated by Whitham [45].

1. Conservation of Phase

The conservation of phase will be derived for simplicity in relation to simple harmonic motion. The expressions to be derived are also applicable to more general wave motion which can be formed by the superposition of individual Fourier components. The expression for the water surface profile for harmonic motion is given by

$$\eta = \frac{H}{2}(x_i)\cos(k_i x_i - \omega t) \qquad i = 1,2 \qquad (2.2)$$

where $\frac{H}{2}(x_i)$ is the amplitude, and the quantity $(k_i x_i - \omega t)$ is called the phase function χ. The wave-number k_i and frequency ω can be defined in terms of the phase function, such that

$$k_i = \frac{\partial \chi}{\partial x_i} \qquad (2.3)$$

$$\omega = - \frac{\partial \chi}{\partial t} \tag{2.4}$$

An important property of the wave-number can be seen immediately by vector identity

$$\vec{\nabla} \times \vec{k} = \vec{\nabla} \times \vec{\nabla} \chi \equiv 0 \tag{2.5}$$

so that the wave-number is irrotational. From Equations (2.3) and (2.4), the kinematical conservation equation for the wave-number can be written

$$\frac{\partial k_i}{\partial t} + \frac{\partial \omega}{\partial x_i} = 0 \tag{2.6}$$

For a single wave component, the conservation of phase says that the rate of increase of the number of waves in a fixed length is balanced by the net inward flux of waves per unit time. If ω can be expressed as a function of k_i and possibly x, from local arguments (such as assuming a uniform simple harmonic wave train locally), and further allowing a mean current $\vec{U}$, then,

$$\omega = \sigma(k, x_i) + k_i U_i \tag{2.7}$$

σ is the local wave frequency and is the apparent frequency to an observer moving with the current. Substituting into Equation (2.6), Whitham (op. cit.) shows

$$\frac{\partial k_i}{\partial t} + c_{gj} \frac{\partial k_i}{\partial x_j} + U_j \frac{\partial k_i}{\partial x_j} = - G_i \tag{2.8}$$

where

$$G_i = \frac{\partial \sigma}{\partial x_i} + k_j \frac{\partial U_j}{\partial x_i}$$

and

$$c_{gj} = \frac{\partial \sigma}{\partial k_j} \tag{2.9}$$

c_{gj} is the speed at which the energy or values of k_j are propagated, commonly called the group velocity. The individual crests propagate with the local phase velocity $c = \frac{\sigma}{k}$. The notation shall be adopted where, if c or k appear without vector notation, it is understood that they represent the modulus of the vector quantity.

Equation (2.8) says that the rate of change of the wave-number k_i, following a point moving with the combined group and convective velocity, is equal to $- G_i$. Changes in G_i are due to variations in the mean current and bottom configuration. These geometrical equations, which state the kinematical conservation for the wave-number, hold for any kind of wave motion (Phillips, op. cit.).

2. Conservation of Mass

The general conservation of total mass per unit area can be expressed

$$\frac{\partial}{\partial t} \rho D + \frac{\partial}{\partial x_i} \tilde{M}_i = 0 \qquad i = 1,2 \tag{2.10}$$

D is the total averaged depth of water which can include a mean elevation $\bar{\eta}$, above (or below) the still water depth h, so that

$$D(x,y,t) = (\bar{\eta} + h) \tag{2.11}$$

The overbar shall be used to signify time averages. The total mass flux $\tilde{M}_i$ can be partitioned into its mean and fluctuating components

$$\tilde{M}_i = \bar{M}_i + M_i \tag{2.12}$$

The mass flux per unit width of the mean flow is

$$\overline{M}_i = \overline{\int_{-h}^{\eta} \rho U_i \, dz} = \rho D U_i \tag{2.13}$$

The mass transport of the wave motion is

$$M_i = \overline{\int_{-h}^{\eta} \rho u_i' \, dz} \tag{2.14}$$

3. Conservation of Momentum

The equation defining the conservation of horizontal momentum is derived by integrating the momentum equation, including shear stresses, over depth and averaging in time. The balance of total momentum per unit area can be expressed

$$\frac{\partial}{\partial t} \tilde{M}_i + \frac{\partial}{\partial x_j} (\tilde{U}_i \tilde{M}_j + S_{ij}) = T_i + R_i \tag{2.15}$$

Here $\tilde{M}_i$ denotes the total horizontal momentum per unit area. Hence, the first term on the left represents the rate of change of the total mean momentum per unit area which includes both the current momentum and wave momentum.

The total mean transport velocity can be expressed in terms of the mass flux per unit area

$$\tilde{U}_i = \frac{\tilde{M}_i}{\rho D} = U_i + \frac{M_i}{\rho D} \tag{2.16}$$

The second term on the left of Equation (2.15) expresses the momentum flux of a steady stream having the same mass flux $\tilde{M}_i$ and mean transport velocity $\tilde{U}_i$ as the actual flow together with an excess momentum flux

term S_{ij} arising from the superposed wave motion, where

$$S_{ij} = \overline{\int_{-h}^{\eta} (\rho u_i' u_j' + p\delta_{ij})\, dz} - \tfrac{1}{2}\rho g D^2 \delta_{ij} - \frac{M_i M_j}{\rho D} \qquad (2.17)$$

and δ_{ij} is the Kronecker delta.

The term T_i is given by

$$T_j = -\rho g(\bar{\eta} + h)\frac{\partial \bar{\eta}}{\partial x_i} \qquad (2.18)$$

and represents the net horizontal force per unit area due to the slope of the free water surface.

R_j is the time mean averaged shear stress which must be included in any realistic treatment of the surf zone where dissipative effects occur. The form of the shear stress was not explicitly stated by Phillips in his derivation so this term will be expanded in detail. Also, insight can be gained into the manner in which the momentum equation was integrated over depth in arriving at the generalized momentum conservation equation. Considering the shear stresses on a column of water (see Figure 4) and integrating over the depth, R_i can be expressed

$$R_i = \overline{\int_{-h}^{\eta} \frac{\partial \tau_{ji}}{\partial x_j}\, dz} + \overline{\int_{-h}^{\eta} \frac{\partial \tau_{zi}}{\partial z}\, dz} \qquad i,j = 1,2 \qquad (2.19)$$

where τ_{ji} includes the combined stresses of waves and currents. The shear stress on the horizontal plane can be integrated over depth, such that

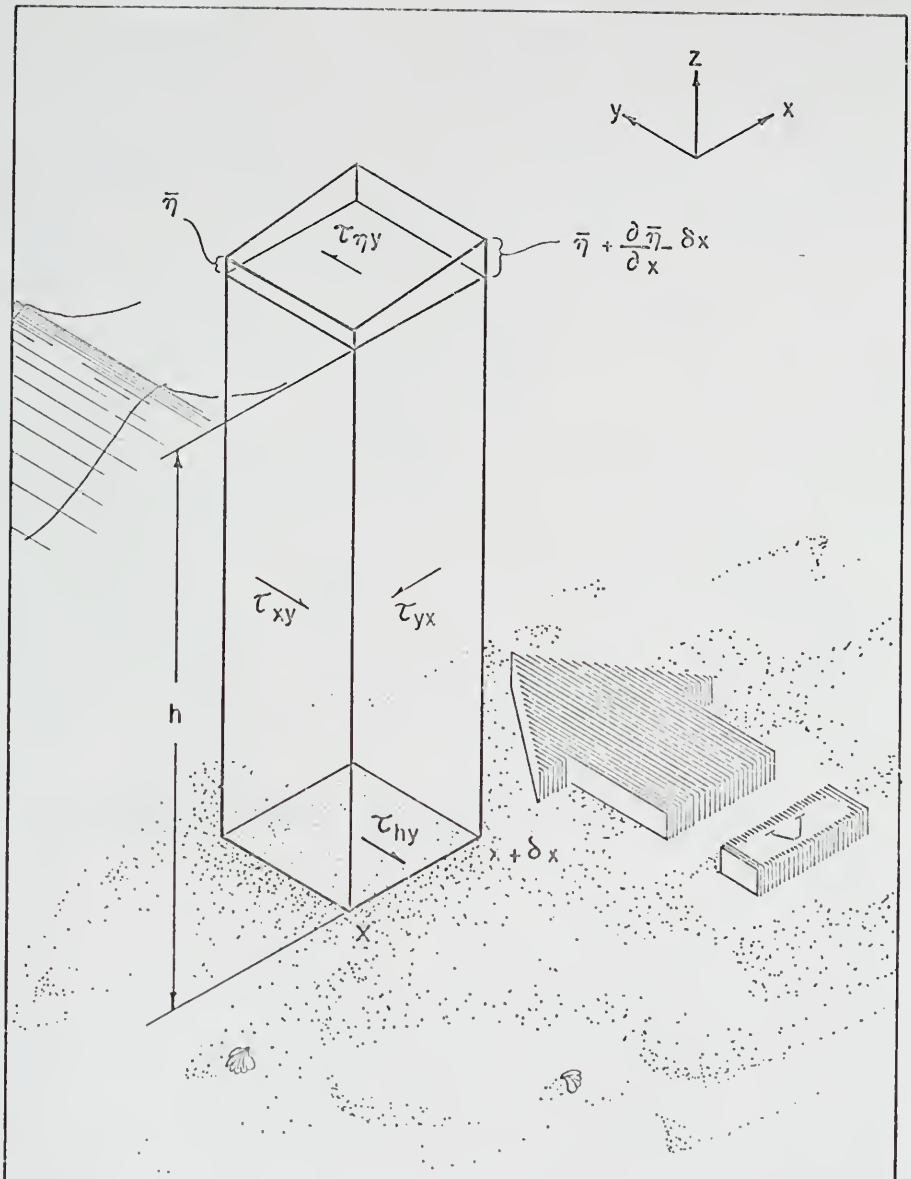

Figure 4. Shear Stresses Acting on the Faces of an Elemental Water Column

$$\overline{\int_{-h}^{\eta} \frac{\partial \tau_{zi}}{\partial z} dz} = \overline{\tau}_{\eta i} - \overline{\tau}_{hi} \tag{2.20}$$

where the subscripts refer to surface and bottom.

The Leibnitz rule of integration must be employed to integrate over depth the stresses occurring on the vertical faces of the water column. Evaluating the shear stress on the vertical faces and taking the time average of the terms

$$\overline{\int_{-h}^{\eta} \frac{\partial \tau_{ji}}{\partial x_j} dz} = \frac{\partial}{\partial x_j} \overline{\int_{-h}^{\eta} \tau_{ji} dz} - \overline{\tau_{ji\eta} \frac{\partial \eta}{\partial x_j}} - \overline{\tau_{jih} \frac{\partial h}{\partial x_j}} \tag{2.21}$$

Thus, the general shear stress term is given by

$$R_i = \frac{\partial}{\partial x_j} \overline{\int_{-h}^{\eta} \tau_{ji} dz} - \overline{\tau_{ji\eta} \frac{\partial \eta}{\partial x_j}} - \overline{\tau_{jih} \frac{\partial h}{\partial x_j}} + \overline{\tau_{\eta i}} - \overline{\tau_{hi}} \tag{2.22}$$

$$i,j = 1,2$$

4. Conservation of Energy for Fluctuating Motion

The equation for the conservation of total energy can be partitioned into the energy contributions from the mean and fluctuating parts with the aid of the conservation of mass and momentum equations. In the following development, it is convenient to work with the energy balance for the fluctuating motion alone, which can be stated

$$\frac{\partial}{\partial t}\left(E - \frac{M_i^2}{2\rho D}\right) + \frac{\partial}{\partial x_i}\left(U_i E + F_i - \frac{\tilde{U}_i M_j^2}{2\rho D}\right) + S_{ij} \frac{\partial U_j}{\partial x_i} = -\varepsilon \tag{2.23}$$

In separating the mean and fluctuating contributions, the mean energy density has been represented as the total energy density of an "equivalent"

uniform flow with the same depth and mass flux as the actual flow, plus the energy density of the fluctuating motion, minus an additional term representing the difference between the energy density of the actual mean motion and that of the equivalent uniform flow. Then, the first term in Equation (2.23) is the rate of change of the energy density of the fluctuating motion minus the correction term. The second term represents the convection of the fluctuating energy E, by the mean flow, the energy flux of the fluctuating motion F, minus the correction term. The transport of energy by the fluctuating motion is given by

$$F_i = \rho \int_{-h}^{\overline{\eta}} u_i' \left[\tfrac{1}{2}(u_j'^2 + w'^2) + g(z - \overline{\eta}) + \frac{p}{\rho}\right] dz \qquad (2.24)$$

which represents the rate of work done by fluctuating water particle motion (for turbulence, this would be the work done by the Reynolds stresses) throughout the interior region of the flow, plus the work done by the pressure and gravity forces. The last term on the left of Equation (2.23) represents the rate of working by the fluctuating motion against the mean rate of shear. Dissipative effects of turbulence have also been allowed where ε is the rate of energy dissipation per unit area.

5. Conservation of Energy for the Mean Motion

The energy budget for the mean motion is given by

$$\frac{\partial}{\partial t}\left[\tfrac{1}{2}\tilde{U}_i\tilde{M}_i + \tfrac{1}{2}\rho g(\overline{\eta}^2 - h^2)\right] + \frac{\partial}{\partial x_i}\tilde{M}_i\left(\tfrac{1}{2}\tilde{U}_j^2 + g\overline{\eta}\right) + U_j\frac{\partial S_{ij}}{\partial x_i} = U_i\tau_i \qquad (2.25)$$

The terms of this equation represent, respectively, the rate of change of the kinetic and potential energy of the mean motion, the transport

of the total mean energy, and the rate of work by mean motion on the fluctuating motion and bottom shear stresses.

In the development of the conservation equations, no restrictions were placed on the wave slopes or amplitudes. Also, no restrictions were placed on the fluctuating motion so that the equations are equally applicable to wave or turbulent motion.

C. Description of the Wave Field

1. Waves outside the Surf Zone

The descriptive equations for the wave field are derived by, first, solving the linearized boundary value problem over a horizontal bed. The solution can, then, be extended to a higher order by perturbation techniques. The development presented here will retain terms to the second order in amplitude (first order in energy and momentum) and neglect all higher order terms. The wave solution can then be substituted directly into the conservation equations providing a means for describing the wave-induced mean motions. In making this substitution and dropping all terms of orders higher than the second, only knowledge of the first order (linear) wave water particle velocities and surface elevation is necessary. This is because, in expanding and then averaging over the period, the terms involving higher order quantities in velocity and surface elevation go to zero. The pressure must be known to the second order in wave height; however, the average second order pressure component can be determined from the first order water particle velocities and surface elevation terms. Thus, only the linear wave solution is required.

In utilizing linear theory, it is assumed that the motion is irrotational and that the fluid is incompressible and inviscid. These have

been shown to be good assumptions, due to the fact that viscosity plays only a very minor role in determining the hydrodynamics of the wave field, and, thus, the vorticity is very weak [44]. The fact that the linear theory is a good approximation is demonstrated by its success in describing many observed phenomena.

Assuming simple harmonic motion, the surface elevation is restated as in Equation (2.2)

$$\eta = \frac{H}{2} \cos(k_i x_i - \sigma t) \qquad i = 1,2$$

where the wave-number components are

$$k_x = k \cos\alpha$$
$$k_y = k \sin\alpha \tag{2.26}$$

The arbitrary angle of wave incidence α is measured between a line parallel to the contours and the wave crests. The velocity potential for the first order solution is given by

$$\phi = -\frac{H}{2} \frac{g}{ck} \frac{\cosh k(h + z)}{\cosh kh} \sin(k_i x_i - \sigma t) \tag{2.27}$$

The velocity is related to the gradient of the velocity potential

$$u_i = -\nabla\phi \tag{2.28}$$

$$u_i = \frac{H}{2} \frac{g}{c} \frac{k_i}{k} \frac{\cosh k(h + z)}{\cosh kh} \cos(k_i x_i - \sigma t) \tag{2.29}$$

The frequency equation relates the frequency to the local wave-number and water depth

$$\sigma^2 = gk \tanh kh \tag{2.30}$$

The pressure can be determined as a function of the depth to the second order by integrating Euler's vertical momentum equation over the depth and retaining terms of second order. Only knowledge of the first order water particle velocities and surface elevation is required to determine the mean second order pressure term. The time-mean pressure is given as

$$\bar{p} = -\rho g z - \frac{1}{8}\rho\sigma^2 H^2 \frac{\sinh^2 k(z+h)}{\sinh^2 kh} \tag{2.31}$$

where the first term is the hydrostatic contribution, and the second term is the second order mean dynamical pressure component.

The group velocity of the waves can be determined from Equation (2.9)

$$(c_g)_i = \frac{k_i}{k}\frac{d\sigma}{dk} = \frac{\sigma}{k} n \frac{k_i}{k} = c_i n \tag{2.32}$$

where the transmission coefficient is

$$n = \frac{1}{2}\left(1 + \frac{2kh}{\sinh 2kh}\right) \tag{2.33}$$

For deep water (infinite depth), $n = \frac{1}{2}$, and, in shallow water, n approaches 1.

The energy of the waves is proportional to the wave height squared and is equally partitioned between the potential and kinetic energy, such that the total energy is

$$E = \frac{1}{8}\rho g H^2 \tag{2.34}$$

Recalling that the group velocity expresses the speed of energy propagation, the energy flux of the wave motion is

$$F_i = E\, c_{gi} \tag{2.35}$$

Assuming negligible wave reflection and a mildly sloping bottom, Equations (2.32) and (2.34) can be substituted directly into Equation (2.35) to obtain the flux of wave energy.

The mass transport of the waves can be determined by recalling Equation (2.14) in which the fluctuating velocity was integrated from the bottom to the surface. Since the water surface elevation is unknown, the integrand is expanded in a Taylor series about the mean water surface level $\bar{\eta}$

$$M_i = \int_{-h}^{\bar{\eta}} \overline{\rho u_i}\, dz + \int_{\bar{\eta}}^{\overline{\eta}} \overline{\rho [u_i(\bar{\eta}) + z \frac{\partial u_i(\bar{\eta})}{\partial z} + \ldots]}\, dz \qquad (2.36)$$

where the time mean average of the mass transport below the trough is zero (first integral), and only terms of second order in amplitude will be retained. Substituting for the wave profile and water particle velocity of the wave motion, Equations (2.2) and (2.29), the mass transport of the waves is

$$M_i = \rho \overline{\eta u_{i\eta}} = \frac{E}{c} \frac{k_i}{k} \qquad (2.37)$$

Simple harmonic motion has been selected to describe the waves because experience has shown that this solution gives fairly good results for the deep water case. Inside the surf zone, however, the approximation is not good, but the assumption of simple harmonic wave trains will be retained with the exception of certain modifications on the celerity and amplitude. The wave field could just as easily (in principle, anyway) have been specified using the cnoidal or other higher order wave theories. It is felt that, for the present investigation, the accuracy gained would not justify the much increased complexity of the resulting equations.

2. Breaking Waves

The seaward edge of the surf zone is usually delineated by the point where the waves first start to break. Inside the surf zone, the waves are unstable, and the fluid motion tends to lose its ordered character. Waves break in different ways, depending primarily upon the wave steepness and slope of the beach. The manner in which they break has a very definite influence on the hydrodynamics inside the surf zone which, in turn, affects such quantities as the sediment transport, longshore currents, and wave runup.

Based on observations by Wiegel [46], breaking waves are usually classified as spilling, plunging, or surging. Spilling occurs when the wave crests become unstable, curl over slightly at the top, creating a foamy advancing face. Plunging occurs on steeper beaches when the wave becomes very asymmetric; the crest curls over, falling forward of the face resulting in the creation of considerable turbulence, after which a bore-like wave front develops. Surging occurs when the wave crest remains unbroken while the base of the front face of the wave, with minor turbulence generated, advances up the beach.

There is a continuous gradation in the type of breaking, and Galvin [34], in a more recent classification, found it convenient to add a fourth category of collapsing to describe a type intermediate to plunging and surging. He performed extensive laboratory investigations to quantitatively classify breaking waves according to the wave and beach characteristics. Combining his results with earlier works, he grouped the breaker type depending on beach slope $\tan\beta$, wave period T, and either deep water or breaker height H. The breaker type can be sorted by either of two dimensionless combinations of these variables,

an offshore parameter, $H_o/(L_o \tan^2\beta)$, or an inshore parameter, $H_b/(gT^2 \tan\beta)$. As either of these parameters increases, breaker type changes from surging to collapsing to plunging to spilling. Spilling breakers are associated with steep, relatively short period waves and flat beaches; plunging breakers are associated with waves of intermediate steepness and the steeper beaches; and surging breakers are associated with waves of small height and steep beaches.

On natural beaches, breakers classed as spilling are most commonly observed, followed in decreasing order of frequency by plunging, collapsing, and surging. In the laboratory tests, spilling breakers are relatively rare compared with collapsing and surging breakers, because slopes used in laboratory tests are usually steeper than slopes commonly found in nature due to the physical limitations of space.

The breaking index curve provides a relationship between the breaking depth D_b, the breaking wave height H_b, and the wave period T. In shallow water, the relationship simplifies to $H_b/D_b = \kappa$, a constant. Reid and Bretschneider [47] compiled breaking wave data from several sources including both laboratory and field data. They found a fairly good correlation for breaking waves as compared to the breaking wave criteria predicted by the solitary wave theory. The solitary wave theory predicts a value for κ of 0.78, while other theories predict slightly different values. Theoretical values range from 0.73, found by Laitone [48], for cnoidal wave theory, to a value of 1.0, found by Dean [49] using a numerical stream function theory. Experiments on steeper laboratory beaches show that the value of κ can be much larger. All the theoretical values have been calculated, assuming a flat bottom, and correspond to beaches with very gentle slopes. The important point is that the breaker height is governed by the depth of water.

3. Waves inside the Surf Zone

Inside the surf zone, energy is dissipated due to the generation of turbulence in wave breaking, bottom friction, percolation, and viscosity. The waves in the surf zone constitute a non-conservative system in which the use of potential flow theory is no longer valid. In fact, there is no analytical description available for the waves in the surf zone. Hence, one is required to make rather gross assumptions and then to test these assumptions experimentally. The linear wave theory will be retained as the input to the conservation equations, but with modification to the wave amplitude and speed. The wave height inside the surf zone is controlled by the depth and is of the same order of magnitude. Thus, even the second order theory in wave height is a rather poor assumption, but seems to agree surprisingly well with measurements of some phenomena.

Spilling breakers lend themselves to a physical treatment since the potential energy and momentum flux of the waves inside the surf zone can be expressed approximately in analytical form. If the beach slope is very gentle, the spilling breakers lose energy gradually, and the height of the breaking wave approximately follows the breaking index curve [50]. The height of the wave is then a function of the depth.

In the breaking process, plunging breaker heights may also be intermittently described by the breaking index; however, due to rapid dissipation of energy in breaking, the height may fall below the breaking index curve, and the residual wave energy may later reform and then break again in shallower water. This was generally noted for moderately gentle slopes in laboratory experiments by Nakamura et al. [51].

In the present analysis, it will be assumed that the waves act as spilling breakers inside the surf zone and that they follow the breaking index, $\kappa = 0.78$, as predicted by the solitary wave theory. The wave height inside the surf zone is then given by

$$H = \kappa D \tag{2.38}$$

It is further assumed that the kinetic and potential energy are equally partitioned so that the total wave energy can be described in terms of the wave height which is a function of the depth

$$E = \frac{1}{8} \rho g \kappa^2 D^2 \tag{2.39}$$

This is a non-conservative statement of the energy distribution within the surf zone.

The waves inside the surf zone are assumed to retain their simple harmonic character so that the wave profile and water particle velocity are described by

$$\begin{aligned} \eta &= \frac{H}{2} \cos(k_i x_i - \sigma t) \\ \vec{u} &= \frac{H}{2} \frac{g}{c} \frac{k_i}{k} \cos(k_i x_i - \sigma t) \end{aligned} \tag{2.40}$$

The expression for the horizontal water particle velocity is based on the Airy wave theory and has been simplified for shallow water.

In very shallow water, the waves are non-dispersive with the wave speed being only a function of the depth. It has been found experimentally that a reasonable approximation to the wave speed in the surf zone is that predicted by the solitary wave theory [52].

$$c = \sqrt{g(H + D)} = \sqrt{g(1 + \kappa) D} \tag{2.41}$$

The wave field has been completely specified. These results may now be substituted into the general conservation equations to describe wave-induced phenomena inside and outside the surf zone.

CHAPTER III

LONGSHORE CURRENT THEORY

A. Statement of the Problem

The study of the area in and about the surf zone presents a difficult problem due to its very complex nature. A proper treatment of the surf zone must consider a three-dimensional problem of unsteady fluid motion and is further complicated by moving interfaces at the upper and lower boundaries, that is, at the water surface and sediment bottom. It was also noted earlier that more than one longshore current system could occur for seemingly similar conditions. Thus, it is necessary to make definite and simplifying assumptions in order to make the problem tenable to a theoretical approach.

This analysis considers the steady-state distribution of quantities on a line normal to the shoreline. A schematic of the surf zone area is shown in Figure 5. The analysis is restricted to the case of an arbitrary bottom profile with straight and parallel contours in the y-direction (parallel to the beach). The water depth is then a function of the x-direction only (perpendicular to the beach). Since the distribution of mean properties of the wave field is a function of the depth, this eliminates any y-dependence.

An exception to this was found by Bowen [7]. Using the fact that incident waves can excite transversal waves, commonly called edge waves, he showed that if these waves are standing waves, or only slowly progressive, gradients in the mean water surface can be developed in the

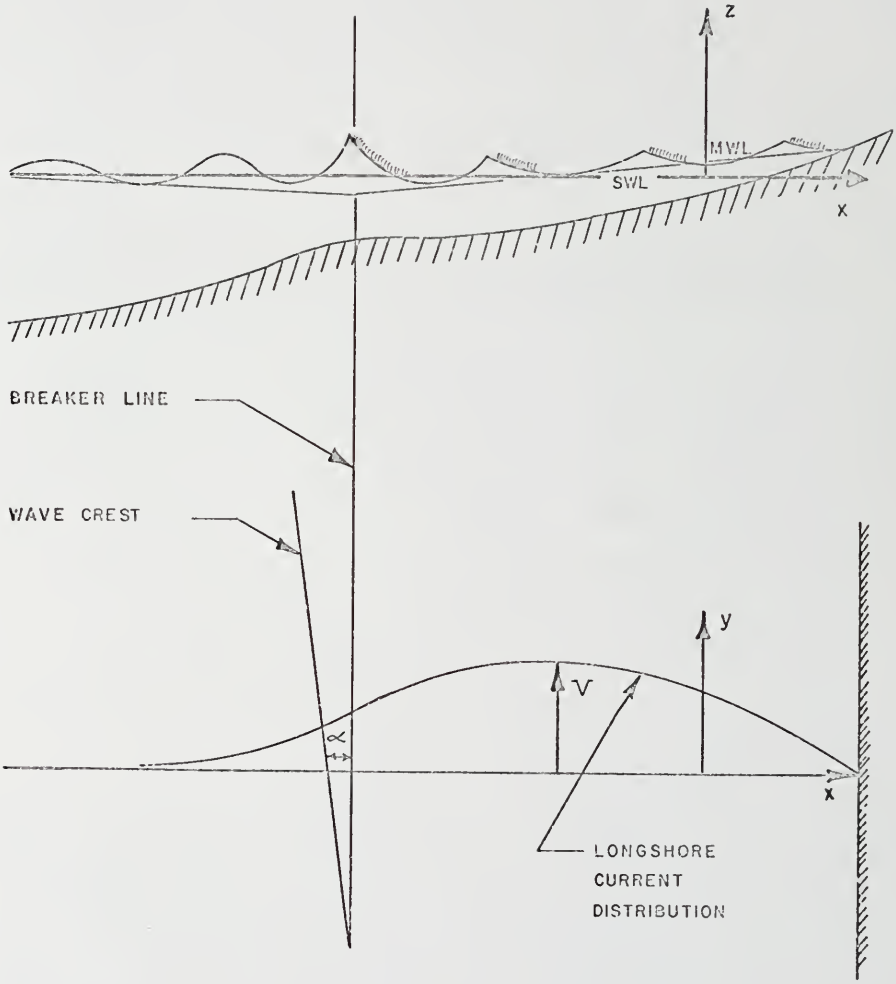

Figure 5. Scheme of the Surf Zone

longshore direction which in turn can result in circulation cells. Thus, a more exact formulation has to assume suitable spatial averaging in the longshore direction so as to preclude the effects of any transversal waves.

It is assumed that wave reflection is negligible. This assumption is justifiable outside the surf zone for gently sloping bottoms. The present analysis is shown to be most valid for spilling breakers which implies a gently sloping bottom. The wave reflection is least for this type of breaker condition and is assumed negligible inside the surf zone as well.

Shear stresses at the surface due to the wind will be neglected.

Summarizing, this is a steady-state problem (except for periodic wave motion) with no y-dependence such that

$$\frac{\partial h}{\partial y} = \frac{\partial E}{\partial y} = \frac{\partial V}{\partial y} = \frac{\partial U}{\partial y} = 0 \tag{3.1}$$

The notation $U_x = U$ and $U_y = V$ will be used henceforth. No restrictions will be placed on the direction of wave approach for, indeed, it is the wave motion in the y-direction that is the driving mechanism in the equations of motion.

The problem can be conveniently discussed by considering separately the areas outside and inside the surf zone. Since conditions inside the surf zone are dependent on the incoming waves, the case seaward of the breakers will be examined first.

B. Currents outside the Surf Zone--Neglecting Bottom Friction

A determination of the distribution of mass transport and energy of the waves is first necessary in order to solve for the wave-induced currents outside the surf zone.

1. Mass Transport Velocity

Due to the absence of any y-dependence, the mass conservation Equation (2.10) reduces to

$$\frac{\partial \tilde{M}_x}{\partial x} = 0 \tag{3.2}$$

Integration gives

$$\tilde{M}_x = \text{constant} = 0 \tag{3.3}$$

which must be equal to zero since the beach forms a boundary in the x-direction. This then says

$$U = -\frac{M}{\rho D}\cos\alpha = -\frac{E}{\rho c D}\cos\alpha \tag{3.4}$$

which states that there is a mean reverse current balancing the mass transport onshore due to the wave motion. This must be true everywhere, both inside and outside the surf zone, to ensure that there is no accumulation of mass or growth of currents in the y-direction in order to maintain steady-state conditions in accordance with the original assumptions.

2. Distribution of Energy outside the Surf Zone

The determination of the energy distribution is necessary as a means of relating the wave heights at various depths. The energy, in turn, must be related to the local angle of wave incidence. The angle of wave incidence is affected by refraction which can occur since the waves are allowed to approach at an arbitrary angle of incidence to the bottom contours. The problem is further complicated since a shear flow is allowed which can also produce wave refraction.

The general statement of the phase relation gives an expression relating the frequency, mean current motion, and wave angle. Equation (2.7) can be expanded to give

$$\omega = \sigma + Vk \sin\alpha + Uk \cos\alpha \tag{3.5}$$

The assumption of steady-state conditions requires that ω be uniform and constant.

The wave-number was shown to be irrotational

$$\frac{\partial k_y}{\partial x} - \frac{\partial k_x}{\partial y} = 0 \tag{3.6}$$

Since the wave length and amplitude of the waves are independent of the y-direction, the gradient of the local wave-number in the y-direction is zero.

$$\frac{\partial k_x}{\partial y} = 0 = \frac{\partial k_y}{\partial x} \tag{3.7}$$

Integrating the gradient of k_y in the x-direction gives

$$k \sin\alpha = \text{constant} = k_o \sin\alpha_o \tag{3.8}$$

where the subscript "o" refers to conditions in deep water. This is a statement that, for straight and parallel contours, the projection of the wave-number on the beach is a constant. Substituting into Equation (3.5), a general expression for the celerity of the waves can be derived where

$$\omega_o = k\left(\frac{\sigma}{k} + V \sin\alpha + U \cos\alpha\right) \tag{3.9}$$

or utilizing Equation (3.8)

$$c = \left(\frac{c_o}{\sin\alpha_o} - V\right) \sin\alpha - U\cos\alpha \tag{3.10}$$

For U = V = 0, this expression simplifies to Snell's law for wave refraction.

The conservation of energy for the fluctuating motion, Equation (2.23), can be expanded for steady-state conditions to give

$$\frac{\partial}{\partial x}\left(EU_x + Ec_{gx} - \frac{\tilde{U}_x M_x^2}{2\rho D} - \frac{\tilde{U}_x M_y^2}{2\rho D}\right) + S_{xy}\frac{\partial V}{\partial x} + S_{xx}\frac{\partial U}{\partial x} = -\varepsilon \tag{3.11}$$

where the gradients in the y-direction are zero. This equation states that the change in energy flux, due to currents and waves plus the work done by the excess momentum flux on the straining motion, is equal to the energy dissipated by turbulence and work done on the bottom. The product of a stress times rate of strain is a quantity that can be associated with power per unit volume. The last two terms on the left of the energy equation can be interpreted in this context where the excess momentum flux tensor then represents a stress and the velocity-shear a rate of strain. Longuet-Higgins and Stewart [53] were the first to take cognizance of this, and named the excess momentum flux tensor a radiation stress.

The excess momentum flux tensor can be determined by substituting the wave expressions into Equation (2.17). In general terms of energy, group velocity, and wave speed, an expression applicable to both inside and outside the surf zone is given by

$$S_{ij} = \begin{vmatrix} E\frac{c_g}{c}\cos^2\alpha + \frac{E}{2}\left(\frac{2c_g}{c} - 1\right) & \frac{E}{2}\frac{c_g}{c}\sin 2\alpha \\ \frac{E}{2}\frac{c_g}{c}\sin 2\alpha & E\frac{c_g}{c}\sin^2\alpha + \frac{E}{2}\left(2\frac{c_g}{c} - 1\right) \end{vmatrix} - \frac{M_i M_j}{\rho D} \tag{3.12}$$

The effects of turbulence and surface tension have not been included.

Referring to Equations (3.4) and (3.12), it can be seen that U and S_{xx} are of order E. The first and last terms of Equation (3.11) involving the product of these terms are of order (E^2) and, hence, will be ignored in this analysis. From the result of the conservation of mass, Equation (3.4), $\tilde{U}_x = 0$, so that the third and fourth terms of the energy equation are zero. Substituting for S_{xy} and F_x, and retaining only terms of first order in energy, the energy equation reduces to

$$\frac{\partial}{\partial x} (Ecn \cos\alpha) + En \frac{\sin 2\alpha}{2} \frac{\partial V}{\partial x} = - \varepsilon \tag{3.13}$$

where the substitution, $c_g = cn$, has been made. Substituting for the wave celerity, as given by Equation (3.10), yields

$$\frac{\partial}{\partial x} En \left[\left(\frac{c_o}{\sin\alpha_o} - V \right) \sin\alpha \cos\alpha - U \cos^2\alpha \right] + En \cos\alpha \sin\alpha \frac{\partial V}{\partial x} = - \varepsilon \tag{3.14}$$

Again recalling that U is of order E, and that all higher order terms involving the product of U can be neglected in this analysis, the energy equation can be written

$$\frac{\partial}{\partial x} En \left(\frac{c_o}{\sin\alpha_o} - V \right) \sin\alpha \cos\alpha + En \cos\alpha \sin\alpha \frac{\partial V}{\partial x} = - \varepsilon \tag{3.15}$$

Expanding and cancelling terms, gives

$$\left(\frac{c_o}{\sin\alpha_o} - V \right) \frac{\partial}{\partial x} En \sin\alpha \cos\alpha = - \varepsilon \tag{3.16}$$

Far outside the surf zone, energy dissipation due to bottom effects can be ignored, and the energy losses due to turbulence can be assumed negligible. Since the term in the brackets of Equation (3.16) is

nonzero, the result of the energy equation outside the surf zone, assuming no energy dissipation, is

$$En \sin 2\alpha = \text{constant} \tag{3.17}$$

The relative amplification of the wave energy is then given by

$$\frac{E}{E_o} = \frac{n_o \sin 2\alpha_o}{n \sin 2\alpha} \tag{3.18}$$

Since the term involving U in the celerity equation resulted in the product of higher order terms that are not included, Equation (3.10) can be written, consistent with this analysis

$$c = \left(\frac{c_o}{\sin\alpha_o} - V\right) \sin\alpha \tag{3.19}$$

or in terms of the wave angle

$$\sin\alpha = \frac{c}{c_o} \sin\alpha_o \left[\frac{1}{1 - \frac{V}{c_o} \sin\alpha_o}\right] \tag{3.20}$$

Equations (3.16) and (3.18) give a complete description of the wave amplitude and direction outside the surf zone.

For no current, Equation (3.10) reduces to Snell's law for wave refraction and can be combined with Equation (3.18) to give

$$E\, c_g \cos\alpha = E_o \frac{c_o}{2} \cos\alpha_o = \text{const} \tag{3.21}$$

where the local quantities are related to the conditions in deep water. The changes in energy density E, or wave height, can be determined from this equation as a function of the local wave-number and water depth. For decreasing depth as the waves approach the shore, the local wave length and the angle of incidence decrease. The effect of shoaling is

determined by the group velocity. The group velocity initially increases slightly so the energy density decreases; the group velocity then decreases resulting in a continual increase in the energy density towards shore. A maximum wave height occurs at breaking. Due to the change in wave angle, which is the result of refraction, the wave crests become more nearly parallel to the beach. The energy density is less for waves approaching at an angle to a constant sloping beach than for waves whose orthogonals are normal to the beach because wave refraction results in divergence of wave energy.

The effect of a shear current on the energy density can be illustrated most simply by considering the case of waves in deep water where the depth is not involved as a parameter. The relative amplification of the energy density as a function of V/c_o is shown graphically in Figure 6 for various values of the initial angle α_o. It can be seen that for the case of currents with a component in the direction of wave propagation (positive ratio of V/c_o) there is a decrease in energy density. For angles greater than zero, there is a point at which the amplification suddenly becomes very large and tends to infinity. As $\alpha \to 90$ degrees, the infinity occurs for all currents in the positive direction. These infinities represent caustics, or crossings of the wave rays. In reality, the theory is no longer valid near such points.

As has been shown, there is an excess of momentum flux due to the presence of the waves. For conservation of momentum flux, there must be a force exerted in the opposite direction such as a hydrostatic pressure force or bottom shear stress to balance this excess momentum flux. It will be presented that outside the surf zone the component of excess momentum flux directed perpendicular to the contours is balanced by mean water level set-down.

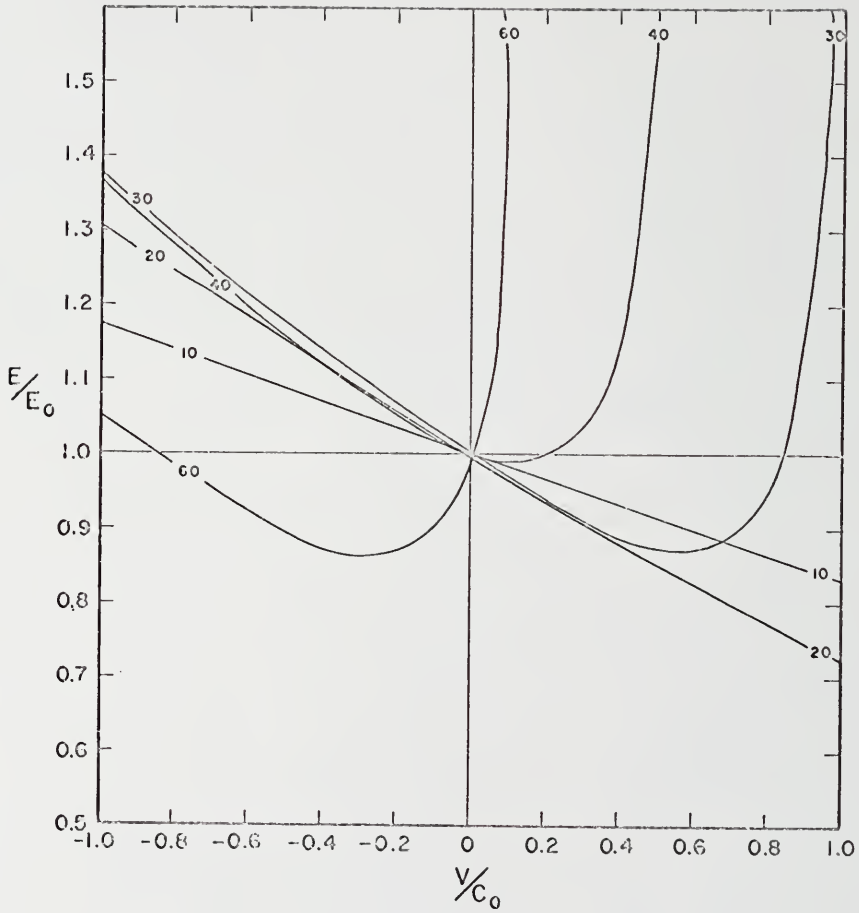

Figure 6. Amplification of Wave Energy Density Due to a Shear Current as a Function of the Incident Wave Angle

3. Distribution of Currents outside the Surf Zone

There is a component of excess momentum flux directed parallel to the shore due to the oblique wave approach. The question of whether this radiation stress can induce a current can be investigated by considering the general y-momentum equation. Neglecting changes in the slope of the free water surface, Equation (2.15) can be written

$$\frac{\partial}{\partial x}\left(V\tilde{M}_x + S_{xy}\right) = R_y \tag{3.22}$$

where the gradients in the y-direction are zero. The conservation of mass equation showed that $\tilde{M}_x = 0$; hence, the first term is zero. Comparison of the energy equation solution, Equation (3.17), and the excess momentum flux tensor, Equation (3.12), shows that

$$S_{xy} = E\frac{c_g}{c}\sin\alpha\cos\alpha = \text{constant} \tag{3.23}$$

Therefore, the change of momentum flux due to the waves and mean motion in the y-direction is zero--there is no driving force for generating a current outside the surf zone. The only wave-induced current far outside the surf zone is then due to the mass transport velocity.

It shall be assumed $V = 0$ since there is no driving force for generating currents. The mean current in the y-direction then reduces to the mass transport velocity

$$U_y = \frac{M_y}{\rho D} = \frac{E}{\rho c D}\sin\alpha \tag{3.24}$$

The mass transport velocity generally decreases as the depth increases so that the longshore currents in deep water are very weak. This is in agreement with observations outside the surf zone. However, very near the surf zone, the mass transport velocity tends to become first

order in amplitude and is no longer negligible; but, at the same time, bottom effects become important making the derivation inaccurate. Thus, very near the surf zone, dissipation of energy must be considered. This will be discussed in Section C.

4. Set-down of Mean Water Elevation outside the Surf Zone

It is interesting to investigate the balance of momentum perpendicular to the beach. The x-momentum flux equation outside the surf zone is given by

$$\frac{\partial S_{xx}}{\partial x} = - \rho g(h + \bar{\eta}) \frac{\partial \bar{\eta}}{\partial x} \tag{3.25}$$

where dissipative effects have been neglected. The excess momentum tensor was shown in Equation (3.12) to be a function of the wave energy. As waves shoal, the amplitude, and hence the energy, increases (except over a short distance in shallow water); thus, the excess momentum flux tensor must also increase. The changes in the flux of excess momentum is balanced by a slope of the mean water level. It can be seen from Equation (3.25) that a positive gradient of the excess momentum flux (increasing) results in a negative gradient of the mean water surface. This results in an increasing set-down as the water becomes shallower. Longuet-Higgins and Stewart [54] have solved Equation (3.25) for the case of waves approaching perpendicular to an arbitrary plane bottom. They found

$$\bar{\eta} = - \frac{H^2}{8} \frac{k}{\sinh 2kh} \tag{3.26}$$

where it is seen that the set-down is a function of the local conditions only. Thus, for the case of waves approaching at an angle, if the curvature of the wave rays is small, one would expect the same solution for

the local set-down. Mei (op. cit.) solved the problem of waves shoaling over a plane bottom by means of a perturbation expansion, taking into account the sloping bottom boundary condition. He derived an expression relating the local set-down to the deep water conditions.

$$\overline{\eta} = -\frac{H_o^2}{8}\frac{\cos\alpha_o}{\cos\alpha}\frac{k \coth kh}{(2kh + \sinh 2kh} \tag{3.27}$$

This can be expressed by the local conditions using the solution to the energy equation which relates deep water conditions to shallow water conditions. Equation (3.27) then reduces to the same expression as Equation (3.26) for the local set-down.

This set-down outside the surf zone has been verified experimentally by Bowen et al. [55] in the laboratory; although close to breaking, the experimental values for set-down were less than the predicted values. As breaking is approached, and the wave height becomes larger, the second order theory becomes less valid and would be expected to give less accurate results. No energy dissipation has been accounted for, which can become important in shallower water. The effect of including energy dissipation would be to decrease the energy density as the waves shoal, which presumably would decrease the energy density gradient. This would result in a decrease in the excess momentum gradient, decreasing the set-down. This would help explain the discrepancy between theory and experiment.

C. Currents outside the Surf Zone--Including Bottom Friction

The energy equation has been used to relate the changes in wave height due to changes in the wave direction, current velocity, and depth at a particular location. Having determined the wave height distribution, the momentum and continuity equations were used to solve for currents

generated parallel to the shore. Dissipative effects were neglected in the above derivation of the longshore currents, and the evaluation of the energy equation was rather straightforward. Near the surf zone, in shallower water, the bottom effects can no longer be neglected, and the dissipation term must be included in the derivation. It will be assumed that all the energy dissipation outside the surf zone is due entirely to bottom friction and percolation. Turbulent and viscous energy dissipation above the boundary layer is very small and will be neglected. Energy utilized in transporting sediment, either along the bed or in suspension, will be assumed to be included in the bottom friction loss term and will not be considered separately. This aspect of the problem will be considered in Chapter IV.

The loss of mechanical energy is due to work done by the turbulent shear stresses acting on the bottom. To evaluate the dissipation due to bottom friction, it is first necessary to investigate the shear stresses occurring at the bottom.

1. Bottom Shear Stress Due to Combined Waves and Currents

The determination of the bottom bed shear stress for uniform steady flow has been fairly well established. For oscillatory flow, and particularly combined waves and currents, the bed shear stress is not so well formulated. This is due primarily to the lack of good empirical data. Jonsson [56] compiled the available laboratory data and conducted additional experiments dealing with turbulent boundary layers in oscillatory flow. From this study, he developed a classification of the flow regimes similar to that for steady flow. The classification is based on a roughness parameter and characteristic Reynolds number. It is found that the wave boundary layer in nature can always be considered in the "hydraulically rough" turbulent regime.

Unlike the boundary layer in open channel flow, which essentially extends over the entire depth of flow, the boundary layer under wave motion constitutes only a very small fraction of the vertical velocity distribution. This is because the boundary layer does not have an opportunity to develop under the unsteady velocity field of the wave action. Above the boundary layer, the free stream is well described by the potential flow theory (at least for small waves).

Jonsson used an oscillating flow tunnel to simulate prototype wave conditions in the laboratory. In the experiments, he was able to measure the vertical velocity profile in the boundary layer and determine the bottom shear stress. He found that for simple harmonic motion the velocity profile in the boundary layer could be approximated by a logarithmic distribution and that the instantaneous bottom shear stress was related to the velocity by the quadratic shear stress formula

$$\vec{\tau}_{hw} = f_w \frac{\rho}{2} \vec{u}_h |\vec{u}_h| \tag{3.28}$$

or

$$\vec{\tau}_{hw} = f_w \frac{\rho}{2} u_{mh}^2 \cos(\omega t - \theta)|\cos(\omega t - \theta)| \tag{3.29}$$

where u_{mh} is the velocity amplitude of the oscillating flow just above the boundary layer, θ is a phase lag, and f_w is a friction factor associated with the wave motion.

He found, further, that the friction factor was practically constant over an oscillation period. The constancy of the friction factor for particular flow conditions is an important result which allows for a better analytical determination of the combined shear stress due to waves and currents. Using the available data from several sources, he found

that the friction factor for wave motion alone for rough turbulent boundary layers could tentatively be represented by

$$\frac{1}{4\sqrt{f_w}} + \log \frac{1}{4\sqrt{f_w}} = - 0.08 + \log \frac{\xi_h}{r} \tag{3.30}$$

where r is a measure of roughness, and ξ_h is the maximum water particle excursion amplitude of the fluid motion at the bottom as predicted by linear wave theory

$$\xi_h = \frac{H}{2} \frac{1}{\sinh kh} \tag{3.31}$$

Equation (3.30) is based on the roughness parameter r being a measure of the ripple height. The wave friction factor is seen to be a function of the wave characteristics. This is because, for granular beds consisting of a particular grain size, the ripples adjust their dimensions according to the wave motion, and it is the ripple geometry that determines the effective roughness.

Unfortunately, there is only, at best, a qualitative understanding of the ripple geometry as related to sand wave characteristics. Generally, the ripples are much more symmetrical in shape and much longer crested as compared to those found in alluvial channels. Inman [57] collected a large number of observations of ripple geometry and wave conditions from Southern California beaches. These observations extended from a depth of 170 feet to the shore. Since the wave and sand characteristics vary from deep water to the beach, the ripple geometry would be expected to vary also. These observations showed that the size of the sand is the most important factor in determining the geometry of the ripple. In general, the coarser the sand, the larger the ripples. Also, there was a general

correspondence of decreasing ripple height with decreasing water depth. The ripples were smallest in the surf zone where the higher orbital velocities of the waves tended to plane the ripples off; the ripples were almost nonexistent for surf zones with fine sands. The ripple wave length was related to the orbital excursion. As the bottom orbital velocity of the shoaling waves increased, the ripple length decreased, increasing the effective roughness, but, at the same time, the ripple height is decreased, decreasing the effective roughness. Since quantitative relationships among ripple geometry, sand grain size, and wave characteristics have not been determined, one is forced to rely on observations to determine the effective roughness, and, for this reason, Inman's data are especially relevant.

It is now desired to superpose a mean current on the wave motion and determine the total shear stress due to waves and currents combined. The difficulty in using the quadratic shear stress formula is in stipulating the friction factors. The wave friction factor was seen to be a function of the wave properties for a deformable bed, that is, the fluid motion; whereas, the friction factor for steady currents for rough turbulent boundary layers is only a function of the system geometry. It would seem reasonable to expect that for weak currents, as compared to the water particle motion of the waves, that the wave dynamics would dominate the hydrodynamical system. For this reason, it is desirable to derive the combined bottom shear stress in terms of the wave friction factor alone, even though it is less well defined than the friction factor for steady currents.

It is assumed that the total instantaneous bed shear stress for combined waves and currents is related to the velocity by

$$\vec{\tau}_h = \rho \frac{f}{2} \vec{v} |\vec{v}| \tag{3.32}$$

where $\vec{v}$ is the resultant instantaneous velocity vector of the combined wave and current motion, and f is the friction factor. Since the problem has been formulated as a combination of wave and current motion, it proves convenient to resolve the shear stresses into components in the direction of the wave and current components. To do so, the velocity is first resolved into components in the direction of the current and wave motion

$$|\vec{v}| = (u_w^2 + V^2 + 2u_w V \sin\alpha)^{\frac{1}{2}} \tag{3.33}$$

where u_w is the instantaneous velocity of the wave motion measured just above the frictional boundary layer near the bottom. V is the mean motion which was assumed uniform over the depth and in the longshore direction only. Resolving the component shear stresses in the direction of the velocity vectors results in the shear stress and velocity vectors being proportional to each other as can be seen from the geometrical representation in Figure 7. The shear stress component for the wave motion can then be written

$$\vec{\tau}_{hw} = \vec{\tau}_h \frac{\vec{u}_w}{\vec{v}} = \rho \frac{f}{2} |\vec{v}| \vec{u}_w \tag{3.34}$$

and, similarly, for the shear stress in the direction of the mean current

$$\vec{\tau}_{hy} = \vec{\tau}_h \frac{V}{\vec{v}} = \rho \frac{f}{2} |\vec{v}| V \tag{3.35}$$

If friction factors for the wave and current motion are now defined,

$$f_w = f \frac{|\vec{V}|}{|\vec{u}_w|} \tag{3.36}$$

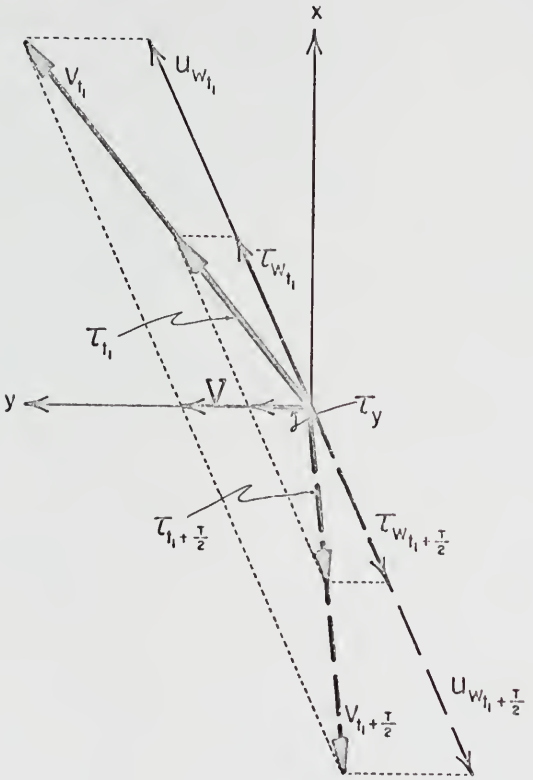

Figure 7. Resolution of Currents and Waves into Respective Velocity and Shear Stress Components

$$f_y = f \left| \frac{\vec{V}}{V} \right| \tag{3.37}$$

the shear stress components can then be written

$$\vec{\tau}_{hw} = \rho \frac{f_w}{2} \vec{u}_w \left| \vec{u}_w \right| \tag{3.38}$$

$$\tau_{hy} = \rho \frac{f_y}{2} V^2 \tag{3.39}$$

The shear stress for waves, as defined in Equation (3.38), is in the same form as given by Jonsson (op. cit.) for which information of the friction factor was found experimentally. Knowing f_w and the velocity of the waves and currents, the other friction factors and, hence, shear stresses can be determined. The total shear stress, in terms of the shear stress components, is

$$\left| \vec{\tau}_h \right| = \left(\tau_{hw}^2 + \tau_{hy}^2 + 2\tau_{hw}\tau_{hy} \sin\alpha \right)^{\frac{1}{2}} \tag{3.40}$$

Combining Equations (3.32) and (3.36), the total shear stress can also be written

$$\vec{\tau}_h = \rho \frac{f_w}{2} \left| \vec{u}_w \right| \vec{v} \tag{3.41}$$

or substituting Equation (3.33)

$$\vec{\tau}_h = \rho \frac{f_w}{2} \left| \vec{u}_w \right| \left(u_w^2 + V^2 + 2u_w V \sin\alpha \right)^{\frac{1}{2}} \frac{\vec{V}}{\left| \vec{V} \right|} \tag{3.42}$$

Since only the steady-state conditions are being considered, it is desired to find the time mean values. It will be assumed a priori that near and inside the surf zone the mean currents are much less than the maximum velocity of the wave motion. Only the case of just outside the surf zone is considered here, but it will be shown later that the

equations developed are valid for inside the surf zone as well. The time mean value of the absolute value of the water particle velocity at the bottom due to the waves is found by integrating over time Equation (2.29) to give

$$\overline{|u_w|} = \frac{2}{\pi} \frac{H}{2} \frac{gk}{\sigma \cosh kh} \tag{3.43}$$

Assuming relatively small incident wave angles α, and that $V \ll \overline{|u_w|}$, as a first approximation

$$|\vec{v}| \approx |\vec{u}_w| \tag{3.44}$$

The total bed shear stress is then given by

$$\vec{\tau}_b = \rho \frac{f_w}{2} \vec{u}_w |\vec{u}_w| \tag{3.45}$$

This result will be used later in calculating frictional energy dissipation at the bottom.

2. Changes in Wave Height outside the Surf Zone Due to Bottom Friction and Percolation

The energy equation, Equation (3.11), can now be written to include the dissipation term. Some of the higher order terms previously neglected become first order in energy in shallow water and might be included. Collectively, the contribution of these higher order terms is only approximately 4 per cent at the breaker line and, considering the inaccuracies in calculating the energy dissipation terms, can be neglected. This leads to a simplified energy equation

$$\frac{\partial}{\partial x} (Ecn \cos\alpha) = - (\varepsilon_f + \varepsilon_p) = - \varepsilon \tag{3.46}$$

where ε_f is the mean rate of energy dissipation due to bottom friction,

and ε_Φ represents the mean rate energy dissipation due to percolation.

It is assumed that the instantaneous rate at which energy is dissipated per unit bed area due to bottom friction is given by

$$\varepsilon_f = \vec{\tau}_h \cdot \vec{v}_h \tag{3.47}$$

The dissipation function is to be substituted into the energy equation concerned only with the fluctuating motion, so that $\vec{v} = \vec{u}_w + \frac{\vec{M}}{\rho D}$. The second velocity term being of second order is much less than the mean of the absolute value of the velocity of wave motion and will be neglected. The bottom shear stress is given by Equation (3.45). Jonsson (op. cit.) evaluated the energy losses experimentally using the dissipation function as given above. He found that the phase shift in the shear stress term could be ignored, and the instantaneous dissipation term evaluated in terms of the wave particle motion at the bottom.

$$\varepsilon_f = \rho \frac{f_e}{2} \left| u_{mh}{}^3 \cos^3 \omega t \right| \tag{3.48}$$

The energy friction factor f_e would not necessarily be expected to be equal to the wave shear stress friction factor f_w since a phase shift was introduced in the shear stress term. Indeed, it was found experimentally by Jonsson that they were not equal for laminar flow. However, for rough turbulent boundary layers, f_w and f_e were, for all practical purposes, the same and constant over the wave period for the experiments conducted. Thus, the energy friction factor can also be given by Equation (3.30).

Since the frictional energy dissipation is defined in terms of the absolute value of the bottom velocity, and the velocity-shear stress product is a symmetrical odd-function, the time mean value is equal to

the average of Equation (3.48) over one-half the wave cycle. The mean frictional energy dissipation is then given by

$$\varepsilon_f = \frac{\rho f_w}{12\pi} \left(\frac{\sigma H}{\sinh kh}\right)^3 \tag{3.49}$$

This is the same dissipation term found earlier by Putnam and Johnson [58] who made similar assumptions in their derivation.

Putnam [59] also theoretically examined the energy losses due to percolation. If the bed consists of permeable material, pressure variations due to the wave motion induce currents in the permeable layer, and these currents will dissipate some of the mechanical energy of the wave.

For a permeable bed whose depth is greater than approximately one-third the wave length L, the amount of mean energy dissipated, ε_ϕ, by viscous forces in the permeable bed per unit area of the bottom per unit time is given by

$$\varepsilon_\phi = \frac{g^2}{2\nu} \frac{\rho \phi k H^2}{(\cosh kh)^2} \tag{3.50}$$

where ϕ is the permeability coefficient of Darcy's law, and ν is the kinematic viscosity of the water. If the depth of the permeable bed is less than 0.3 L, a more complicated expression must be used so that it will be assumed here that the bed layer is always greater than this depth.

It is necessary to evaluate Equation (3.46) numerically due to the nonlinear dissipation terms. This can be written in terms of the wave height in a difference form

$$H_n = H_{n-1} K_s K_r \left[1 - \frac{8}{\rho g} \frac{\varepsilon_n}{\left(H^2 c_g \cos\alpha\right)_{n-1}} \Delta x\right]^{\frac{1}{2}} \tag{3.51}$$

where

$$K_s = \left(\frac{(c_g)_{n-1}}{(c_g)_n}\right)^{\frac{1}{2}} \tag{3.52}$$

is the shoaling coefficient reflecting the changes in the group velocity, and

$$K_r = \left(\frac{\cos\alpha_{n-1}}{\cos\alpha_n}\right)^{\frac{1}{2}} \tag{3.53}$$

is the refraction coefficient for a constant sloping bottom. The term in the brackets of Equation (3.51) includes the effect of energy dissipation. This equation is equivalent to Equation (3.18) for no dissipation, $\varepsilon = 0$. The wave height can then be evaluated by starting at a known value and proceeding to any desired position where the changes in the wave height compared to the initial wave height are found by integrating the dissipation term.

Savage [60] conducted laboratory studies to test the above equations and found reasonable agreement for the changes in wave height due to frictional dissipation. He further found that the energy losses by percolation were less than the theoretical values by a factor of between 4 and 10. The tests indicated that for sand sizes less than 0.5 millimeters, there is practically no loss due to percolation. On the other hand, for sand grain sizes larger than 2 millimeters, the percolation losses could become very large.

Bretschneider [61] tested the above equations with field data from the Gulf of Mexico. Percolation losses were not considered in his analysis since the bottom consisted of relatively impermeable fine sediments. Comparison of field measurements showed that using friction factors that

were close to those predicted by Equation (3.30) gave results in reasonable agreement with the theory. Thus, it is assumed that the use of Equation (3.51) for predicting the wave height at a particular position is valid and will be used in this analysis.

3. Distribution of Currents

Having determined the wave height as a function of the incident wave angle, wave period, and local depth, the wave-induced currents parallel to the shoreline can be determined from the y-momentum equation

$$\frac{\partial S_{xy}}{\partial x} = \frac{\partial}{\partial x}\left(\frac{1}{8}\rho g H^2 n \cos\alpha \sin\alpha\right) = -\tau_{hy} \tag{3.54}$$

This equation states that the change of the y-component of momentum in the x-direction is balanced by the bottom shear stress directed in the y-direction. Only the shear stress acting on the bottom is taken into account. Since the wave height could not be expressed in an explicit form, it becomes necessary to solve for the changes in the excess momentum flux numerically. The longshore velocity is then found from the calculated bottom shear stress as related by the quadratic shear stress formula

$$\tau_{hy} = \rho f_y \frac{V^2}{2} \tag{3.55}$$

where the time mean value of f_y can be determined from Equations (3.36), (3.37) and (3.43)

$$f_y = \left|\frac{\overline{u_{wh}}}{V}\right| f_w = \frac{1}{\pi}\frac{f_w}{V}\frac{H g k}{\sigma \cosh kh} \tag{3.56}$$

and f_w is determined by Equation (3.30). Therefore, the velocity outside the surf zone, taking bottom friction into account, is

$$V = -\frac{\pi}{8}\frac{\sigma}{f_w}\frac{\cosh kh}{kH}\frac{\partial}{\partial x}(H^2 n \sin 2\alpha) \qquad (3.57)$$

This gives the velocity in terms of measurable quantities.

D. Longshore Currents inside the Surf Zone

It has been shown that longshore currents could be induced by changes in the momentum flux of the waves directed parallel to the shore outside the surf zone. The wave height inside the surf zone and, hence, the water particle motion of the waves decreases due to intense energy dissipation. It might be expected that, due to the more rapid changes in momentum flux inside the surf zone, faster currents can be generated.

A simplified approach will be investigated first, and, then, additional refinements will be included to illustrate various aspects of the problem and to obtain more accurate results. A uniformly sloping bottom is initially assumed so that the physical principles involved are not lost in the algebraic details. A more general profile is then considered later. Also, the first solution considers the resisting force parallel to shore to be only due to shear on the bottom, and internal shear stresses are neglected.

Again, it is first necessary to specify the energy distribution across the surf zone in order to determine the distribution of momentum flux. The energy, as related to the wave height, was shown to be a function of the local depth. Outside the surf zone, it was shown that, due to the excess momentum flux directed perpendicular to shore, there was a set-down of the mean water surface. The changes in the mean water surface elevation inside the surf zone are investigated next.

1. Wave Set-up inside the Surf Zone

Both the wave height and speed are a function of the total local depth of water. Since there is an unknown change in the mean water level to balance the excess momentum flux of the waves, the total depth of water is unknown and must be derived to specify these quantities.

Conservation of momentum flux in the x-direction states

$$\frac{\partial}{\partial x}\left(\tilde{U}_x \tilde{M}_x + S_{xx}\right) = T_x \tag{3.58}$$

where there are no gradients in the y-direction. It was explicitly assumed that the net mass flux perpendicular to the beach was zero so that there is no contribution from the mean motion to the momentum flux perpendicular to shore. This is necessary to comply with the steady-state assumption. If a net mass transport were allowed into the surf zone and there were no rip currents or other offshore return, the currents would grow unbounded. Dissipative effects, such as bottom friction and turbulence, have not been explicitly stated but are accounted for in the potential energy decay. Equation (3.58) reduces to

$$\frac{\partial}{\partial x} S_{xx} = T_x = -\rho g D \frac{\partial \bar{\eta}}{\partial x} \tag{3.59}$$

which states that the change of excess momentum flux due to wave action is balanced by a change in the mean water level.

It is assumed that the excess momentum flux tensor inside the surf zone can be expressed in terms of the energy and wave speed in the same form as in shallow water. This assumption implies that, even under the breaking waves, water particle motion retains much of its organized character as described by linear wave theory.

Experiments conducted in the field by Miller and Zeigler (op. cit.) show that this assumption is not as extreme as one might first expect. Velocity meters were used in these experiments to measure the internal velocity fields in breaking waves. The results showed that the internal velocity field of the near breaking and breaking waves, corresponding to spilling-type breakers, could be qualitatively described by Stokes' third order wave theory. The tests also showed that different types of breakers had different internal velocity fields as would be expected, and that the spilling-type breaker was the most organized.

From Equation (3.12)

$$S_{xx} = E(\cos^2\alpha + \frac{1}{2}) - \frac{E^2}{\rho c^2 D} \cos^2\alpha \tag{3.60}$$

where S_{xx} is a function of the energy density which decreases inside the surf zone. Hence, both the momentum flux and the balancing force have a negative gradient so that the change in the mean water level inside the surf zone will be positive, representing a wave set-up.

The phase relation, as given by Equation (3.20), relates the velocity and wave speed to the incident angle relative to the conditions at the breaker line, and can be written

$$\sin\alpha = \frac{c}{c_b} \sin\alpha_b \left[1 + \frac{(V_b - V)}{c_b} \sin\alpha_b\right]^{-1} \tag{3.61}$$

In this investigation, waves having a range of periods of approximately 4-18 seconds are considered. Waves of these periods are greatly refracted before reaching the depth at which they break. Thus, the angle of wave incidence at the edge of the surf zone is generally small--usually much less than 30 degrees. Assuming the maximum value of the

longshore current velocity would be approximately equal to the component of the wave speed in the longshore direction, then

$$|V_b - V| \leq V \leq c_b \sin\alpha_b \tag{3.62}$$

so that

$$\frac{|V_b - V|}{c_b} \sin\alpha_b < \frac{(c_b \sin\alpha_b)}{c_b} \sin\alpha_b << 1 \tag{3.63}$$

Thus, an approximation for Equation (3.61), using the binomial expansion, can be conveniently employed.

$$\sin\alpha = \frac{c}{c_b} \sin\alpha_b \left[1 - \frac{(V_b - V)}{c_b} \sin\alpha_\beta + \ldots\right] \tag{3.64}$$

The $\cos^2\alpha$ term is given by

$$\cos^2\alpha = 1 - \frac{c^2}{c_b^2} \sin^2\alpha_b \left[1 - 2 \frac{(V_b - V)}{c_b} \sin\alpha_b + \ldots\right] \tag{3.65}$$

or as first approximations

$$\sin\alpha = \frac{c}{c_b} \sin\alpha_b \tag{3.66}$$

$$\cos\alpha = 1 - \frac{1}{2} \left(\frac{c}{c_b}\right)^2 \sin^2\alpha_b \tag{3.67}$$

Putnam et al. [16] used the same assumption as in Equation (3.63) and verified it in the laboratory and field. He found that the longshore current never exceeded the longshore component of the wave celerity.

Galvin [24] makes a special point to take exception with this assumption, and, thus, it is necessary to justify its use here. In his laboratory experiments, he found that the mean longshore velocity

often exceeded the component of the wave speed in the longshore direction. This was also found in a similar laboratory study by Brebner and Kamphuis (op. cit.). Galvin points out that this is because much of the water composing the breaking waves has been extracted from the surf zone and that this water already has a longshore velocity which is added to the breaking wave component.

This seeming discrepancy in experimental results is clarified by examining the kinematics of breaking waves. The waves broke by plunging in Galvin's experiments; whereas, in the experiments of Putnam et al., it is implied the waves broke by spilling. Iversen [62] conducted laboratory studies of breaking waves on various beach slopes. He found that the backwash velocity in spilling breakers was much less than in plunging breakers so that the fluid contribution to the spilling breaker is relatively less. Also, surf zones with spilling breakers are much wider with the backwash having much less effect. Galvin's argument does not apply to spilling breakers on flat beaches which derive little fluid from the surf zone at incipient breaking. Thus, the assumption given by Equation (3.63) appears to be valid for spilling waves.

Changes in the total water depth can now be solved by substituting Equations (2.39), (2.41), (3.60) and (3.67) into (3.59), resulting in

$$\frac{\partial}{\partial x}\frac{1}{8}\rho g\kappa^2 D^2\left[\left(1-\frac{\kappa^2}{8(1+\kappa)}\right)\left(1-\frac{1}{2}\frac{D}{D_b}\sin^2\alpha_b\right)+\frac{1}{2}\right] = -\rho g D\frac{\partial}{\partial x}(D-h) \tag{3.68}$$

Expanding and combining terms, this equation can be easily integrated to give

$$\left[3\frac{\kappa^2}{8}\left(1-\frac{\kappa^2}{12(1+\kappa)}\right)+1\right]D-\frac{3}{8}\kappa^2\left(1-\frac{\kappa^2}{8(1+\kappa)}\right)\frac{\sin^2\alpha_b}{2D_b}D^2 = h + \text{constant} \tag{3.69}$$

Imposing the boundary condition that $D_b = h_b + \bar{\eta}_b$ at the edge of the surf zone, and using the equivalent approximate form of Equation (3.66),

$$\sin^2\alpha = \sin^2\alpha_b \frac{D}{D_b} \tag{3.70}$$

The total depth variation is

$$D = \frac{(1 - K(\alpha))}{(1 - K(\alpha_b))} D_b + (1 - K(\alpha)) (h - h_b) \tag{3.71}$$

where $K(\alpha)$ is a function of the local wave angle such that

$$K(\alpha) = \frac{1}{1 + \frac{8}{3\kappa^2} \frac{1}{\left[1 - \frac{\kappa^2}{12(1+\kappa)} - \left(1 - \frac{\kappa^2}{8(1+\kappa)}\right) \frac{\sin^2\alpha}{2}\right]}} \tag{3.72}$$

This form corresponds to an earlier formulation by Longuet-Higgins and Stewart [54]. It should be noted that this equation is applicable to an arbitrary bottom profile and that the wave set-up depends only on the local still water depth. The only restriction on the bottom profile is that it monotonically decreases shoreward in order that the assumption of spilling breakers be fulfilled across the surf zone, that is, that the wave height must always be a function of the local depth.

The effect of oblique wave incidence on the set-up can be investigated most simply by assuming a constant sloping beach. Figure 8 shows the relative changes in the local wave set-up for various angles of wave incidence. It can be seen that the wave set-up decreases for increasing angles, as would be expected.

For all practical angles of wave incidence, as shown in Figure 8, the change in the total local depth is less than 2 per cent. The set-up is important in this analysis for calculations of the wave height. Recalling that the wave height is assumed proportional to the total depth,

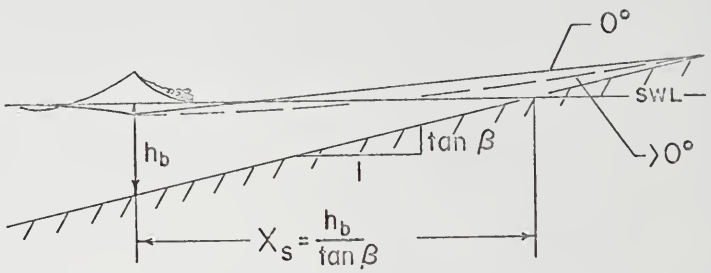

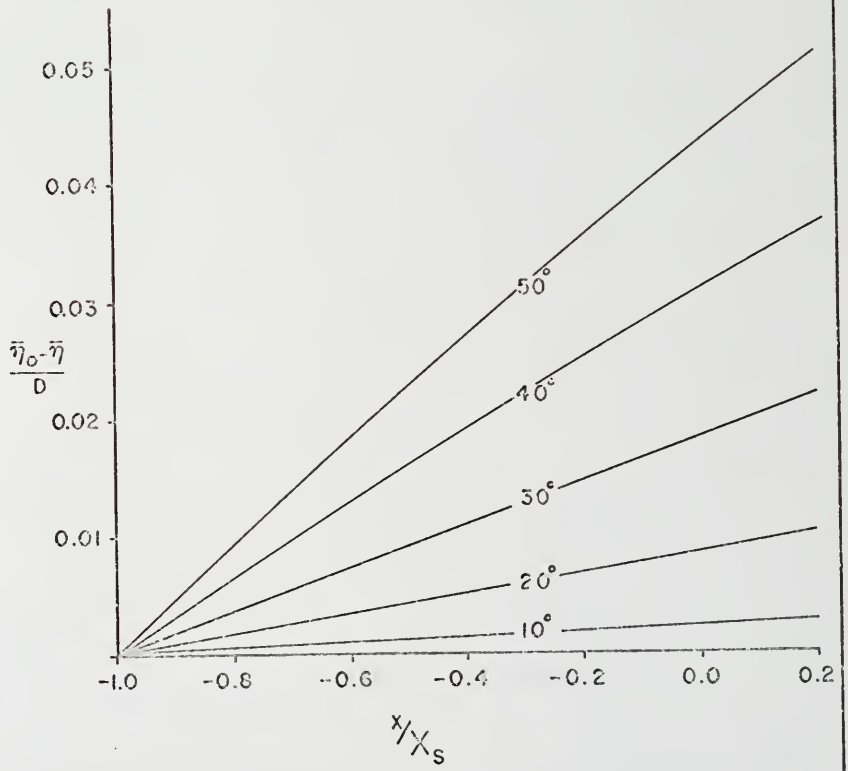

Figure 8. Relative Changes in Wave Set-up inside the Surf Zone as a Function of the Incident Wave Angle

an error of less than 2 per cent in the wave height calculations is introduced by neglecting the angle of wave incidence. This approximation is certainly within the accuracy of the basic assumption that the wave height is proportional to the depth. Hence, for purposes of this analysis, the effect of oblique wave incidence on the wave set-up inside the surf zone will be neglected to simplify calculations. The equation for wave set-up then reduces to the case of waves normal to the beach. This is essentially the same solution obtained by Longuet-Higgins and Stewart (ibid.) where they considered the case of waves normal to a beach only. The difference in the solution given here is due to the inclusion of the momentum flux of the mean wave motion in the radiation stress term.

The depth inside the surf zone simplifies to

$$D = (1 - K)\, h + Kh_b + \bar{\eta}_b \tag{3.73}$$

and the wave set-up inside the surf zone is given by

$$\bar{\eta} = K(\alpha)\, (h_b - h) + \bar{\eta}_b \tag{3.74}$$

where the set-down at the breaker line $\bar{\eta}_b$ can be determined from Equation (3.26).

Bowen et al. [55] conducted laboratory studies to verify the theory predicting the changes in mean sea level for waves normally incident to the shoreline. In his experiments, a plane beach was used with a slope of 1:12. The breaking waves were of the plunging type, and, after breaking, the residual energy propagated shoreward in the form of a bore.

Well outside the breaking point, the prediction of the set-down by Equation (3.26) and the measured values compared very well. Figure 9 shows a typical observation from Bowen's experiments of the wave height envelope and mean water level.

Just outside the breaking point, the assumptions of linear theory are no longer justified, and the measured values of the set-down are less than predicted by the theory. Between where the waves start to break and the plunging point, the set-down was found experimentally to be rather constant. The measurements showed that inside the plunging point the wave height is very nearly proportional to the mean water depth. This supports the basic assumption of this analysis that $H = \kappa D$. As Bowen points out, it is surprising that the set-up is so well described by theory using the approximation for the wave momentum flux since linear theory is essentially assumed valid inside the surf zone.

2. Velocity Distribution--Constant Sloping Bottom

With the mean water profile and energy distribution specified, the variation of the longshore current across the surf zone can be determined. The y-momentum equation inside the surf zone can be written similarly to that outside the surf zone.

$$\frac{\partial S_{xy}}{\partial x} = R_y \qquad (3.75)$$

Again, recall that the net mass transport perpendicular to the beach is zero, and that there is no y-dependence. This equation says that the change in the momentum flux parallel to the shore due to the waves is balanced by the force required to overcome bottom friction and internal lateral shear stresses which must maintain a longshore current. A loss

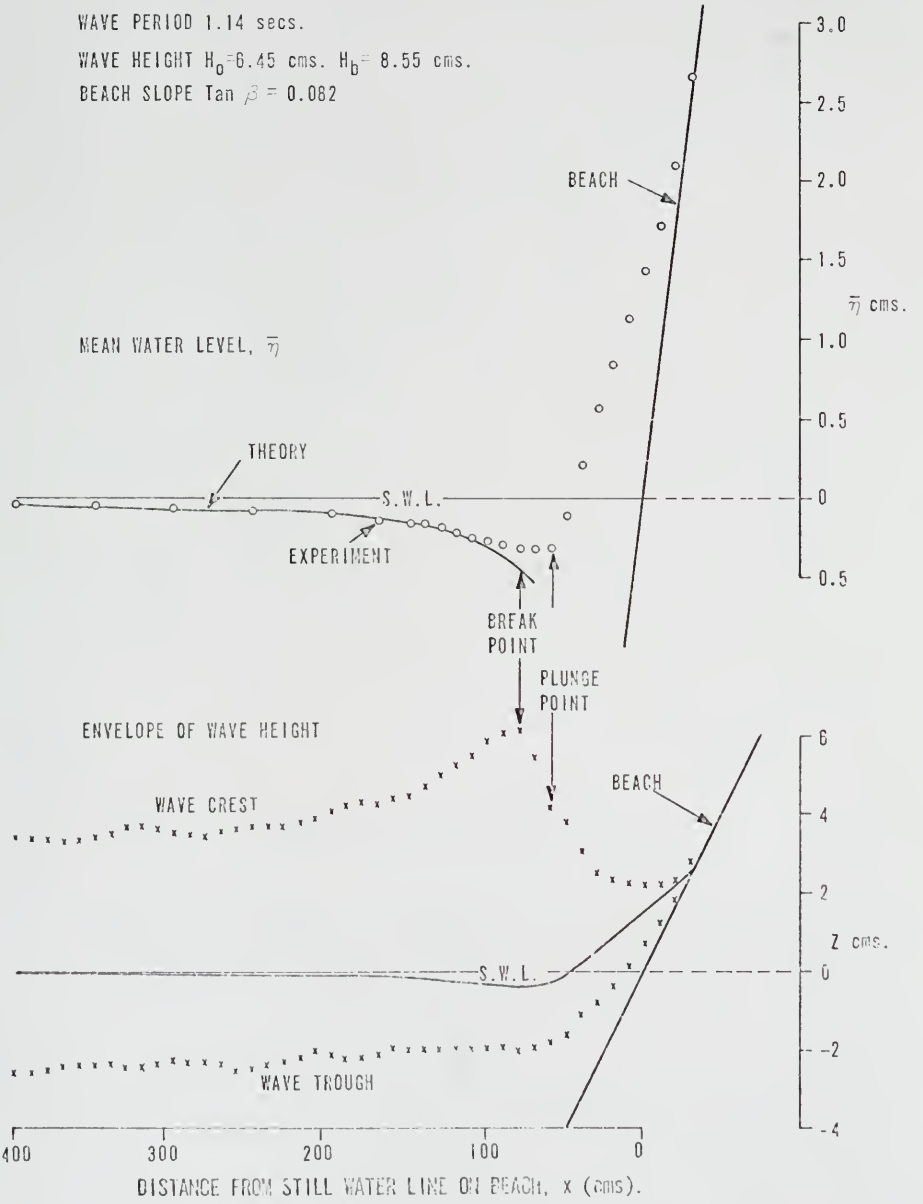

Figure 9. Laboratory Measurements of Wave Set-down and Set-up (after Bowen [55])

of momentum due to potential energy decay across the zone is also implied.

It is assumed that the changes in momentum flux are balanced solely by the bottom shear stress parallel to shore, $R_y = -\tau_{hy}$. Substituting for S_{xy} from Equation (3.12) gives

$$\frac{\partial}{\partial x}\left[E \sin\alpha \cos\alpha - \frac{E^2}{\rho c^2 D} \cos\alpha \sin\alpha\right] = -\tau_{hy} \tag{3.76}$$

The height, celerity, refracted angle of the waves, and, hence, changes in momentum flux inside the surf zone can be expressed in terms of the local depth of water. Substituting Equations (2.38), (2.41), (3.66), and (3.67) into Equation (3.76) gives

$$\frac{\partial}{\partial x}\left[\frac{1}{8}\rho g \kappa^2 \left(1 - \frac{1}{8}\frac{\kappa^2}{(1+\kappa)}\frac{\sin\alpha_b}{\sqrt{D_b}} D^{5/2} \left(1 - \frac{D}{D_b}\frac{\sin^2\alpha_b}{2}\right)\right)\right] = \tau_{hy} \tag{3.77}$$

which can be written

$$AD^{3/2}\left(1 - 0.7\frac{D}{D_b}\sin^2\alpha_b\right)\frac{\partial D}{\partial x} = -\tau_{hy} \tag{3.78}$$

where

$$A = \frac{5}{16}\rho g \kappa^2 \left(1 - \frac{\kappa^2}{8(1+\kappa)}\right)\frac{\sin\alpha_b}{\sqrt{D_b}}$$

This is a general equation expressing the changes in momentum flux across the surf zone in terms of the total local depth of water. Included in the formulation is the set-up of water and the effects of wave refraction inside the surf zone. This equation is subject to the restriction that the waves be described as spilling breakers, and, hence, the depth continuously decreases shoreward from the breaker line. Thus, the momentum flux decreases monotonically inside the surf zone since both the energy and wave angle decrease with decreasing depth.

It will be assumed that the bottom shear stress is described by Equation (3.39) such that

$$\tau_{hy} = \rho \frac{f_y}{2} V^2 \tag{3.79}$$

The friction must be specified in order to utilize Equation (3.79). Recalling Equation (3.43), where the time mean water particle velocity over half a wave cycle just above the boundary layer inside the surf zone is given,

$$\left|\overline{u}_{wh}\right| = \frac{2}{\pi}\left(\frac{H}{2}\frac{g}{c}\right) = \frac{\kappa}{\pi}\sqrt{\frac{gD}{1+\kappa}} \tag{3.80}$$

such that the time mean friction factor can be expressed

$$f_y = \frac{\kappa}{\pi}\sqrt{\frac{gD}{1+\kappa}}\frac{f_w}{V} \tag{3.81}$$

Solving for the velocity by substituting Equations (3.80) and (3.81) into (3.78), a general expression for the velocity distribution for an arbitrary bottom profile is

$$V(D) = -\frac{A'}{f_w} c_b \sin\alpha_b \frac{D}{D_b}\left(1 - 0.7\frac{D}{D_b}\sin^2\alpha_b\right)\frac{\partial D}{\partial x} \tag{3.82}$$

where

$$A' = \frac{5}{8}\pi\kappa\left(1 - \frac{\kappa^2}{8(1+\kappa)}\right)$$

For the case of the uniform sloping bottom, Equation (3.82) can be simplified by making a simple transformation of the independent variable. The equation for the still water depth, $h = -x\tan\beta$, can be substituted into Equation (3.73).

$$D = Kh_b + \overline{\eta}_b - (1 - K)\, x \tan\beta \tag{3.83}$$

so that

$$dx = \frac{-1}{(1 - K)\ \tan\beta}\, dD \tag{3.84}$$

The longshore velocity distribution across the surf zone assumes the form

$$V(D) = \frac{A''}{f_w} c_b \sin\alpha_b \tan\beta \frac{D}{D_b} \left(1 - 0.7 \frac{D}{D_b} \sin^2\alpha_b\right) \tag{3.85}$$

where f_w is given by Equation (3.30), and

$$A'' = \frac{5}{8} \pi (1 - K)\ \kappa \left(1 - \frac{\kappa^2}{8(1 + \kappa)}\right)$$

This solution, assuming a plane beach, shows that the maximum velocity always occurs at the maximum depth--the edge of the surf zone, and that the velocity goes to zero at the beach ($D = 0$).

The predicted velocity distribution (Equation (3.85) is compared to a measured velocity profile obtained by Galvin and Eagleson (op. cit.) in the laboratory in Figure 10. The velocity distribution outside the surf zone, as predicted by Equation (3.57), is also shown. As can be seen, the velocity distributions do not compare very well. One reason for this discrepancy, as mentioned before, is that the waves in the laboratory do not generally fulfill the spilling breaker criteria due to the relatively steeper beaches (1:10, in this case). Other reasons, and more reasonable approximations, will be discussed subsequently.

The set-down and set-up of the water surface, as predicted by Equations (3.26) and (3.74), respectively, are also shown. The experimental and predicted results, in this case, compare quite favorably.

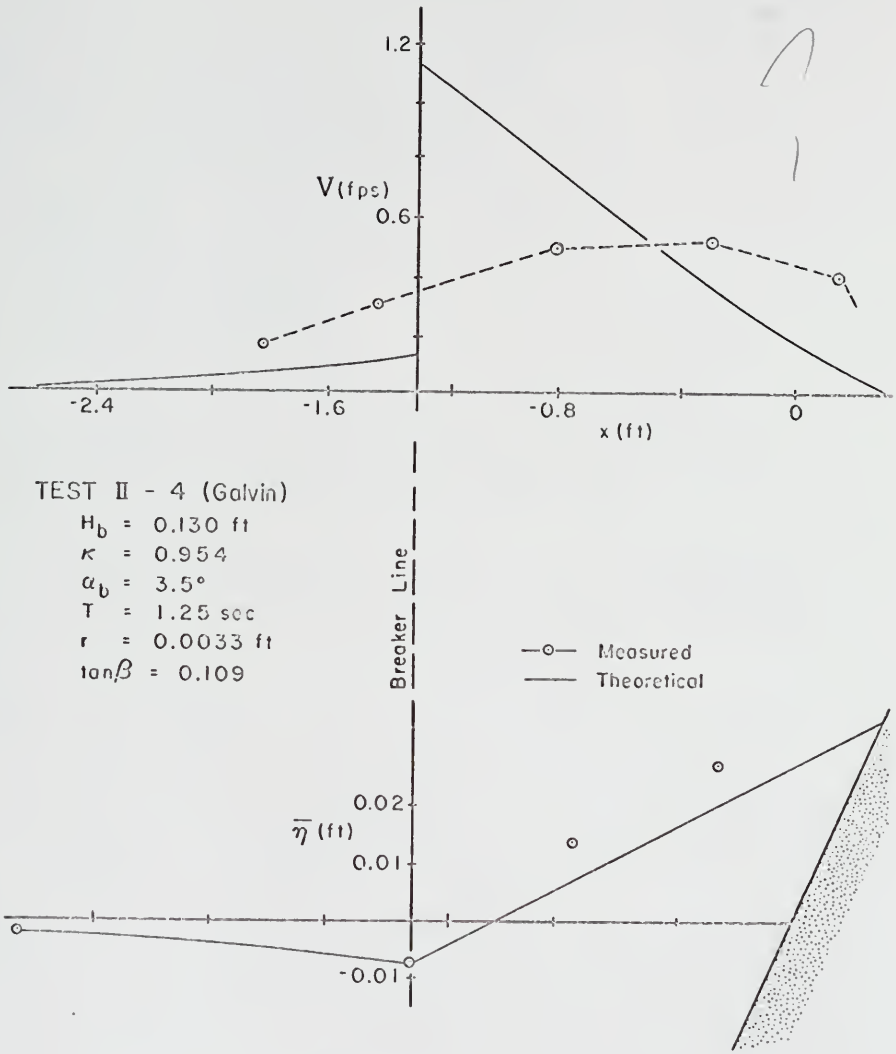

Figure 10. Longshore Velocity Distribution across the Surf Zone for a Constant Sloping Beach

3. Mean Longshore Current--Constant Sloping Bottom

The mean longshore current can be found by integrating Equation (3.85) across the width of the surf zone, $X_s = D_b/(1 - K)\tan\beta$, corresponding to $D = D_b$ to $D = 0$

$$\overline{V} = \frac{1}{X_s} \int_{D_b}^{0} \frac{-1}{(1 - K)\tan\beta} V dD \tag{3.86}$$

It is necessary to make an assumption concerning the friction factor f_w in order to integrate Equation (3.86). An investigation into the nature of Equation (3.30) shows that $f_w \to \infty$ as $D \to 0$ so that a spatial mean of f_w across the surf zone cannot be determined. Numerical calculations of f_w across the surf zone for a wide range of situations showed that, if only the region between the breaker line and $x = 0$ is considered, the choice of f_w calculated at $D = D_b/2$ is very close to a mean value for the surf zone. Choosing f_w as a constant, in this manner, Equation (3.86) can be integrated, and the mean longshore current velocity is given by

$$\overline{V} = \frac{B}{f_w} \sin\alpha_b \tan\beta \, (gH_b)^{\frac{1}{2}} (1 - 0.467 \sin^2\alpha_b) \tag{3.87}$$

where

$$B = \frac{5}{16} \pi \sqrt{\kappa(1 + \kappa)} \, (1 - K) \, \left(1 - \frac{\kappa^2}{8(1 + \kappa)}\right) = 0.71, \; \kappa = 0.78$$

This equation is tested using data from several sources, both in the laboratory and field, as shown in Figure 11. Only experiments using sand bottoms have been included in the comparison so that the determination of the friction factor, using the formulation presented, can be rationally specified. A value for the ripple height of 0.05 feet

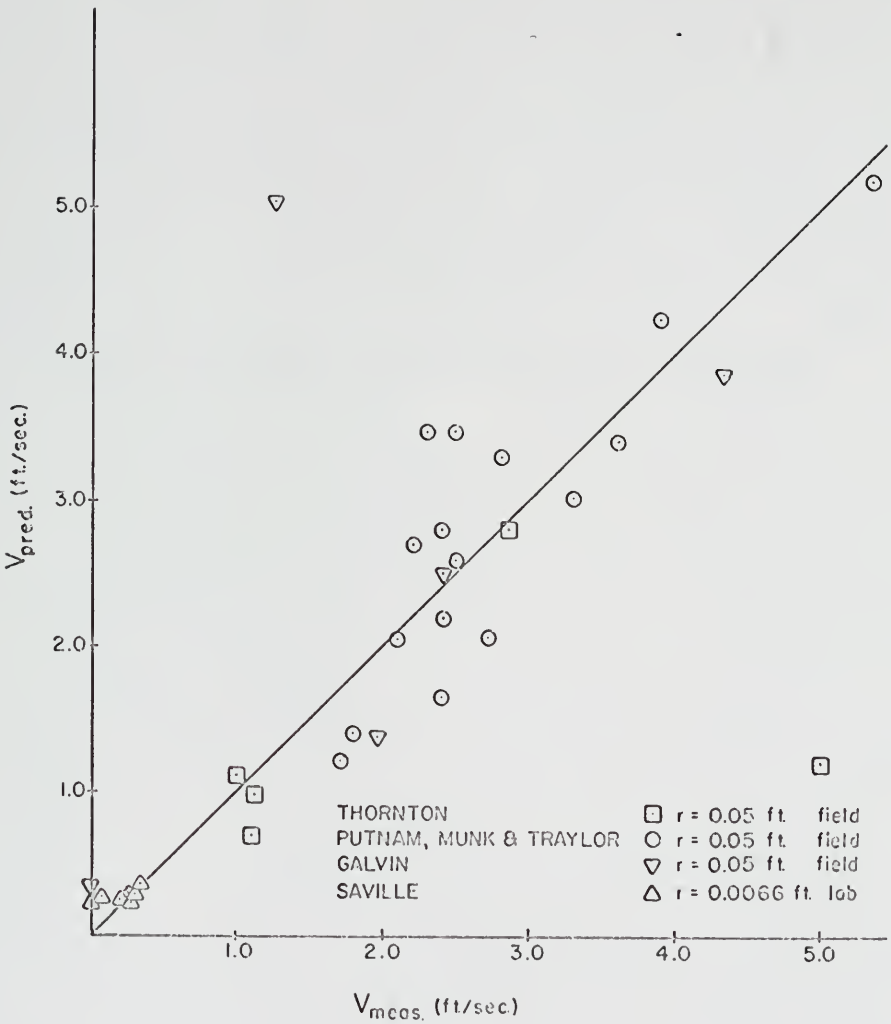

Figure 11. Comparison of Predicted and Measured Mean Longshore Currents

for inside the surf zone was chosen as representative for all the field tests. This value appears reasonable considering the measured ripple heights obtained by Inman [57]. Laboratory data obtained by Saville, using a movable bed model, is also included.

4. Longshore Current--General Profile

Beach profiles in nature have variable slopes and are not plane as has been previously considered in this presentation. Measurements of equilibrium beaches show that the foreshore slope is usually considerably steeper, 10-30 degrees, compared to the bottom slope offshore which ranges roughly from 1-10 degrees. A more realistic approach to the problem then is to consider a more general bottom profile. If the depth can be related to the distance offshore, the relationship can be inserted into the equations already derived, and a more general velocity distribution determined.

Bruun [63] examined many Danish and California beach profiles and found that they could be generalized by an n^{th} degree parabola. He found that the equation giving the best fit was of the form

$$h = B|x|^{2/3} \tag{3.88}$$

where B is a constant of proportionality. A set-up of the mean water level will be allowed in the present analysis so that a more general equation has to be used to avoid the singularity at the intersection of the water line and beach. Translating the axis by increments of δx and δh, the bottom profile can be expressed

$$h + \delta h = B|x + \delta x|^{1/n} \tag{3.89}$$

The total depth of water, including the set-up, is found by substituting the still water depth h into Equation (3.73)

$$D = Kh_b + \bar{\eta}_b + (1 - K)\ [B(x + \delta x)^{1/n} - \delta h] \qquad (3.90)$$

This formulation allows three degrees of freedom in choosing the desired profile δh or δx, B, and n.

Having specified the bottom profile, the velocity distribution can be found by substituting into Equation (3.82). A predicted velocity profile is shown in Figure 12 compared to field data obtained by Ingle [5]. This particular profile was chosen because of the regularity of the bottom. A parabola, giving the best fit, is used to establish the bottom profile, and the velocity distribution is predicted from this profile. The maximum velocity no longer occurs only at the breaker line, but can occur somewhere between the breaker line and the beach. It is noted that after the velocity abruptly changes at the breaker line, it is almost constant across the surf zone. This is qualitatively more in agreement with observations.

An almost exact fit, describing the bottom profile, can be obtained using a higher order polynomial equation. It was found that a fourth degree polynomial very closely represented the profile shown in Figure 12; no difference in the measured and fitted curve can be discerned in the line drawings. The corresponding velocity profile was calculated using Equation (3.82), and is also shown. An excellent correspondence to the measured velocity distribution is found (for this particular case, anyway) although it can be seen that the predicted velocity distribution is very sensitive to small changes in the bottom profile. This was particularly noted in other cases in which the bottom profiles were more irregular.

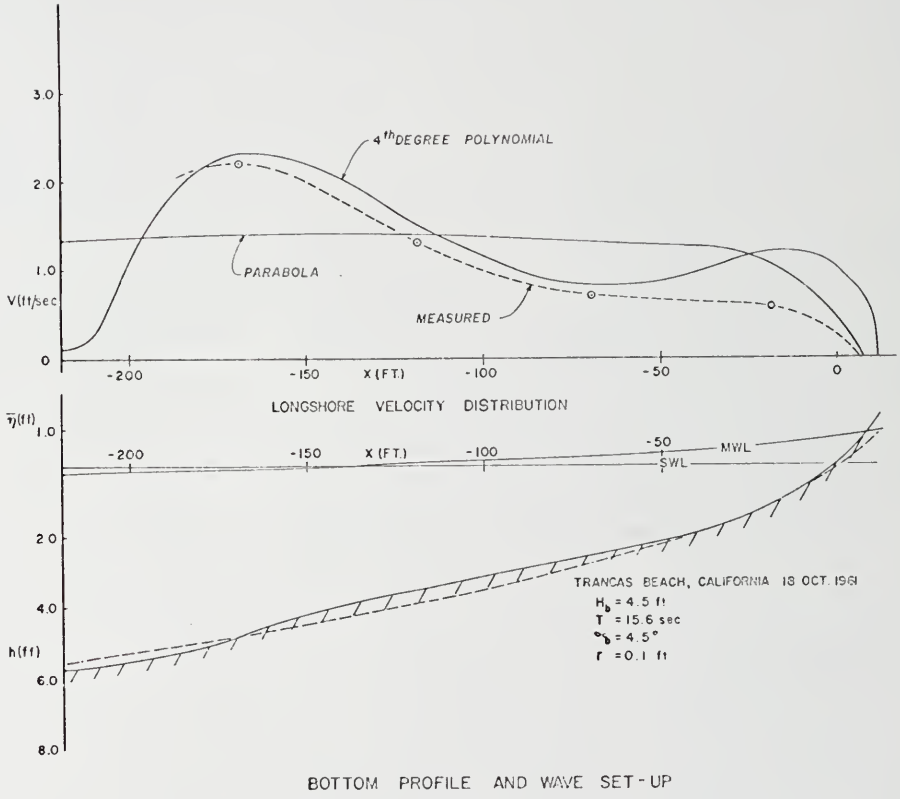

Figure 12. Longshore Velocity Distribution across the Surf Zone for a Beach Described by an n^{th} Degree Polynomial

The reason for this is that the differential water columns being considered are mathematically uncoupled from adjacent water columns by the assumption that the only shear acting is on the bed.

Figure 13 shows a comparison with the velocities, predicted in the above manner, to the measured velocity at various relative distances from the breaker line, $x = 0$, across the surf zone to the intersection of the mean water line with the beach, $x = X_s$. The measured field data were taken by Ingle [5] on various Southern California beaches. The velocity distributions have been adjusted by changing the measured angle of wave incidence so that the measured and predicted velocities are equal at the midpoint of the surf zone. This was done to present an easier interpretation of how well the theory predicts the distribution across the surf zone, but not necessarily the absolute value. The incident wave angle was chosen to adjust because this is the most difficult parameter to measure accurately and, hence, most subject to error. As can be seen, the velocities near the breaker line are generally over predicted, and the velocities near the still water line are predicted smaller than measured. This can be attributed, at least partially, to the fact that internal shear stresses have been neglected in this derivation.

5. Longshore Current Distribution--Including Internal Shear Stress and Bottom Friction

A more complete description of the hydrodynamics inside the surf zone would include vertical shear between adjacent infinitesimal control volumes (see Figure 4). A discontinuity was noted at the breaker line in the previous models. Adjacent control volumes are coupled by including shear stresses on the vertical planes so that the distribution of velocity across the surf zone is continuous.

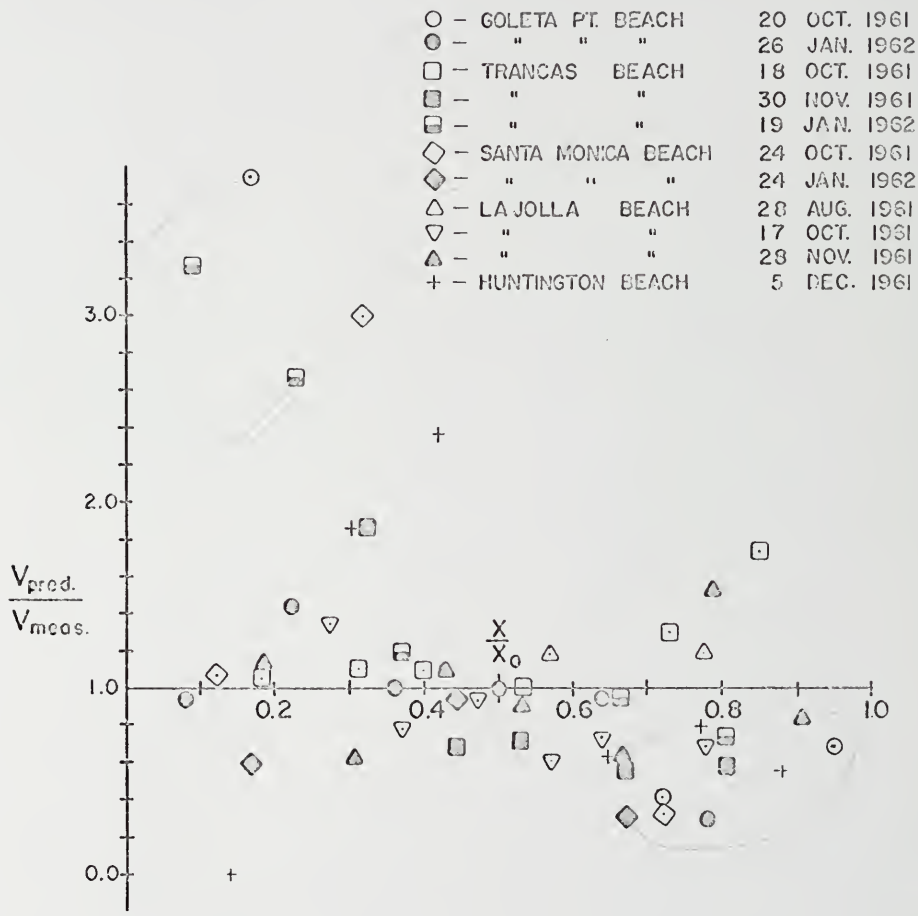

Figure 13. Comparison of Predicted and Measured Velocity Distributions for Natural Beaches

Considerable success has been achieved using Prandtl's mixing length hypothesis for specific problems. This concept will be utilized to relate the internal shear stresses to the mean flow. The expression for the internal shear stress can be given in terms of the mean turbulent Reynolds stress

$$\tau_{xy} = - \rho \overline{u'v'} \tag{3.91}$$

The variation of the turbulent velocity component in the y-direction is given in accordance with Prandtl's hypothesis by

$$v' = \ell' \frac{\partial V}{\partial x} \tag{3.92}$$

where ℓ' denotes a mixing length which can fluctuate with time. Equation (3.91) gives

$$\tau_{xy} = - \rho \overline{u'\ell'} \frac{\partial V}{\partial x} \tag{3.93}$$

This formulation can be compared to a "Boussinesq" approach in which it is assumed

$$\tau_{xy} = \rho \varepsilon_v \frac{\partial V}{\partial x} \tag{3.94}$$

where ε_v is the kinematic eddy viscosity. Combining Equations (3.93) and (3.94) results in an expression for ε_v

$$\varepsilon_v = - \overline{u'\ell'} \tag{3.95}$$

For the case of superposed waves and currents, it is natural to consider the length over which momentum is transferred as equivalent to the water particle excursion due to the wave motion and the velocity fluctuation u' equal to that of the water particles in the waves.

Because u' and ℓ' are in quadrature, it is necessary to assume

$$\overline{u'\ell'} = |\overline{u'\ell'}| \tag{3.96}$$

in order to obtain a non-zero value. The mixing length ℓ' can be interpreted as a measure of the turbulent scale and u' as a measure of turbulent intensity. This interpretation is not unreasonable physically. Examination of actual energy spectra of turbulence occurring in the surf zone shows that most of the fluctuating energy is associated with the waves.

The kinematic eddy viscosity can be evaluated by recalling Equations (2.29) and (3.31). It will be assumed for simplicity that shallow water wave conditions apply, so that

$$\varepsilon_v = \frac{H^2}{8\pi^2} \frac{gT}{h} \cos^2\alpha \tag{3.97}$$

The general shear stress term can be determined by referring to Equation (2.19). Evaluating the internal shear stress term first by substituting Equation (3.94) gives

$$\overline{\int_{-h}^{\eta} \frac{\partial \tau_{xy}}{\partial x} dz} = \int_{-h}^{\eta} \rho \frac{\partial}{\partial x} \left(\varepsilon_v \frac{\partial V}{\partial x}\right) dz = \rho D \frac{\partial}{\partial x} \left(\varepsilon_v \frac{\partial V}{\partial x}\right) \tag{3.98}$$

where ε_v and V are independent of z. The bottom shear stress can be determined by substituting Equations (3.80) and (3.81) into Equation (3.79)

$$\tau_{hy} = \frac{\rho f_y}{2} V^2 = \rho \frac{f_w}{2} |\overline{u_{wh}}| V \tag{3.99}$$

where the shallow water wave assumption gives

$$\tau_{hy} = \rho f_w \frac{H}{2\pi} \frac{g}{c} V \tag{3.100}$$

The total resistance term, including internal and bottom shear stresses, is given by

$$R_y = \rho D \frac{\partial}{\partial x} \left(\varepsilon_v \frac{dV}{dx}\right) - \rho \frac{f_w}{2\pi} \frac{g}{c} H V \tag{3.101}$$

The variation of the longshore current inside the surf zone can be solved by equating the changes in excess wave momentum to the resistance forces as given by the general Equation (3.78)

$$AD^{3/2} \left(1 - 0.7 \frac{D}{D_b} \sin^2\alpha_b\right) \frac{\partial D}{\partial x} = \rho D \frac{\partial}{\partial x} \left(\varepsilon_v \frac{\partial V}{\partial x}\right) - \frac{\rho\kappa}{2\pi} f_w \sqrt{\frac{gD}{(1 + \kappa)}}\, V \tag{3.102}$$

This development is similar to that by Bowen [19] in an investigation limited to a plane beach in which he assumes linear bottom friction and constant kinematic eddy viscosity in order to obtain an analytical solution.

The inclusion of the kinematic eddy viscosity and bottom friction requires Equation (3.102) to be solved numerically. Boundary conditions imposed on the problem inside the surf zone are: for $D = 0$, $V = 0$ corresponding to conditions at the intersection of the water line and the beach; and for $D = D_b$, $V = V_b$ corresponding to conditions at the breaker line.

A similar solution can be sought outside the surf zone where it is now assumed that the driving force for the currents outside the surf zone is zero--the changes in the momentum flux directed parallel to shore are zero. This is in accordance with the formulation in Section B.3 where it is assumed that there were no energy losses as the waves propagated shoreward outside the surf zone. The y-momentum Equation (3.102) reduces to

$$D \frac{\partial}{\partial x} (\varepsilon_v \frac{\partial V}{\partial x}) - \frac{f_w}{2\pi} \frac{g}{c} H V = 0 \qquad (3.103)$$

where now the force driving the currents is due to lateral momentum flux resulting in a coupling of the adjacent vertical faces of the differential water column across the breaker line. This is to say that currents outside the surf zone are being driven by the longshore currents inside the surf zone due to coupling across the breaker line.

The boundary conditions imposed on the formulation outside the surf zone are that the velocity approaches zero far away from the breaker line ($D \to \infty$) and that the velocities and velocity gradients inside and outside the surf zone match at the breaker line.

The laboratory results of Galvin, given previously in Figure 10, are used to test the predictive equations. The only parameter that is necessary to be chosen is the roughness in order to utilize the predictive equations. A value of r = 0.0033 feet (1 mm) was chosen for the concrete beach, which is a reasonable value. The kinematic eddy viscosity is completely specified by the kinematics of the flow field. Figure 14 shows the velocity distribution including both internal and bottom shear stresses. This distribution can be compared to the distribution in Figure 10 which only accounted for bottom friction. A more reasonable velocity distribution is predicted, particularly, for a plane beach.

The distributions of the kinematic eddy viscosity and friction factor are also shown in Figure 14. The kinematic eddy viscosity is a maximum at the point of breaking, where the maximum momentum exchange would be expected to take place, and decreases to zero at the shoreline. The friction factor varies slowly except near the beach where f_w increases

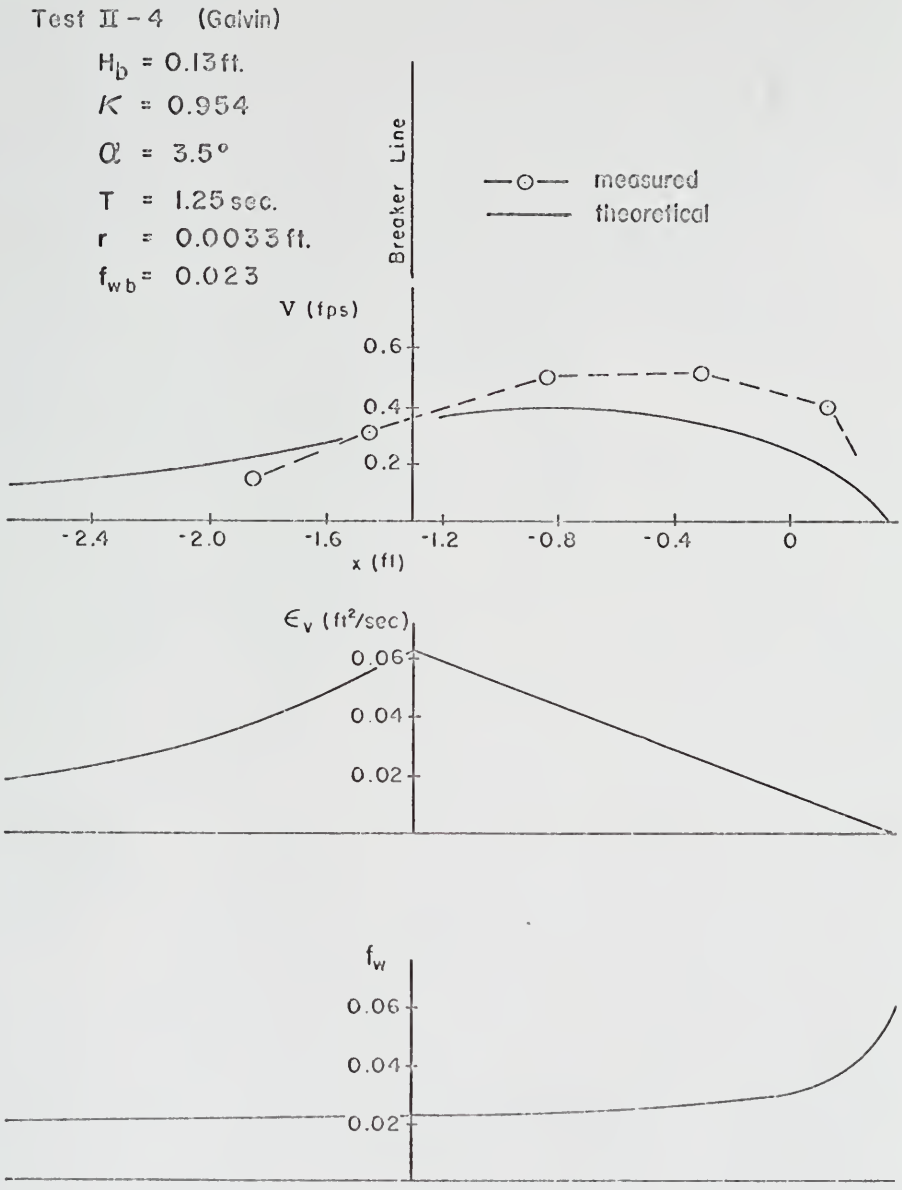

Figure 14. Velocity Distribution across the Surf Zone for Low Velocities Including Internal and Bottom Shear Stresses

very rapidly and approaches infinity at the intersection of the beach and the still water line.

Two other cases are presented in Figure 15 for more severe wave conditions. The friction factor at the breaker line f_{wb} is given; it varies only slightly for the three cases. The kinematic eddy viscosity $\varepsilon_{v_{max}}$ is also given and is seen to be much more sensitive to differences in wave conditions than the friction factor. The velocity is predicted too large for Test II-3 and is probably a consequence of the relatively large wave height. Surprisingly good correlation is found considering that the only parameter chosen is the roughness in order to completely specify the longshore velocity distribution.

The same equations are applied to the field data presented previously in Figure 12. Information concerning the bathymetry outside the surf zone is lacking so a bottom slope of 0.01 is assumed. The velocity distributions, both including and not including the internal shear stresses, are shown in Figure 16. The kinematic eddy viscosity and friction factor distributions are also shown and are similar to those found for the laboratory beaches. The friction factors for the laboratory and field are of the same order of magnitude, owing to the fact that the friction factor is not only dependent on the roughness but also the wave characteristics. The kinematic eddy viscosity for field conditions is several orders of magnitude greater than the value found for laboratory conditions. The predicted values for the kinematic eddy viscosity for the field appear possibly too large and may tend to overly smooth the velocity distribution. More comparison of theory with field data needs to be obtained to better test the formulation before any definite conclusions can be made; this constitutes an area for future endeavor.

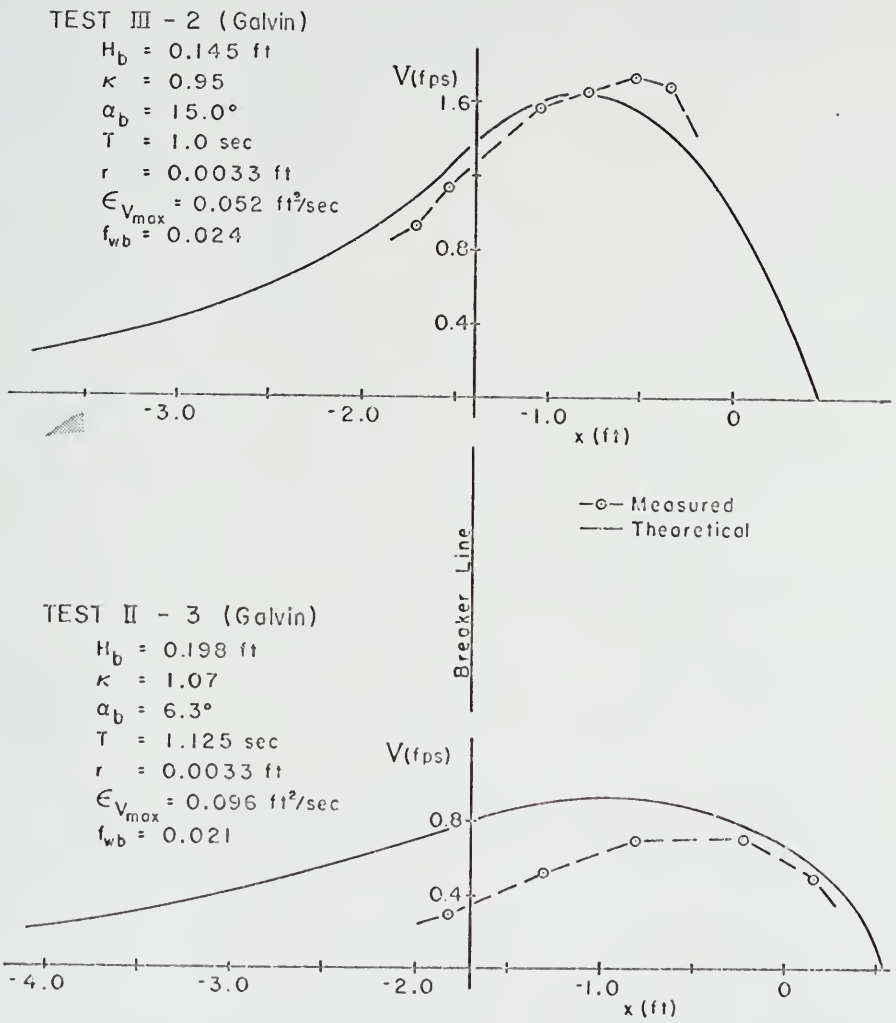

Figure 15. Velocity Distribution across the Surf Zone for Moderate Wave Conditions Including Internal and Bottom Shear Stresses

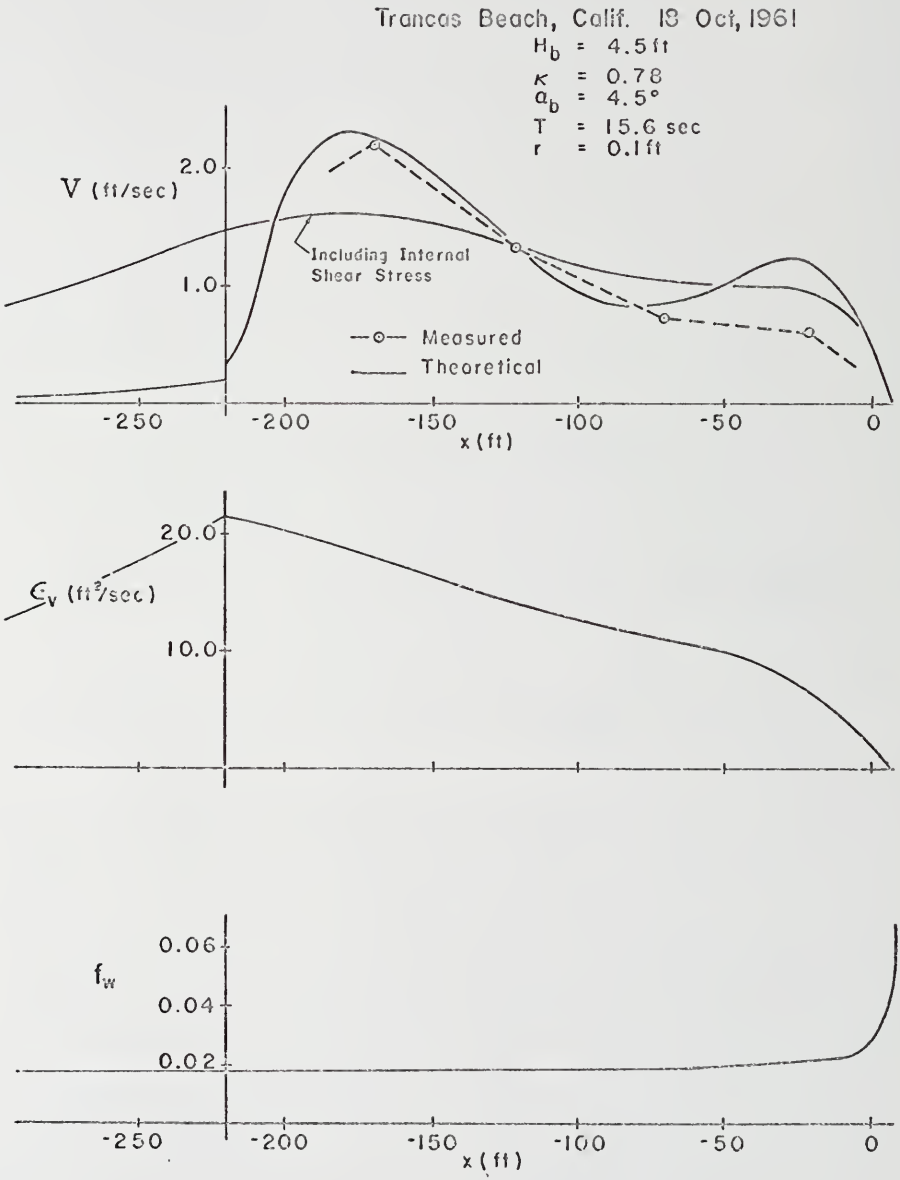

Figure 16. Velocity Distribution across the Surf Zone for Field Conditions Including Internal and Bottom Shear Stresses

The efforts to include the internal shear stresses were developed in the latter stages of this investigation and are not included in the sediment transport formulation. This restriction is not severe for natural beaches with movable beds. Peaks in the velocity distribution also indicate points of higher bottom shear stress. The bed will tend to readjust itself to minimize the shear acting on the bottom. This will result in a smoother velocity profile. Hence, omitting the coupling effect of the internal shear stresses is not a limitation on the resulting equations for prototype conditions which generally have movable beds.

CHAPTER IV

LITTORAL TRANSPORT--ENERGY PRINCIPLE

A. Introduction

An energy principle approach is utilized to relate the work expended in transporting a quantity of sand to the energy available for transporting purposes. The development follows basically that of Bagnold (op. cit.) with some modifications to better suit the assumed conditions. The same basic principles and physical laws applicable to the unidirectional flow problem also pertain to the sediment transport due to combined wave and current action. Thus, many of the concepts of sediment transport in rivers and streams will be utilized. The inherent advantage of an energy approach is the simplicity and ease of physical interpretation. This type of approach also has had the most success for engineering applications in the oceans. However, the use of the word "success" in reference to predictability of sediment transport formulas must be qualified. Accuracy within 100 per cent is good for the more predictable river problem. For the more complicated sediment transport problem in the littoral zone, order of magnitude approximations are acceptable at present.

Both bed load and suspended load transport, due to combined wave and current action, are considered. The areas inside and outside the surf zone are discussed separately. Bagnold applied his analysis only to waves in deeper water, but the principle would be expected to be equally valid inside the surf zone.

B. Bed Load Transport

The work, or energy, required to move a certain quantity of sediment is certainly related to the weight of the sediment transported. Bagnold considers an idealized situation where bed load consists of a top layer of grains simultaneously (in the statistical sense) sliding over the bottom. Since the sediment is heavier than the fluid, the grains are pulled toward the bed by a gravity component normal to the bed surface. For sake of argument, it will be assumed that there is a demarcation plane between the moving and stationary grains. Equilibrium requires that there be a normal stress exerted across the plane equal to the gravity component of the mass of sediment. This implies the grains remain in contact with each other and that the lift forces are neglected. If the mass of the moving sediment along the bottom per unit area is m_h of density ρ_s, and the bed is inclined at an angle β, the normal stress then has the value

$$N_h = (1 - \frac{\rho}{\rho_s}) \, g m_h \cos\beta \qquad (4.1)$$

There must also exist a tangential stress equal to $(1 - \frac{\rho}{\rho_s}) \, g m_h \sin\beta$ due to the tangential component of gravity. It is assumed, in the problem being considered, that the bottom contours are straight and parallel so that the bed slope in the direction of net sand transport (parallel to the beach) is zero. It is further assumed that the slope of the beach is very small such that there is no net transversal (perpendicular to the beach) movement of sand. Hence, the slope of the beach will not affect the net sand transport and can be neglected. This is to say that the sand grains will maintain, on the average, the same relative position with respect to the bottom profile (distance offshore).

The moving sand results in shearing of the sediment grains over one another and over the bed surface. This sediment shearing stress is denoted by T_h. Also, there is a shearing of the inter-granular fluid τ_s due to the sediment movement. Bagnold found in experiments that, except for very low concentrations of bed load transport, the inter-granular fluid shear τ_s could be neglected relative to the shearing of the sediment particle interaction, $T_h >> \tau_s$.

For moving sediment, grain collisions simultaneously give rise to the dynamic grain stresses, T_h and N_h, which can be considered proportional to each other with the proportionality being a function of angle of collision. Bagnold likens this angle of collision to the angle of repose for static condition and considers it to be a friction factor f_h'. This coefficient must certainly be a function of the grain properties--the most important of which is the sand grain size. Constant transport conditions require tangential stress equilibrium at the bed surface. Hence, the stress acting on the bed, due to fluid flow, is equal to the resisting stress of the sand grains per unit area

$$\tau_F = T_h = (1 - \frac{\rho}{\rho_s}) \, g m_h \, f_h' \qquad (4.2)$$

where τ_F is the tangential stress required to maintain the bed load in motion due to the waves and currents. This is shown schematically in Figure 17. A local increase or decrease in this fluid shear stress at the bottom results in erosion or deposition, respectively.

Embodied in most of the sediment transport formulas for alluvial channels is the critical shear stress--defined as the shear stress at which incipient motion of the sand grains occurs. However, in or near the surf

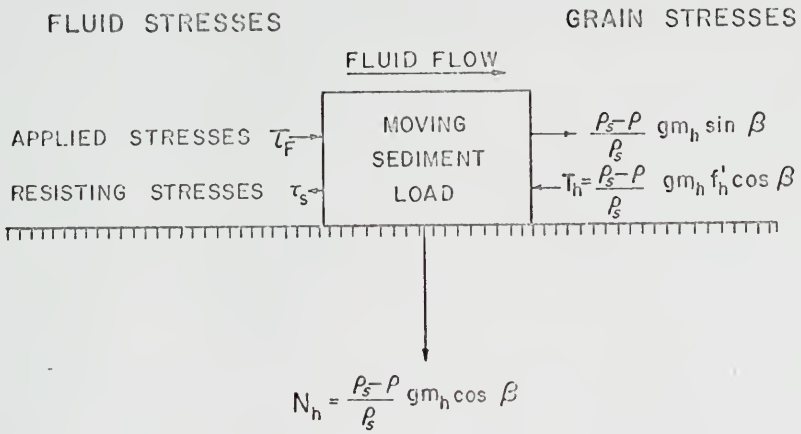

Figure 17. Schematic Diagram Representing Stresses Acting to Cause Bed Load Transport

zone, the critical shear stress assumes less importance since the instantaneous maximum shear stress of the waves greatly exceeds the critical shear stress--the sediments can be thought of as always in a state of to-and-fro motion. Rough calculation shows that the combined shear stress of waves and currents is several orders of magnitude greater than the critical shear stress predicted by Shield's formula which is applicable to uniform flow conditions. Therefore, the critical shear stress will not be incorporated into the oscillatory flow formulation.

The work per unit bed area per unit time required to overcome the resisting stress and maintain the bed load movement P_h is equal to

$$P_h = \tau_F \left|\vec{u}_{sh}\right| = (1 - \frac{\rho}{\rho_s})\, g m_h \left|\vec{u}_{sh}\right| f_h' \tag{4.3}$$

where $\left|\vec{u}_{sh}\right|$ is the velocity of the sand grains moving along the bed. The absolute value sign is necessary since the sand grains can oscillate back and forth in response to the wave motion.

The average power expended per unit bed area in transporting the bed load can be found by averaging in time Equation (4.3)

$$\overline{P} = (1 - \frac{\rho}{\rho_s})\, \overline{g m_h \left|\vec{u}_{sh}\right| f_h'} \tag{4.4}$$

The fluid motion responsible for the sediment transport is that of the waves and currents. The waves were assumed simple harmonic with zero mean motion, so that the net transport is due to the mean current in the longshore direction only. The net mass transport of the sediment per unit time per unit width perpendicular to the beach is defined

$$\overline{q}_h(x) = \overline{m}_h V_{sh} \tag{4.5}$$

where $\overline{m}_h = \overline{m}_h(x)$ is the average mass of moving sediment per unit area of the bed with the mean velocity, $V_{sh}(x)$, in the longshore direction.

The fluid power available to transport the bed load is measurable as the product of the bottom shear stress due to the motion of the fluid times a representative flow velocity. This available power is equal to the work done on the bottom. The bed shear stress must be considered composed of both the wave and mean current components. The action of this combined, or total, bed shear stress can be thought of as the loosening of the sand grains off the bed which are then available for transport by the mean current. The mean current is the longshore current alone as the wave motion has little or no net motion. The average power expended on the bed by the waves and currents was previously determined by Equation (3.49). The total power expended is due to the combined wave and current action.

The mean work done in transporting the bed load and the available power are assumed proportional to each other. This implies that the work done in moving the sand grains is proportional to the frictional energy dissipated on the bottom. Outside the surf zone, there is normally little turbulent energy dissipated. Provided percolation can be neglected, the frictional energy dissipated on the bottom represents most of the energy dissipated. The reduction in wave energy, measurable as a decrease in wave height, is then indicative of the energy spent in sediment transport outside the surf zone. In this case, the available power for sediment transport would be proportional to the total change in energy flux.

The proportionality factor will be denoted e_h and can be considered equivalent to a measure of the transporting efficiency of the available

power. Assuming only bed load transport, this leads to the expression

$$\overline{q}_h \left(1 - \frac{\rho}{\rho_s}\right) g f_h' \frac{|\overline{u}_{sh}|}{\overline{V}_{sh}} = e_h |\overline{u_{wh} \tau_h}| \tag{4.6}$$

For transport of sand in the surf zone, the coefficient e_h will certainly be a function of the manner in which the waves break--just as the wave-induced currents inside the surf zone.

The actual mean velocities of the sand grains are very difficult to measure. The mean sand grain velocities must be related to more measurable quantities in order to make Equation (4.6) workable. It is assumed, as a first approximation, that the mean velocity of the moving sand grains is proportional to the mean shear velocity in the direction of the sand particle motion. The mean shear velocity is defined

$$|\overline{u_*}| = \sqrt{\frac{|\overline{\tau}_h|}{\rho}} \tag{4.7}$$

The ratio of the mean particle velocities is then given by

$$\frac{|\overline{u}_{sh}|}{\overline{V}_{sh}} = b \left| \frac{\overline{\tau}_h}{\overline{\tau}_{hy}} \right|^{\frac{1}{2}} \tag{4.8}$$

where b is a constant of proportionality. The ratio of the sand velocities can be related to the fluid velocities by recalling Equations (3.39) and (3.45) for the shear stress in the direction of mean motion and the total bottom shear stress, respectively.

$$\frac{|\overline{u}_{sh}|}{\overline{V}_{sh}} = b \sqrt{\frac{f_w}{f_y}} \frac{|\overline{u_w}|}{\overline{V}} \tag{4.9}$$

It can be seen from Equations (3.36) and (3.37) that the friction factors are related to mean water particle velocities by

$$\frac{f_w}{f_y} = \frac{V}{|\overline{u}_{wh}|} = \frac{\pi}{2}\frac{V}{u_{mh}} \tag{4.10}$$

Hence, the ratio of the sand velocities is proportional to the square root of the water particle velocity ratio

$$\frac{|\overline{u}_{sh}|}{V_{sh}} = b' \left(\frac{u_{mh}}{V}\right)^{\frac{1}{2}} \tag{4.11}$$

The mean bed load transport of sand per unit time per unit width in the longshore direction can then be expressed

$$\overline{q}_h = \frac{B}{g(1 - \frac{\rho}{\rho_s})}\sqrt{\frac{V}{u_{mh}}}\,|\overline{u_{wh}\,\tau_h}| \tag{4.12}$$

where the proportionality factors have been combined, $B = e_h/b'f_h'$, and must be determined experimentally. The basic idea to underline is that the mass of sand transported is proportional to the available power.

C. Total Sand Transport outside the Surf Zone

The total transport of sand includes both bed and suspended load. Bagnold (op. cit.) also presents a derivation for determining the quantity of suspended sand transport by energy considerations. The basic arguments are similar to those for the bed load transport. For a steady transport of suspended material of mass m_s, there must be a normal stress $N_s = (1 - \frac{\rho}{\rho_s})\, gm_s$ in order to support the load. The mass of the suspended sand is the total suspended sand in a water column per unit bed area. To keep the suspended sand particles at statistically constant elevations above the bed, the fluid must do an amount of work $N_s w_s$ where w_s is the fall velocity of the sand grains. The mean power expended by the fluid in a water column representing a unit area of the bed is

$$\overline{P}_s = (1 - \frac{\rho}{\rho_s})\, g\overline{m}_s\overline{w}_s \tag{4.13}$$

The mean mass transport rate of the suspended load per unit width perpendicular to the beach over the water column is defined similarly as before

$$\overline{q}_s = \overline{m}_s V_{ss} \tag{4.14}$$

where V_{ss} is the mean horizontal velocity of the suspended sand particles. It is assumed that V_{ss} is proportional to the mean longshore current $V_{ss} = S'V$. It is also assumed that the suspended load is proportional to the power available. Outside the surf zone, the energy dissipation is almost entirely due to work done on the bottom so that in this area the power available for transporting the suspended load is the residual power available after transport of the bed load. The mean power available for transport of the suspended sand transport is

$$\overline{P}_s = e_s(1 - e_h)\, |\overline{u_{wh}\tau_h}| \tag{4.15}$$

The mean suspended transport rate per unit width of the profile then is

$$\overline{q}_s = \frac{S}{g(1 - \frac{\rho}{\rho_s})} \frac{V}{w_s} |\overline{u_{wh}\tau_h}| \tag{4.16}$$

where the proportionality factors have been combined. The bed load and suspended load can be combined to give the total mean transport per unit width outside the surf zone

$$\overline{q} = \overline{q}_h + \overline{q}_s = \frac{1}{g(1 - \frac{\rho}{\rho_s})} [B\sqrt{\frac{V}{u_{mh}}} + S\frac{V}{w_s}]\, |\overline{u_{wh}\tau_h}| \tag{4.17}$$

Equation (4.17) is a rational equation for predicting the total sediment transport outside the surf zone. Unfortunately, unknown proportionality factors, or energy coefficients, have been introduced in an attempt to distinguish between bed load and suspended load for which functional relations to the other variables are unknown.

Experiments have been conducted in laboratory flumes by Inman and Bowen [64] to experimentally determine the functional relationship of the coefficients. These experiments were conducted by superposing waves on a current moving in the same direction. Unfortunately, no such relationships have evolved empirically to date.

D. Total Sand Transport inside the Surf Zone

Inside the surf zone, the dissipation of energy is greatly increased and is largely due to turbulent dissipation. The transport inside the surf zone is much greater than outside, and the transport is primarily suspended load for which there is much more energy available for transporting purposes. The actual bed load is still a function of the energy dissipated on the bottom which decreases with decreasing depth. There is also an additional amount of work done on the bed by turbulent energy being diffused and convected downward due to the breaking waves. It is assumed that inside the surf zone the bed load as well as the suspended load is a function of the total energy dissipated including both the energy dissipated on the bottom due to friction and turbulent energy dissipation due to the breaking waves. Within the surf zone, all the energy flux perpendicular to the beach is dissipated as the wave height goes to zero at the beach providing no energy is reflected. It is assumed some portion of this energy is available for sediment

transport so that the available power for sand transport inside the surf zone is proportional to

$$P_s = \frac{-\partial \vec{Ec}_g}{\partial x} \tag{4.18}$$

The total mean transport inside the surf zone is then

$$\bar{q} = \bar{q}_h + \bar{q}_s = \frac{-1}{g(1 - \frac{\rho}{\rho_s})} \left[B_s \sqrt{\frac{V}{u_{mh}}} + S_s \frac{V}{w_s} \right] \frac{\partial \vec{Ec}_g}{\partial x} \tag{4.19}$$

where B_s and S_s are proportionality factors for inside the surf zone.

CHAPTER V

FIELD EXPERIMENTS

A. Description of Experiments

A meaningful field investigation of the sand transport processes in the surf zone requires the synoptic measurement of a number of hydrodynamic and sediment variables. Fairly complete and extensive data are required to evaluate the validity of the proposed sand transport relationships.

Field experiments were conducted in the surf zone at Fernandina Beach, located on the northeastern coast of Florida. The emphasis of the tests was to obtain information concerning the distribution of alongshore sand transport across the surf zone and the physical processes causing such movement. Sediment transport in the surf zone has been shown to be caused by a combination of shear stresses and turbulence due to wave and current action. Hence, an attempt to correlate sediment transport with physical parameters must include adequate wave and current measurements.

Experiments have been conducted intermittently at this location since 1962. The author has been responsible for the experiments conducted after the fall of 1965. Data from experiments conducted since the summer of 1964 are used for testing the equations. In the course of this time, the method of measuring the various parameters has changed, evolving to a relatively sophisticated level. Much of the test equipment was designed and developed especially for these experiments and is unique. Since the

fall of 1966, much more elaborate electronic equipment has been utilized to carry out many of the measurements, and these experiments will be referred to as the "later experiments."

The experiments were conducted at various times of the year so that a variety of wave and weather conditions prevailed during the experiments. The beach and nearshore bottom profile is typically a one- or two-bar system with a gentle slope of 2 to 3 per cent. The mean tidal range is 5.6 feet.

The measurements were conducted from a pier traversing the surf zone seaward to the outer bar. A plan of the pier and location of the instrumentation are shown in Figure 18. A typical bottom profile taken adjacent to the pier is also shown in this figure. The experiments were limited to the study of the sand transport in the area bounded by the outer and inner bar.

The sand characteristics have been studied thoroughly including size distribution, mineral composition, and differences of characteristics across the surf zone. Sand samples were taken periodically during the year to check these characteristics. The results generally showed the sand to be evenly sorted in the area of the sand transport measurements. The mean grain diameter at Fernandina Beach is approximately 0.2 millimeters. A typical sand grain size analysis is shown in Figure 19.

The physical parameters measured during the experiments were the wave height, wave direction, currents, tides, wind direction and speed, quantity of sediment transport, bottom contour profiles, and sediment characteristics.

The experiments were conducted typically over approximately half a tidal cycle, usually four to six hours. The tide recorder, anemometer,

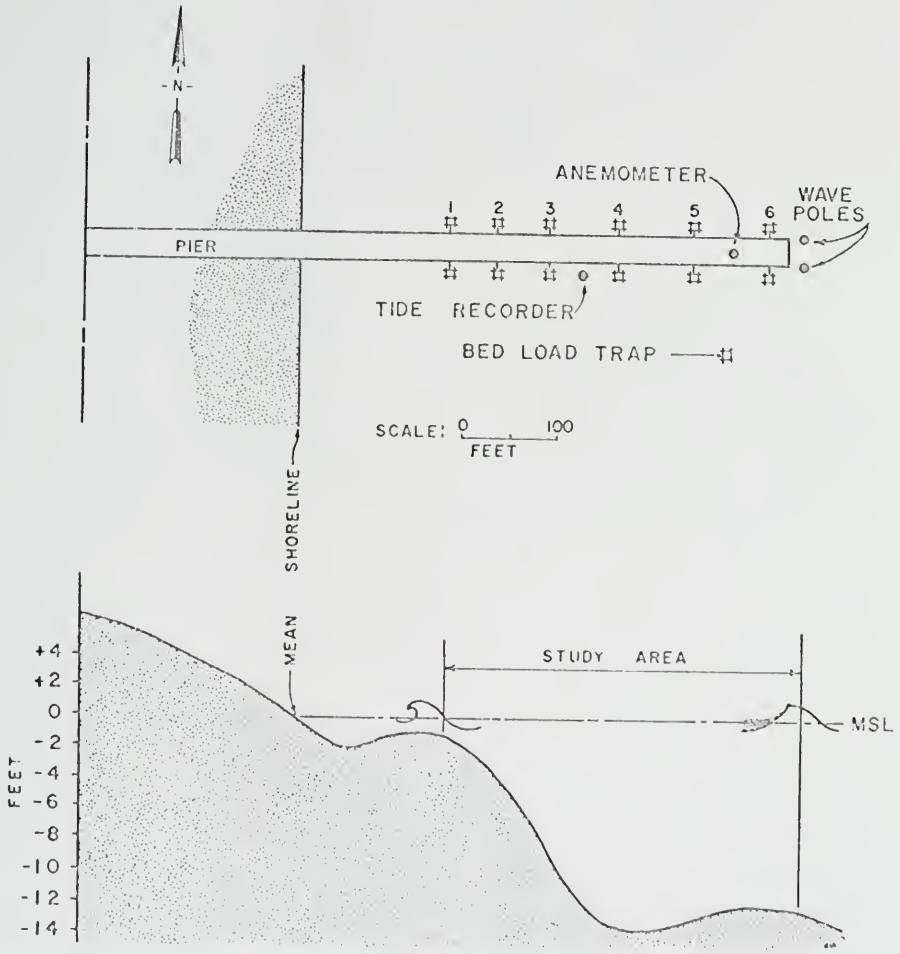

Figure 18. Plan of Pier Showing Instrument Locations and Typical Bottom Profile at Fernandina Beach, Florida

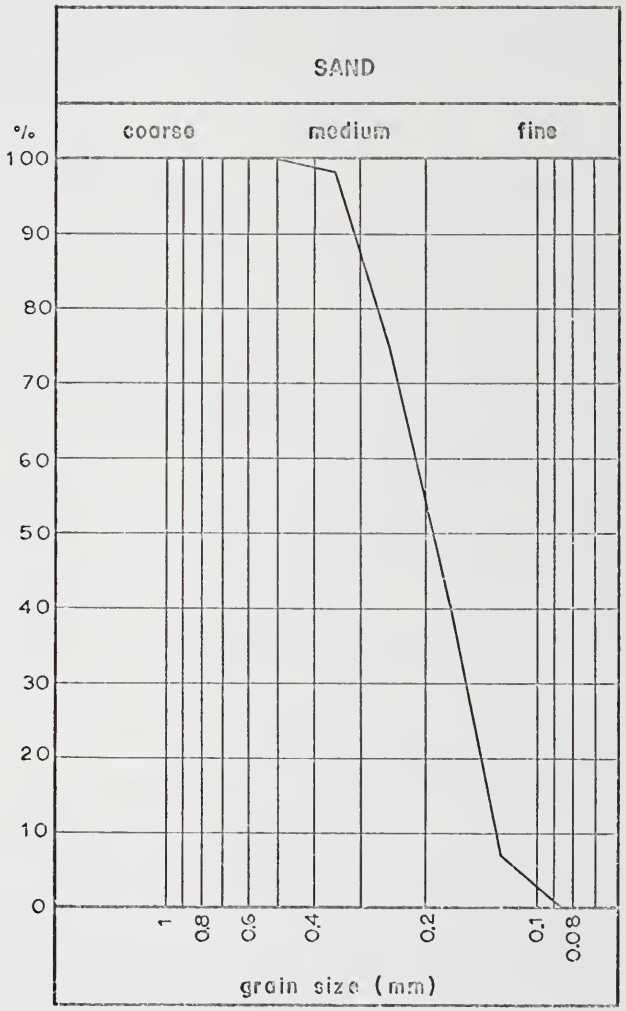

Figure 19. Typical Sand Grain Size Analysis Taken at Fernandina Beach, Florida

and sand traps operated continuously during the experiment. Current measurements were taken by means of floats and current meters. The wave heights and direction were measured simultaneously. The instrumentation and details of measurements are described below.

Taking measurements in the surf zone is usually a difficult problem due, in part, to the tremendous forces exerted by the waves. It is almost essential for synoptic measurements to have a stable platform from which to work. This platform, a fishing pier in this case, exerts some local influence on the environment being measured and care must be taken to minimize this effect. Thus, all measurements were made as far from the pier and its piling as possible, and the measurements were taken on the updrift side of the pier on which the incident waves impinge first.

A pier or similar structure extending out from the beach can also exert an influence on the general circulation patterns of the surf zone. The pier can act as a perturbation on the longshore current system, and one often observes a rip current generated near the tip of such structures. Care was taken to note the occurrence of rip currents being generated at the pier, and such occurrences have been treated as being anomalous. Data taken during such experiments have been excluded.

Another effect of the pier was noted on occasion from the bathymetry of the area adjacent to the pier. It was found that there was considerable scour about the seaward end of the pier which certainly influences the sediment transport in this vicinity. Similar scour about the ends of other piers has also been found elsewhere. It was also noted that there was often some slight accretion of sand at the shoreward end of the pier in the swash-zone area.

Profiles of the beach and offshore area were taken during every test from the pier. A complete bathymetric survey extending 1,000 feet to the north and south of the pier and 3,000 feet offshore was taken periodically during the year. A typical bathymetric chart of this area is shown in Figure 20 (see also Appendix A).

1. Sand Transport Measurements

The quantity of sand transport was measured by means of bed load traps. The traps are aligned in the direction of the longshore current and are designed to intercept the bed load portion of the littoral drift. These traps rest on the bottom and sample an area 20 centimeters high by 40 centimeters wide. The bed load movement here is defined by the height of the traps and, as such, includes saltation. Up to six traps were operated simultaneously from the pier and are located as indicated in Figure 18.

The unique design of these traps evolved over several years of use, and they have proven to be very rugged and dependable for the severe conditions to which they are subjected. Figure 21 shows a bed load trap rigged for use with its doors open in sampling position. An abbreviated description is given below. For a more complete description of the traps and attendant system, see Bruun and Purpura [65].

The body of the traps is elliptical in shape which serves two functions: to decrease current velocities due to the divergence from the entrance allowing sediment to fall from suspension during sampling, and to act as a circular tank in which a swirling motion is developed to put sediment in suspension for pumping out. The trap base is a sheet metal apron which is extended to reduce scour.

The trap was lowered from the pier by a crane as shown in Figure 22.

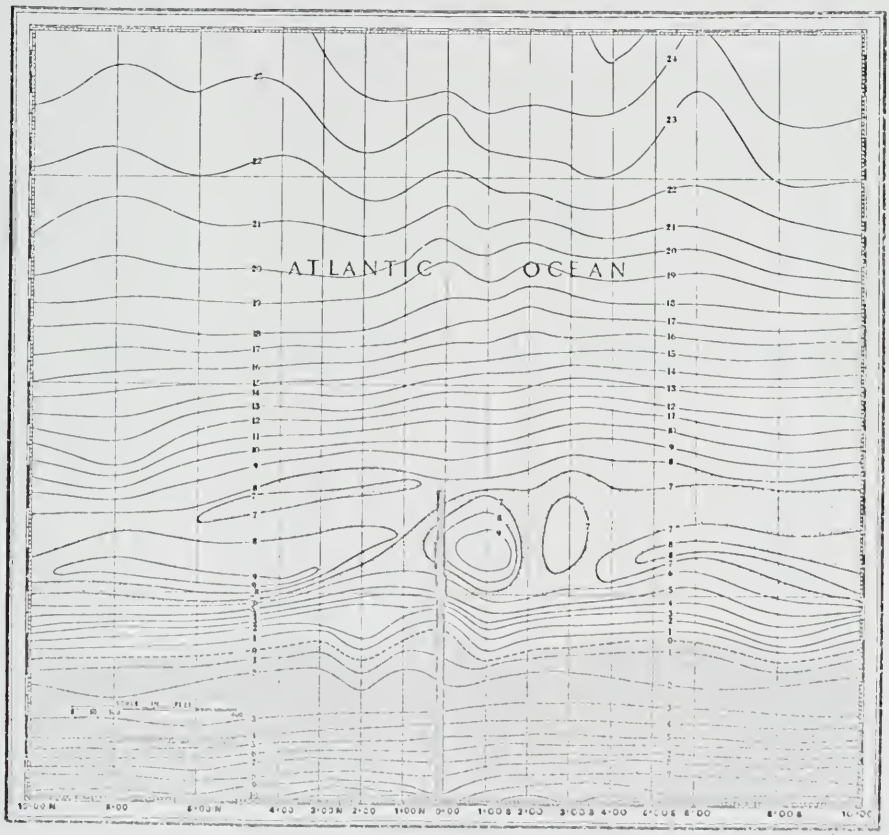

Figure 20. Bathymetry Adjacent to the Fishing Pier at Fernandina Beach, Florida, December 17, 1968

Figure 21. Sand Trap with Doors Open

Figure 22. Lowering Sand Trap from the Pier, Showing View of Crane

Tag lines were attached to assure proper orientation. The traps were run typically on a sampling sequence of 15 minutes sampling with the doors open and 5 minutes pumping out with the doors closed. The doors operate pneumatically from the pier. During the pumping-out cycle when the doors are closed, two jets of fresh water from inside the trap create a swirling action to put sediment in suspension. Simultaneously, the water-sand mixture is pumped out of the traps into filter baskets and drained of the water. The wet sand is put in sample bags and taken back to the laboratory where it is dried and weighed.

2. Current Measurements

Simultaneous with the sand transport measurements was a complete measurement of the physical environment. The currents were measured using two means: floats in the earlier experiments and combined floats and a current meter in later tests. The float measurements consisted of filling large balloons (one foot in diameter when filled) with fresh water and releasing these from the pier and measuring their travel time over a prescribed distance. The fresh water makes the balloons slightly buoyant so that just the top of the balloon is visible. These proved to be a very effective means of measuring the longshore currents.

The current meter was used to measure the water particle velocities. The measurement of water particle velocities in the presence of a wave field, such as the surf zone, has long been a problem. An electromagnetic flowmeter was used during these experiments and proved applicable for use in the surf zone. This instrument was used essentially as a turbulence meter whereby not only the mean, but the fluctuations about the mean, or the turbulent velocities, are measured.

Problems encountered in the surf zone with conventional current meters are due to the suspended sediments and rapid water particle accelerations. The suspended sediments tend to wear out bearings or moving parts. Propeller- or rotor-type meters have a poor response to rapid accelerations due to the inertia of the blades. These problems are not encountered since the electromagnetic current meter utilizes no moving parts.

The current meter mounted on a tripod is shown in Figure 23. Its overall length is 6 inches with an inside bore diameter of 3/8 inches. Calibration of the instrument showed it to have very linear characteristics over the velocity range of less than 0.1 foot per second to more than 16 feet per second, which was the range of the calibrating facilities. The tests also showed the instrument to have a fairly flat response up to frequencies of one cycle per second.

It was found necessary to mount the current meter on a tripod as shown in Figure 24, rather than on the pier, in order to have the desired rigid mounting. The pier, although a reasonably stable platform, responds to the wave motion with a frequency approximately the same as the frequency of the waves. The motion of the pier is predominantly lateral. This motion has negligible effect on the wave measurements but would superimpose a substantial component on the measured current. The natural frequency of the tripod is much higher than frequencies of interest for the measured water particle velocities and has proven to be an excellent mounting.

3. Wave Measurements

The waves were measured by a variety of methods which all consisted of measuring the water surface elevation in time. The measurements were made at one or several locations along the pier. Initially, the water

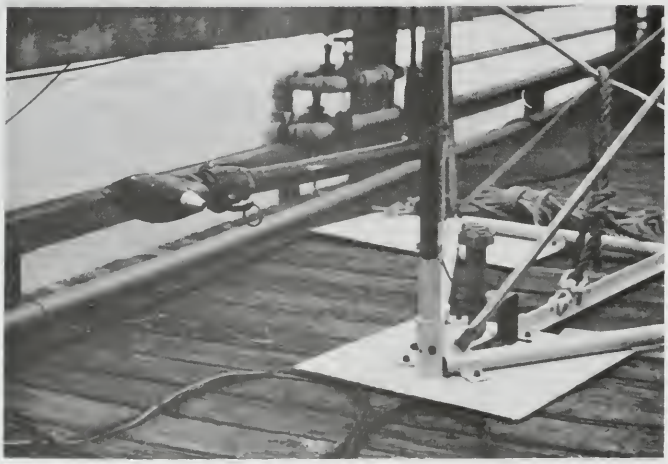

Figure 23. Current Meter and Pressure Transducer (Mounted on Tripod)

Figure 24. Attaching Instruments to Tripod

surface elevation was determined by noting the changes in the elevation of a float inside a perforated transparent tube. Both visual and motion picture records were made of these observations. This procedure was improved by using a mechanical wave height meter that recorded the time history of the wave heights on a strip chart. Finally, these methods were superseded by the use of electronic resistance wire wave staffs and pressure transducers. All measurements were complemented with visual observations.

Waves, as they occur in nature, are essentially aperiodic or random in appearance and, as such, have to be treated as a statistical phenomenon. The studies were conducted over a relatively short duration of time, and the physical environment may be assumed quasi-stationary. Hence, spectral analysis or other statistical inference can be employed in treating this aperiodic phenomenon. Spectral analysis was used in the later experiments and provided valuable information concerning the energy distribution in and about the surf zone. The relations derived previously assume a single component wave system and are not formulated to accommodate a spectrum of waves. For this reason, and due to the variety of methods used in measuring waves, it is convenient to extract from the wave measurements a single parameter characterizing the energy content of the waves. This parameter was selected as the significant wave height which is commonly used in oceanographic studies and which is defined statistically as the average of the highest one-third waves.

A pressure transducer used to measure wave heights was mounted on the same tripod as the current meter so that a direct correlation of the water particle velocity and wave height could be obtained at the same location in the surf zone.

The wave direction was measured by sighting with a compass and noting the angle between the pier alignment and the wave crest. Aerial photography was also employed in a number of the experiments. The incident wave angle at particular points inside and outside of the surf zone were determined in this manner. These measurements refer to the angle of the "significant" wave. Wave measurements conducted in the later experiments, using two wave staffs stationed at the end of the pier and aligned parallel to the shore, allowed directional features of the waves to be determined. A directional spectrum is obtained by computing the Fourier transform of the cross-correlation function of the two wave records which associates one direction with each frequency component and is essentially a measure of the phase difference between the two sensor locations for each Fourier component. A more complete description of the spectral aspects of the experiments is given by Thornton [66].

4. Wind Measurements

A portable anemometer was located atop a 10 foot mast on the pier. The elevation above mean sea level was 29.5 feet. Periodically, during a test, the wind velocity and direction were recorded.

5. Tide Record

The tide was measured continuously by means of a float-type water level gauge with the float inside a stilling well. The tide was mechanically recorded on a strip chart.

B. Error Analysis

The angle of wave incidence is the most importantly weighted variable in the predictive equations for the longshore current and sediment transport equations; it is also the most difficult parameter to measure

accurately. Galvin and Savage [9] compared several methods for measuring waves from a pier using a compass and sighting along the wave crests. They concluded that the error in measuring wave angle may be easily ± 2 degrees, and this same variability will be assumed here. This amount of uncertainty in the measured angle can result in considerable error in the longshore current and sediment transport calculations--particularly, for small angles of approach.

The wave angle, like the wave height, is a stochastic process, that is, a random process varying in time. Hence, a number of measurements must be taken to insure that a representative sample has been obtained. The difficulty of using aerial photography is that, although the wave angle can be measured quite accurately, the number of waves, or total sample, is usually very limited. It will be assumed that the wave angle measurements obtained from aerial photography, usually determined from only two or three waves for an individual experiment, also fall within the ± 2 degree accuracy range.

The directional spectrum obtained by spectral analysis of two simultaneous wave records associates a direction with each particular frequency component. A single representative direction must be chosen from this spectrum. The direction selected was that corresponding to the significant wave frequency which, in turn, corresponds closely to the frequency at which the maximum energy density of the spectrum occurs. This direction is then defined as the "significant direction." Comparisons of wave directions, measured in this way with visual measurements, generally were within the ± 2 degrees.

The wave heights generally were determined from wave records greater than five minutes in length. Hence, the significant wave height was

determined with a high degree of confidence. Visual measurements were used in the first experiments. Galvin and Savage (op. cit.) state an accuracy of the breaking wave height of ± 25 per cent for both wave meter and visual measurements. There is an uncertainty even for the wave meter measurements since there is a spatial variation due to variations in bottom topography. The wave meter measures only at one point that may not be representative of the general area.

The beach profile can be measured quite accurately and varies only slowly with time. There is a certain subjectiveness in choosing a single beach slope for use in the mean longshore current formula (Equation 3.87) when a bar-trough profile exists. The actual depth measurements and local slope of the bottom were used in all other formulations. The limits of variability are judged at certainly less than ± 10 per cent.

The accuracy of the sand traps is dependent on their efficiency in retaining the sand that passes into the trap. The trap efficiency is dependent on the wave conditions, being more efficient for light wave conditions where the turbulence and induced currents are less. The traps tend to become clogged for very heavy wave conditions, and all the sand cannot be pumped out in the sampling cycle; the traps also tend to bury themselves for extreme wave conditions. The traps were observed in the laboratory and field under light wave conditions and appeared to function very well. It was not possible to observe the traps under heavier wave conditions due to the increased turbidity of the water. A trap efficiency of between 40 and 100 per cent is estimated as the representative range for most conditions. As will be discussed subsequently, it is possible that the traps could collect more than the actual net transport.

C. Results and Comparison with Theory

The sediment transport test results are given in Table II. Thirty-one experiments were conducted in all, fourteen of which were judged appropriate for comparison with theory. The other experiments were deleted because of the presence of rip currents, lack of correlating data, equipment failure, or unfavorable weather. Listed in Table II are the station (measured from the baseline) where the trap was located, significant wave height H_s, significant wave period T, wave angle measured at the wave height meter α, mean water depth during experiment $\bar{h}$, and mean bed-load transport per unit width q_h.

The sand transport, like the waves and water particle motion causing the transport, is a stochostic process. The bed load transport per unit width as a function of time for Test Number 26 is shown in Figure 25. Most notably, the bed load transport is seen to vary considerably with time. Each break in the curves represents a twenty-minute average which was the sampling interval. The tidal height variation during the experiment is also shown.

Generally, the mean transport decreases seaward from the breaker line and increases shoreward of the breaker line. This is evidenced in Figure 25 where all the measurements were taken outside the surf zone, with Station 1 being nearest the breaker line, proceeding offshore to Station 4 which was located in the trough of the profile. This suggests that the transport is a function of the depth, and, therefore, the tidal stage could be important although no tidal influence on the sediment transport quantities is obvious for this particular test. What appeared to be tidal influence was noted in some of the experiments, but no definite correlation has yet been established. Unfortunately, the lengths of the

TABLE II

SEDIMENT TRANSPORT

Test	Date	Station (ft)	H_s (ft)	T (sec)	α (°)	$\bar{h}$ (ft)	$q \times 10^5$ lb/sec/ft
4	7/28/64	450	1.0	4.0	25.0	4.4	85.0
		555				6.2	11.3
		690				9.0	6.7
5	10/2/64	340	5.0	4.5	5.0	5.2	436.0
		460				6.4	252.5
		700				12.4	104.8
8	11/16/64	685	2.0	6.0	12.0	15.7	14.4
		440				5.0	222.0
11	12/2/64	575	2.0	11.0	10.0	10.0	22.0
		685				14.6	36.2
13	12/18/64	460	1.7	8.0	10.0	7.7	34.7
		580				13.0	9.3
		700				13.6	4.6
14	1/19/65	450	1.7	4.0	22.0	11.6	13.0
		555				16.7	4.3
		690				13.9	4.6
16	4/14/65	450	3.3	6.0	10.5	10.9	54.2
		570				13.1	38.6
		690				13.1	21.9
17	5/13/65	350	1.7	4.5	5.0	6.8	123.0
		440				10.9	8.4
		575				16.9	1.7
		685				13.9	9.8
19	2/11/66	395	3.8	6.0	3.5	7.0	182.8
		440				10.3	43.7
		570				18.3	20.0
		650				14.3	32.8
		730				12.4	26.9

TABLE II - continued

Test	Date	Station (ft)	H_s (ft)	T (sec)	α (°)	$\bar{h}$ (ft)	$q \times 10^5$ lb/sec/ft
22	4/26/66	395	3.76	7.7	4.0	5.2	504.0
		440				6.4	810.0
		500				11.3	22.0
		730				13.3	89.0
23	5/9/67	395	0.9	10.0	6.0	5.0	21.0
		440				6.9	4.0
		490				10.3	1.5
		570				14.8	0.3
		730				14.2	2.4
24	5/10/67	395	1.6	4.0	10.0	4.9	58.4
		440				6.6	121.0
		570				14.9	4.3
25	5/23/67	395	4.7	7.7	7.0	3.8	476.0
		490				11.8	90.0
		570				16.9	18.0
26	5/24/67	395	3.2	7.0	7.0	6.7	312.0
		440				8.3	83.0
		490				13.6	120.0
		570				18.8	34.0

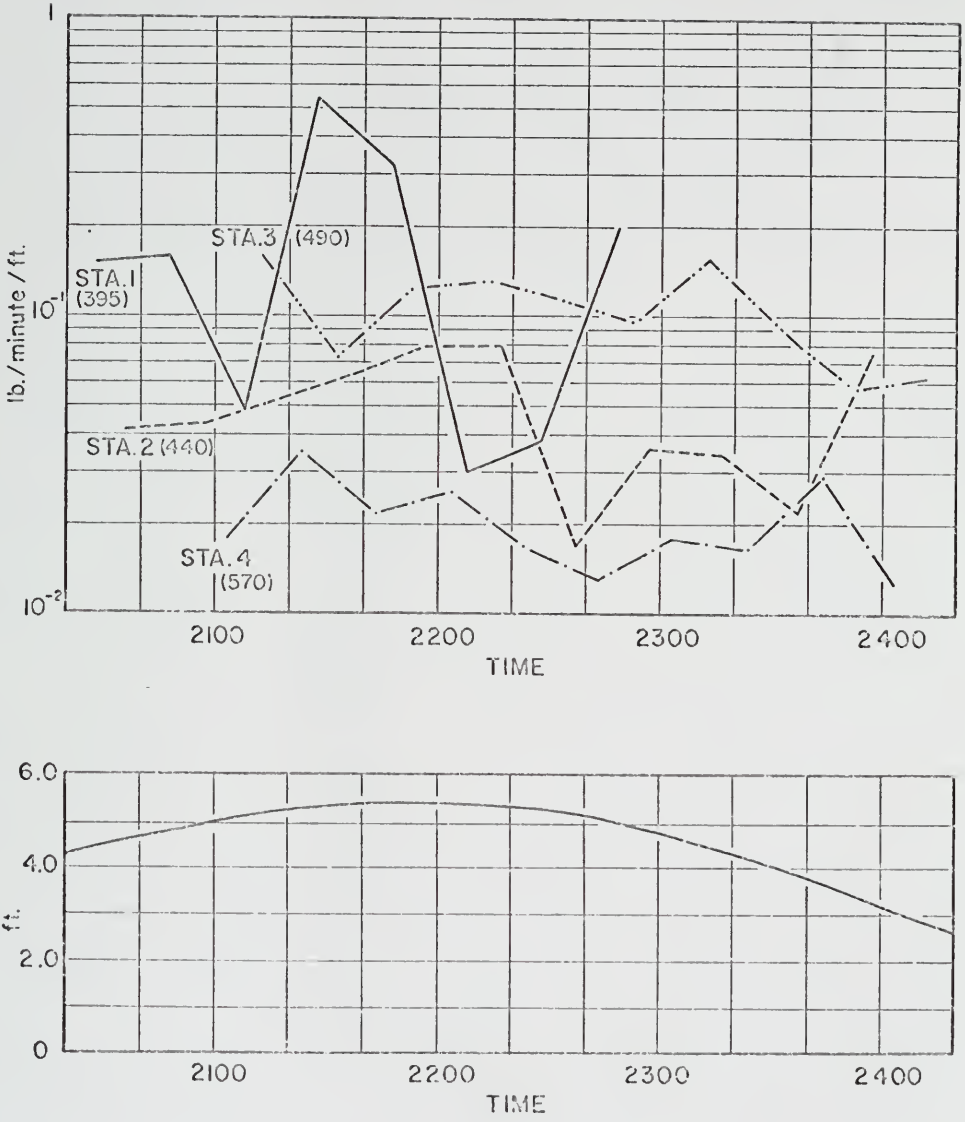

Figure 25. Variation of Measured Sediment Transport with Time, Test Number 26

experiments were not adequate to fully investigate this. The tests were designed to minimize tidal influence by conducting them over the peak of the tide in order to approximate as stationary a system as possible.

All data given in Table II are mean values representing an assumed stationary system. These values can be used to test the bed load transport theory, Equation (4.12) for outside the surf zone and Equation (4.19) inside the surf zone. It is necessary to make several assumptions in the application of the predictive equations. It is assumed that the ripple height was everywhere constant and equal to 0.05 feet. The same ripple height was used for predicting the mean longshore currents inside the surf zone and gave reasonable results (see Figure 11). A constant ripple height is not necessarily a good assumption, but was made as a first approximation due to there not being enough information to assume otherwise.

Energy losses due to percolation have been neglected for application to the Fernandina Beach data because the mean grain size is much less than 0.5 millimeter, recalling that percolation losses were found empirically to be very small for sand sizes less than this value. A mean specific gravity of 2.65 was measured for Fernandina Beach sand, and this value was used in all calculations.

The theory requires wave and current information everywhere along the profile. The measured wave parameters, taken at one location, are used to obtain wave characteristics at each trap location by theoretically carrying the waves shoreward accounting for shoaling, refraction, and frictional dissipation. Predicted longshore currents were used in the littoral transport equations since there was a lack of measurements at each station. The objective is to obtain equations that can be easily utilized to predict the littoral transport from the

measured physical environment, and the wave information at one point is all that is usually available. The longshore currents were predicted from the wave information using Equations (3.57) and (3.82), representing the longshore current outside and inside the surf zone, respectively.

The distribution of the measured and predicted bed load transport are compared for Test Numbers 19 and 22 in Figures 26 and 27. During Test Number 19, all the traps were outside the breaker line which was the case in most of the experiments. A number of equations were utilized to arrive at the final sediment transport predictive equations, and these are summarized in Table III.

Different values of the proportionality factor B were chosen for predicting the sediment transport distribution so that a best fit between theory and experiment for each test could be obtained. The rationale, in doing so, is that if one of the measured variables in the experiments, such as wave height or direction, was substantially in error, this error could change the absolute value of the prediction considerably, but have little effect on the relative distribution along the profile. The B values for inside the surf zone range from 0.42 to 1.0 for all tests except one. The exception was Test Number 25 for which a value of B = 0.13 was used.

There appears to be a definite correlation of sediment transport with depth of water which is graphically illustrated in Figure 27 for Test Number 19. The energy density of the waves in the process of shoaling outside the surf zone generally increases with decreasing depth (provided frictional energy dissipation is not too great) to a maximum at near breaking. Since the energy density is generally a function of depth, the correlation of sediment transport with depth is explained. Indeed,

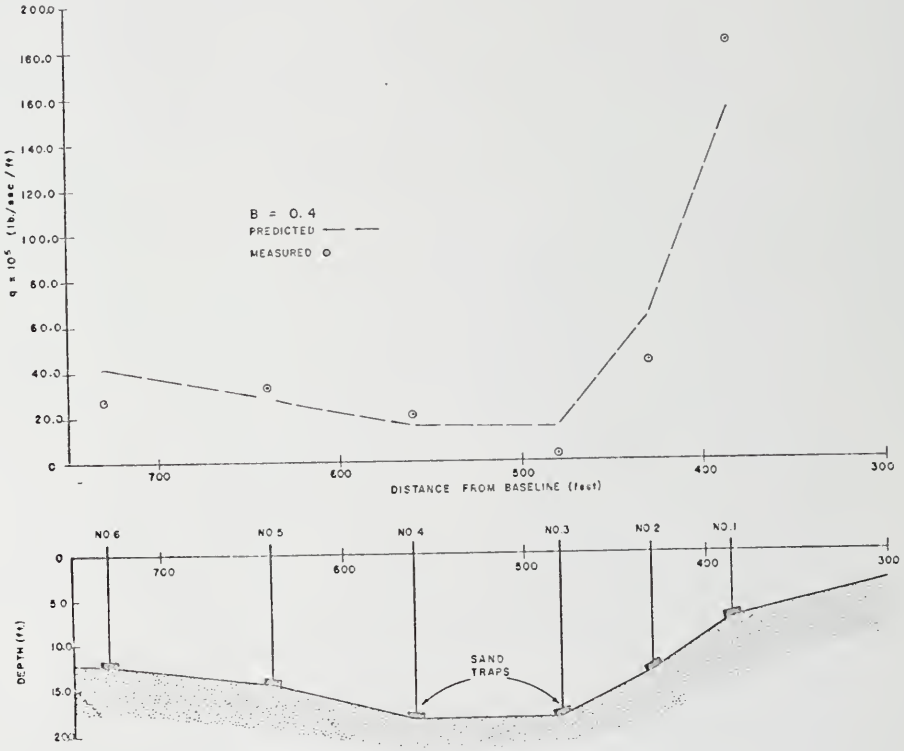

Figure 26. Distribution of Bed Load Transport outside the Surf Zone, Test Number 19

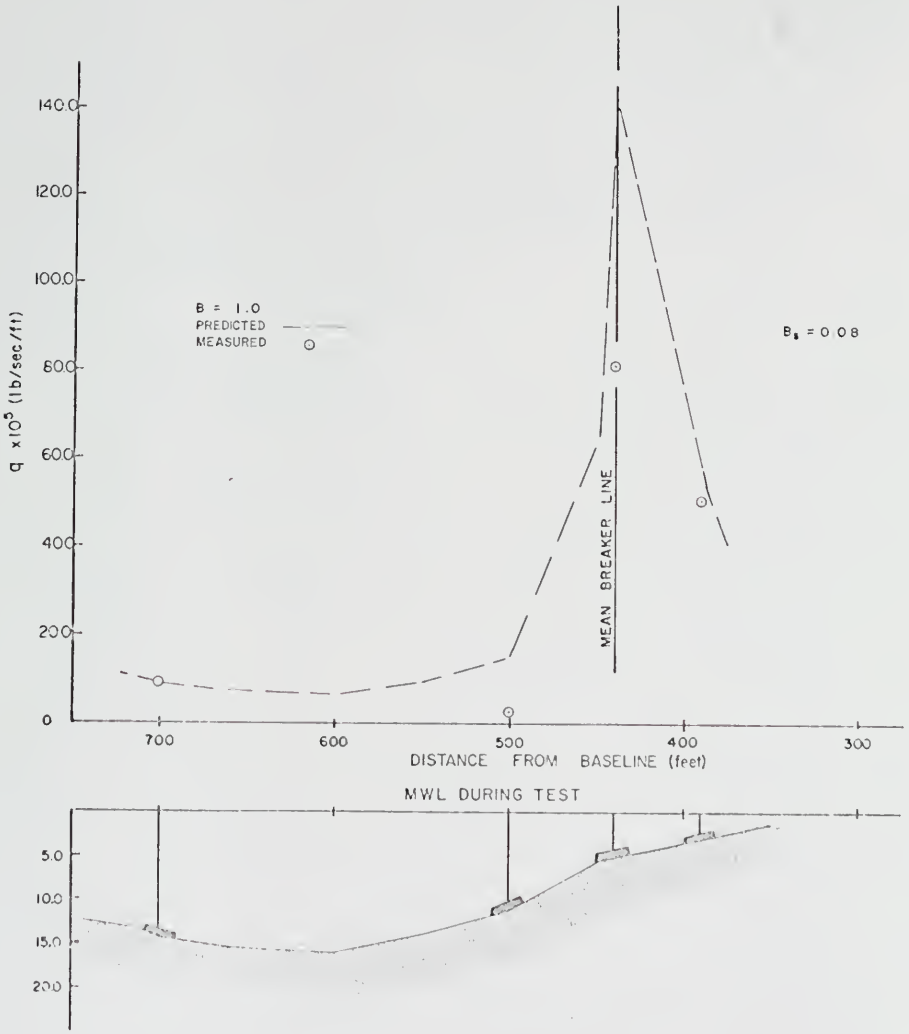

Figure 27. Distribution of Bed Load Transport across the Surf Zone, Test Number 22

TABLE III

SUMMARY OF THE LITTORAL TRANSPORT
PREDICTIVE EQUATION FORMULATION

Outside the Surf Zone (H_s, α_s, T_s, h(x), r)	Inside the Surf Zone (H_b, α_b, h(x), r)
Wave Angle, α	
$\sin\alpha = \frac{c}{c_s} \sin\alpha_s$	$\sin\alpha = (\frac{D}{D_b})^{\frac{1}{2}} \sin\alpha_b$
Friction Factor, f_w	
$\frac{1}{4\sqrt{f_w}} + \log \frac{1}{4\sqrt{f_w}} = -0.08 + \log \frac{\xi_h}{r}$	
Refraction Coefficient, K_r	
$K_r = (\frac{\cos\alpha_{n-1}}{\cos\alpha_n})^{\frac{1}{2}}$	
Shoaling Coefficient, K_s	
$K_s = (\frac{(c_g)_{n-1}}{(c_g)_n})^{\frac{1}{2}}$	
Wave Height, H	
$H_n = H_{n-1} K_s K_r [1 - \frac{8}{\rho g} \frac{\epsilon_n}{(H^2 c_g \cos\alpha)_{n-1}} \Delta x]^{\frac{1}{2}}$	$H = \kappa D$
Energy Dissipation, ϵ	
$\epsilon_f = \lvert\overline{u_{wh}\tau_h}\rvert = \frac{\rho f_w}{12\pi} (\frac{\sigma H}{\sinh kh})^3$	$\epsilon = \frac{\partial}{\partial x} \vec{Ec}_g$
Longshore Current, V(x)	
$V = -\frac{\pi}{8} \frac{\sigma \cosh kh}{f_w kH} \frac{\partial}{\partial x} (H^2 n \sin 2\alpha)$	$V = -A' \frac{c_b}{f_w} \sin\alpha_b \frac{D}{D_b} (1 - 0.7 \frac{D}{D_b} \sin^2\alpha_b) \frac{\partial D}{\partial x}$
Littoral Transport, q	
$q = \frac{1}{g(1 - \frac{\rho}{\rho_s})} [B\sqrt{\frac{V}{u_{mh}}} + S \frac{V}{w_s}] \lvert\overline{u_{wh}\tau_h}\rvert$	$q = -\frac{1}{g(1 - \frac{\rho}{\rho_s})} [B_s\sqrt{\frac{V}{u_{mh}}} + S_s \frac{V}{w_s}] \frac{\partial \vec{Ec}_g}{\partial x}$

the transport is shown to be a minimum in the trough of the profile, greater over the bar, and a maximum near the breaker line where the energy density is greatest.

Measurements both inside and outside the surf zone were obtained in Test Number 22. Again, there is a general correspondence of transport with depth outside the surf zone; a maximum occurs at the breaker line. The energy density gradually decreases for spilling breakers inside the surf zone, and a corresponding decrease in sediment transport is expected. This is clearly shown in Figure 27. It should be noted that a different proportionality factor has been used for inside and outside the surf zone which might be expected. The bed load distribution curves for all other tests are given in Appendix B.

All the results for outside the surf zone are summarized in Figure 28. The same constant of proportionality, B = 1.0, has been used for all the predicted values so as to provide a comparison between the various tests. There are forty values in all to form the correlation. As can be seen, the data span a very large range of values, almost three decades on a log-log graph. The heavy line denotes a one to one correspondence between predicted and measured values for the proportionality factor given by B. The dashed line indicates the expected range of variability of the measured values due to the efficiency of the traps in catching the bed load. The dashed line as drawn indicates that the traps are estimated to be at least 40 per cent efficient in collecting the bed load. It is possible that, in some cases, the traps were more than 100 per cent efficient, that is, they collected more than the actual net littoral transport. This might happen when there is no net flow in one

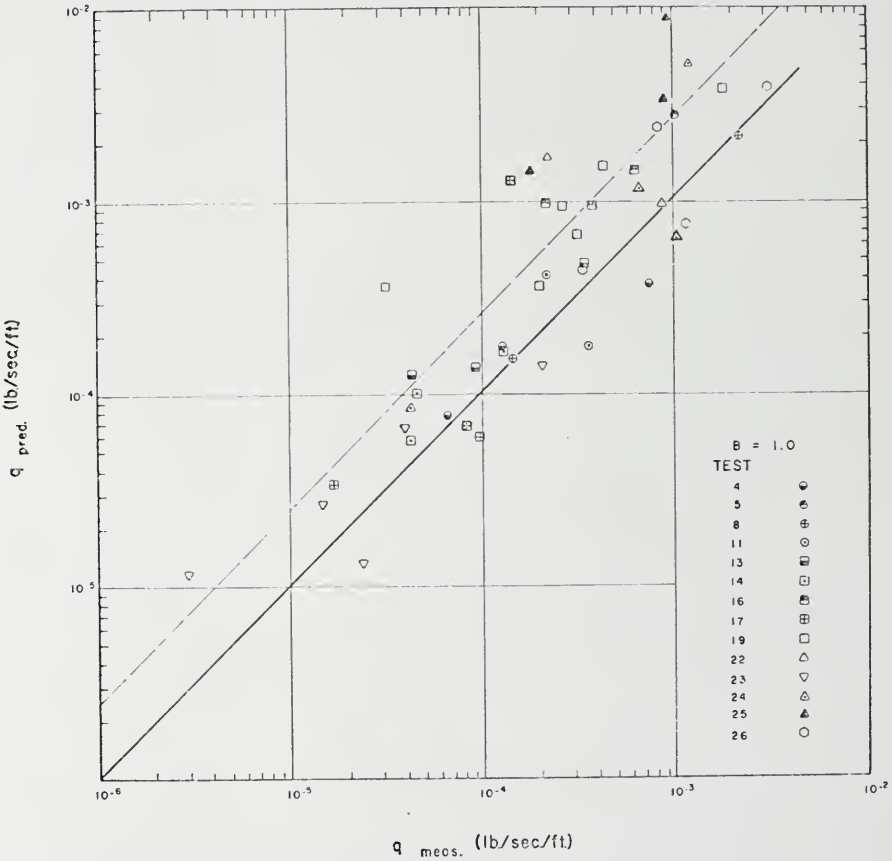

Figure 28. Comparison of Measured and Predicted Bed Load Transport outside the Surf Zone

direction alongshore, and the traps would collect sand moving in both directions, indicating a larger than actual net transport.

The predicted and measured values for inside the surf zone are shown in Figure 29. Unfortunately, there is a paucity of data for sediment transport inside the surf zone. This is primarily due to the design of the traps in that they function poorly for very high transport rates as generally occurs inside the surf zone and have a tendency to become buried. A proportionality factor of $B_s = 0.08$ was used for all experiments inside the surf zone. The estimated limits of variability extend the same range as before. All the values except one fall within the estimated variability of traps. This, in itself, is considered to be very good correlation for predicting conditions so complicated and varied as occurring inside the surf zone.

The values of B are necessarily limited to the particular sediment characteristics found at Fernandina Beach. The most important characteristics are the mean grain size, $d = 0.2$ millimeter, and the specific gravity, $\rho_s = 2.65$. Although the distributions were indicative of only one grain size, the relative distributions are expected to vary little. This is due to the fact that the influence of grain size (provided percolation is not important) would be primarily to change the factor B and the friction factor f_w. Since B is assumed to be constant, and f_w varies only slowly, the relative distribution would not be expected to differ substantially for different grain sizes.

As mentioned previously, the measured currents were not used in comparing the results. The current measurements for the tests are given in Table IV. Most measurements were made outside the actual breaker line in the vicinity of the traps. The measurements taken inside the surf zone

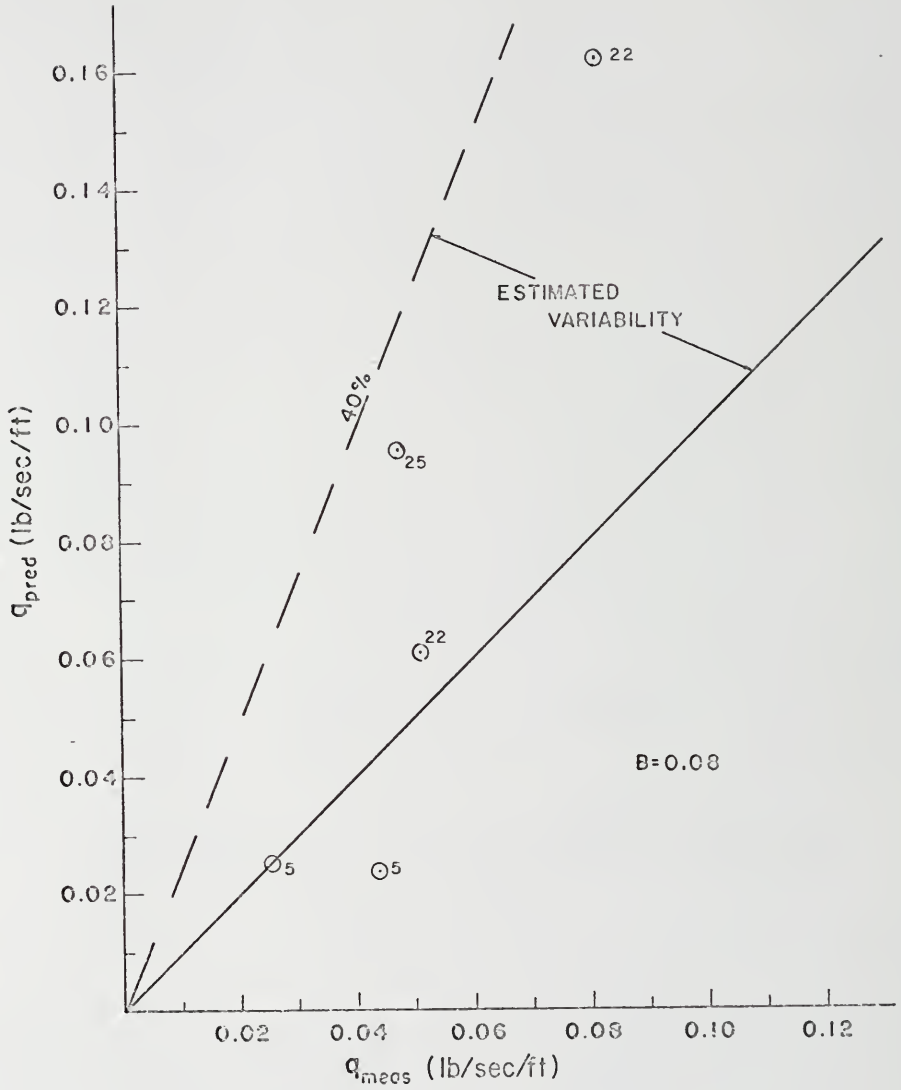

Figure 29. Comparison of Measured and Predicted Bed Load Transport inside the Surf Zone

TABLE IV

LONGSHORE CURRENTS

Test	Date	Station (ft)	H_s (ft)	T (sec)	α (°)	tanβ	V (fps)	Wind (mph)
4	7/28/64	500	1.3	4.0	25.0	0.016	1.8	14 SSE
5	10/2/64	340	5.5	4.5	5.0	0.019	5.0*	18 ENE
8	11/16/64	575	2.0	6.0	12.0	0.020	0.1	3 E
11	12/2/64	460 685	2.0	11.0	10.0	0.019	1.1* 0.7	12 SE
13	12/18/64	580 700	1.7	8.0	10.0	0.019	0.25 0.25	17 NWN
14	1/19/65	350 450 555 690	1.7	4.0	22.0	0.019	0.25 0.25 0.25 0.25	12 S
19	2/11/66	420 530	3.8	6.0	3.5	0.025	1.1* 0.7	9 S
22	4/26/66	700	3.8	7.7	4.0	0.029	1.49	14 SW
23	5/9/67	495	0.9	10.0	6.0	0.031	0.8	8 WNW
24	5/10/67	370 485	1.6	4.0	10.0	0.031	0.06* 0.25	15 S
25	5/23/67	490	4.7	7.7	7.0	0.035	2.86*	20 NNW
26	5/24/67	370 495 495 565 565	3.2	7.0	7.0	0.035	1.0* 0.91 0.75 0.42 0.76	6 NE

are marked by an asterisk. These values have been used in comparing the mean longshore current theory given earlier in Figure 11.

The measured longshore currents outside the surf zone are generally several times greater than the predicted values. The bathymetry at Fernandina Beach is not ideal for the application of the derived theory in that there is typically a bar-trough formation. The bar may tend to trap the shoreward mass transport of the waves between the bar and the shoreline. This fluid contribution over the bar could constitute a considerable influence on the longshore velocity outside the breaker line. The discrepancies between theoretical and measured longshore currents could also be a result of neglecting the influence of internal shear stresses. The coupling across the breaker line, due to lateral transport of momentum offshore, would increase the predicted longshore current values outside the surf zone.

If the actual values of the longshore current were used, instead of the predicted values, the proportionality factor B would be decreased for outside the surf zone. This would result in the proportionality factors, applicable to inside and outside the surf zone, being more nearly equal. The predicted and measured longshore current velocities inside the surf zone correspond well so that the substitution of the measured values would not substantially change the B_s value inside the surf zone.

CHAPTER VI

CONCLUSIONS

A. Longshore Currents

An attempt has been made to describe the wave-induced longshore current and sand transport for a simplified model. The following basic assumptions were made: (1) steady-state conditions prevail, (2) the bottom profile is two-dimensional, but may vary arbitrarily in a direction normal to the shoreline, (3) the waves are adequately described by linear theory, and (4) spilling breakers persist across the surf zone. The equations of motion were analyzed to the second order in wave amplitude (first order in energy). Emphasis in the analysis was placed on formulating usable predictive equations for engineering practice. The wave-induced currents generated parallel to shore were investigated first. The littoral sand transport, which is dependent on the strength of the longshore current and the intensity of the wave action, was subsequently examined.

Conservation equations of mass, momentum, and energy, which have the steady and unsteady contributions separated, were used to describe second order wave-induced phenomena of shoaling waves approaching at an angle to the beach. It was assumed that linear theory described the waves adequately, and that, inside the surf zone, the waves approximated spilling breakers such that the wave height is dependent on the local depth. The specification of the wave field determines the form of the

excess momentum flux due to the presence of the unsteady wave motion (sometimes called a "radiation stress"). The component of excess momentum flux perpendicular to the beach is responsible for wave set-down outside the surf zone and wave set-up inside the surf zone. These changes in the mean water level were included in the longshore current formulations.

It was shown that the component of excess momentum flux directed parallel to shore can generate longshore currents. Changes in the excess momentum flux, as the waves shoal, must be balanced by a resistance force in order to maintain the assumed steady-state conditions. Longshore current equations were derived and discussed for various assumed bottom profiles and resistance forces, including both bottom and internal shear stresses. A logical means of introducing the friction factor associated with the bottom shear stress term was presented--the friction factor being related to the wave and bottom roughness characteristics. An equation for the mean longshore current for plane sandy beaches was developed by assuming the resistance term is due to bottom shear alone. This equation compares well with several laboratory and field experiments.

In the case of a fixed plane laboratory beach, there is an abrupt change in the predicted excess momentum flux at the breaker line which introduces an unrealistic discontinuity in the longshore current distribution. It is therefore necessary to include in the resistance term the internal shear stresses which act to transport momentum laterally. This couples the adjacent elemental water columns, resulting in a continuous velocity distribution.

The driving force for currents outside the surf zone was shown to be small. The internal shear stresses at the breaker line act to drive the current outside the surf zone which is otherwise very weak. The current outside the surf zone is increased by the seaward transfer of momentum across the breaker line, and, conversely, the current inside the surf zone is retarded near the breaker line, displacing the maximum velocity shoreward.

A mixing length hypothesis and the kinematics of the wave motion were combined in order to define the internal shear stresses. Favorable results were obtained for both laboratory and field cases in predicting the velocity distributions when incorporating the internal shear stresses in this manner. This method is tentative, pending further investigation, but the results obtained appear promising.

Natural beaches usually have movable beds which can modify themselves to minimize the shear stress acting on the bottom. This results in bottom profiles with gradual changes in slope and, hence, gradual changes in the shoreward excess momentum flux across the breaker line and inside the surf zone. Reasonable comparison of measured field data with predicted velocity distributions can be obtained by assuming the resistance force is only due to bottom friction where the bottom slope is small and "well behaved," changing only gradually shoreward.

A number of relationships for the longshore current have been investigated for varying bottom profiles, and the physical significance of including different resistance terms has been examined. The wave set-down and set-up have been included in the formulation. Comparison of experimental results from the laboratory and field with the derived

theory shows that the predicted results compare favorably if the assumed conditions are approximately fulfilled.

B. Littoral Transport

The wave-induced sand transport alongshore was investigated by an energy principle approach. Again, the aim of the investigation was to present usable predictive formulas. Both bed and suspended load transport equations were formulated for outside and inside the surf zone. Although the energy approach has been used before, this is the first application to predict the distribution of littoral transport along a line perpendicular to the beach.

The quantity of sand transported is a function of the energy available for transporting the sediments. This energy is related to the energy utilized in bottom friction, viscous dissipation, and turbulence. For the case of waves and currents superposed, wave energy is utilized to put the sediment in motion, and, once in motion, the sediments can be acted upon by weak secondary currents. Hence, littoral drift can be considered as a stirring by the waves, which induces little net motion, and transport by the longshore current, which has net motion in the direction parallel to shore.

Energy dissipation outside the surf zone is primarily due to bottom friction, that is, most of the work is done on the bottom. Hence, the primary mode of transport outside the surf zone is by bed load. Energy is dissipated inside the surf zone primarily by the turbulence in the breaking waves and by friction acting on the bottom so that both bed and suspended load transport are important.

The determination of the energy dissipation by bottom friction

requires the specification of the energy friction factor f_e. Experiments have shown that the energy friction factor (for wave conditions of the intensities that occur in or near the surf zone) is very nearly equal to the shear friction factor f_w. This allows using the same friction factor for both the momentum analysis for the longshore currents and the energy analysis for the littoral sand transport. The specification of f_w as a function of the ripple characteristics and wave velocities appears to give very reasonable results.

Sand transport data were collected in the field using bed load traps. Wave, tide, wind, and current information was collected simultaneously in order to verify the derived predictive equations for longshore current and sediment transport. The longshore current equation including only bottom shear stress was used in the sediment transport predictive equations. Quite reasonable predictions were obtained for the relative distribution of bed load transport, both inside and outside the surf zone, although the absolute values were not as well predicted.

The field data were correlated with the predictive equations to determine separate proportionality factors for inside and outside the surf zone. The proportionality factors are limited to the particular parameters found at the experimental site. In particular, the sediment transport rates would certainly be dependent on the sand characteristics such as grain size and sediment density. However, the comparison of theory and experiment show that the relative distributions, which would be expected to have little dependence on sand characteristics, were fairly well predicted. Hence, the equations could be used as a qualitative predictive relationship for engineering application.

APPENDIX A

BATHYMETRY AT FERNANDINA BEACH, FLORIDA

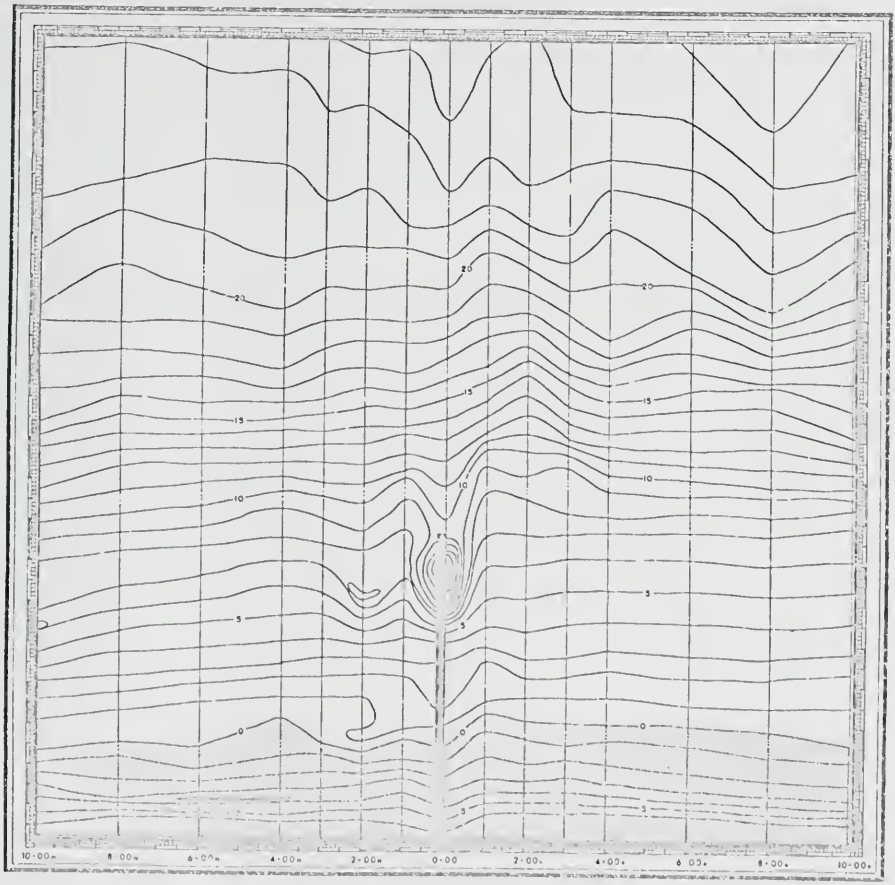

Figure 30. Bathymetry, November 22, 1966

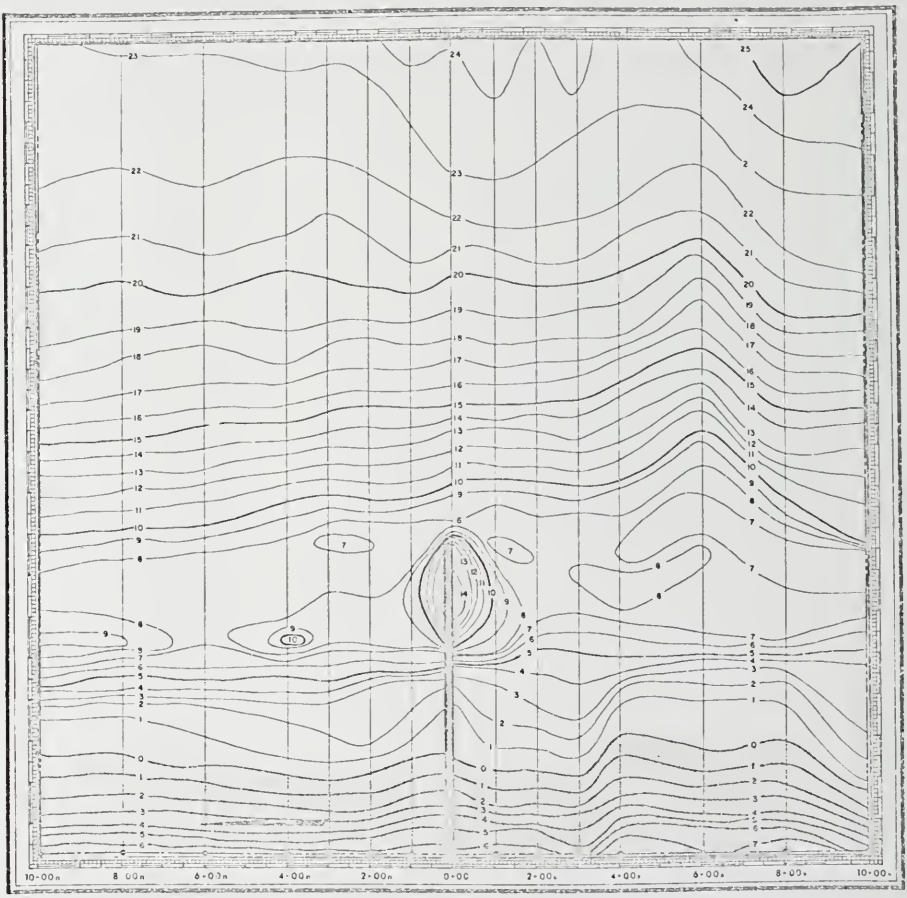

Figure 31. Bathymetry, May 26, 1967

Figure 32. Bottom Profiles Adjacent to Pier, July 24, 1964 - April 14, 1965

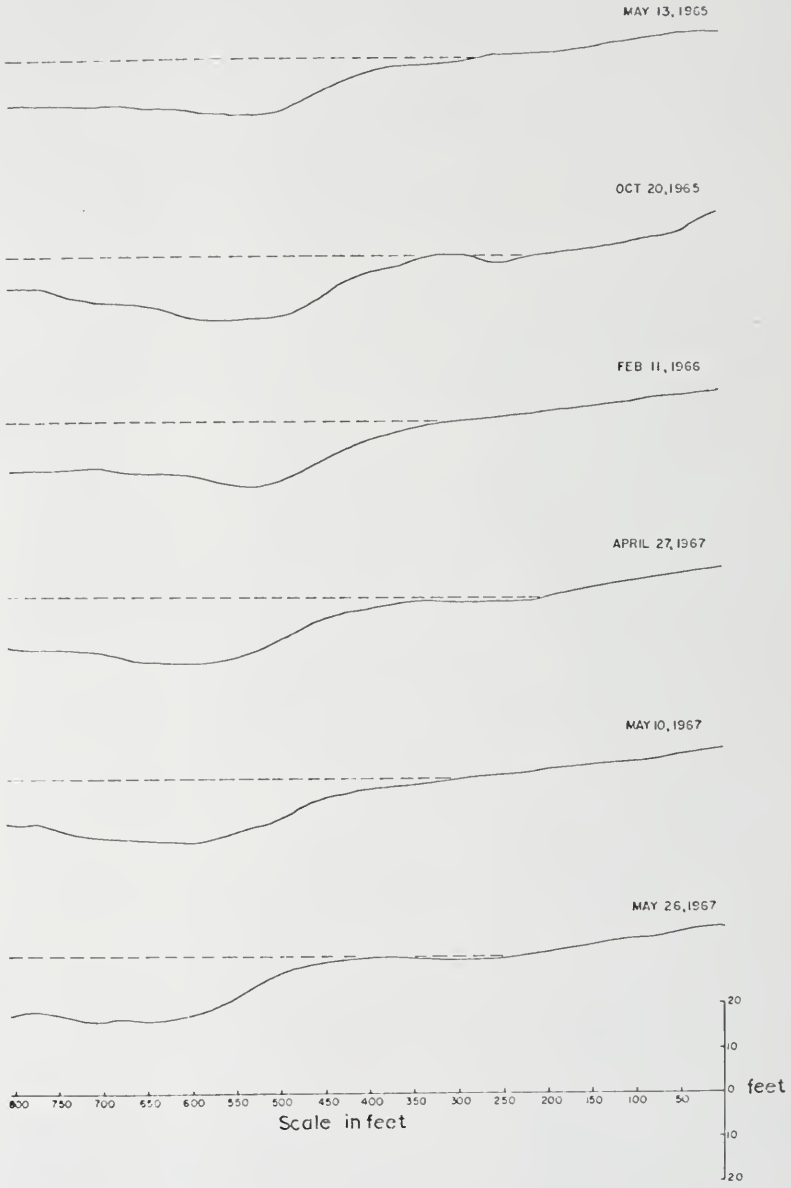

Figure 33. Bottom Profiles Adjacent to Pier, May 13, 1965 - May 26, 1967

APPENDIX B

PREDICTED AND MEASURED DISTRIBUTIONS OF BED LOAD TRANSPORT

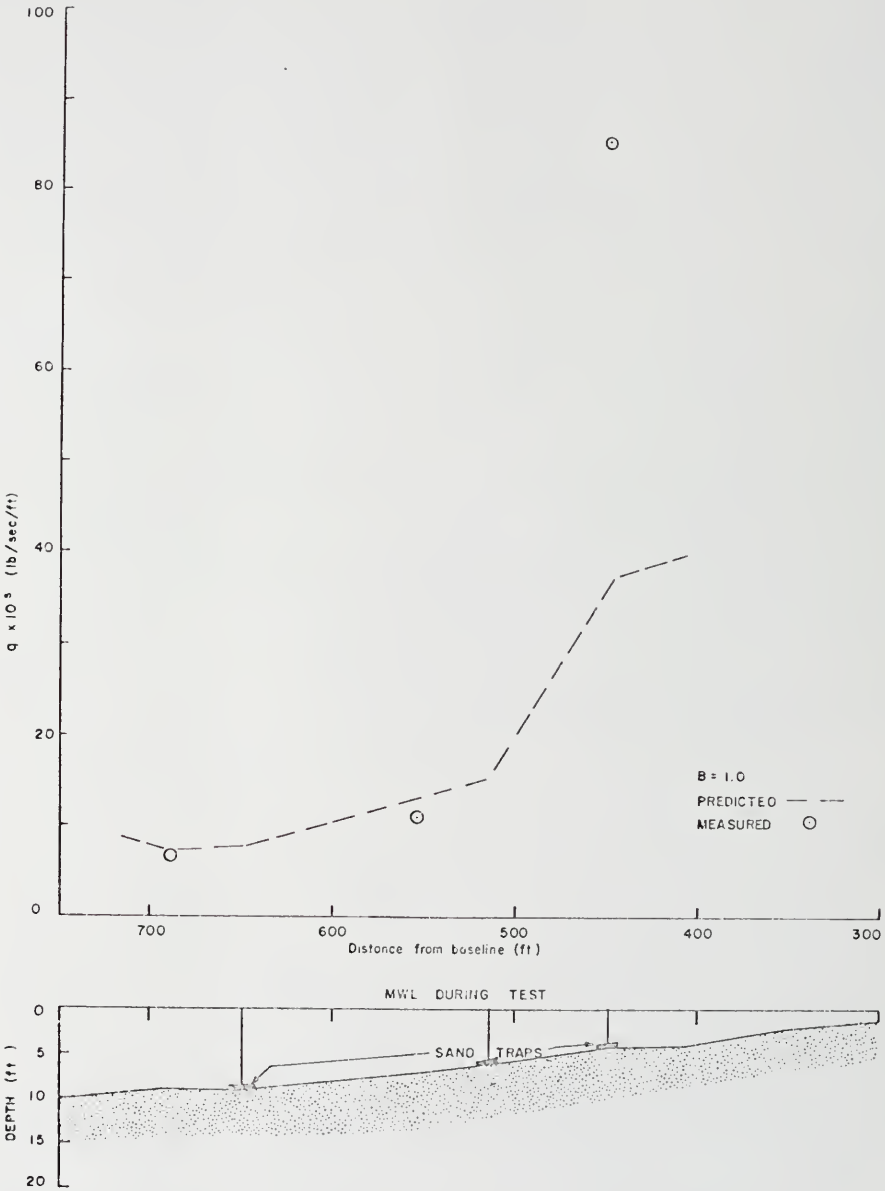

Figure 34. Distribution of Bed Load Transport, Test Number 4

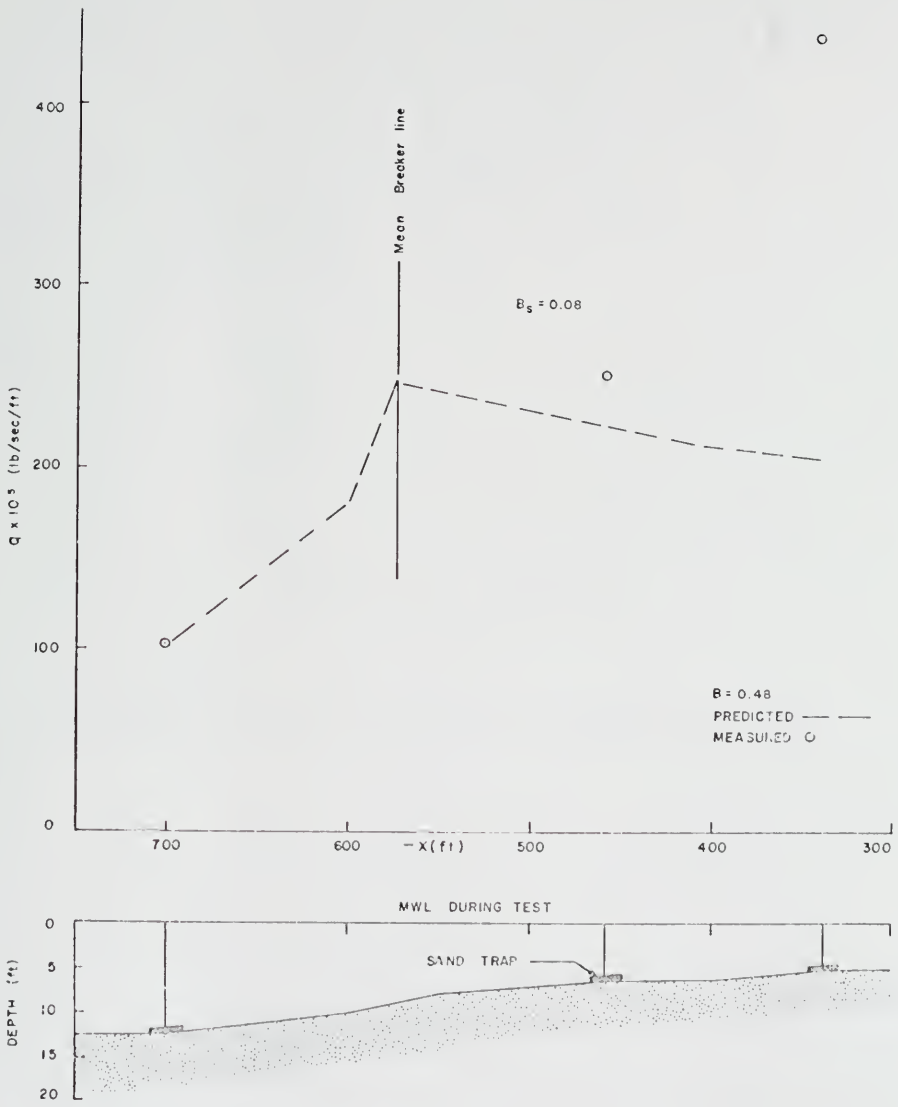

Figure 35. Distribution of Bed Load Transport, Test Number 5

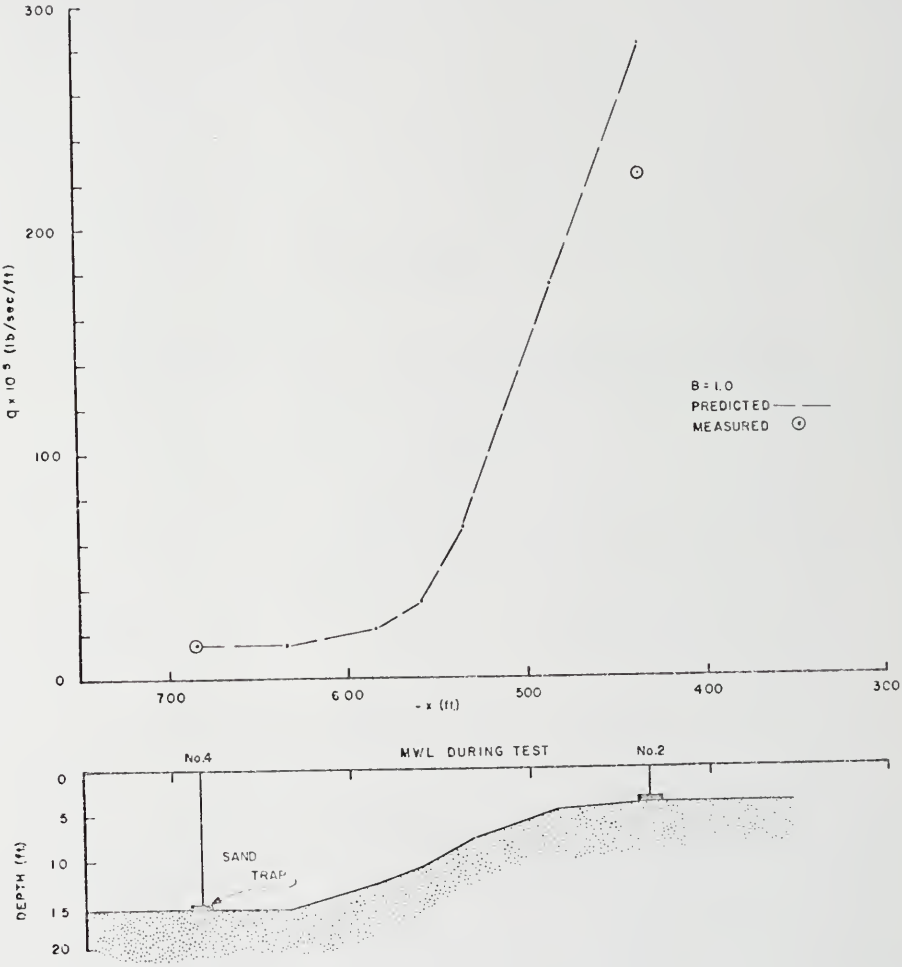

Figure 36. Distribution of Bed Load Transport, Test Number 8

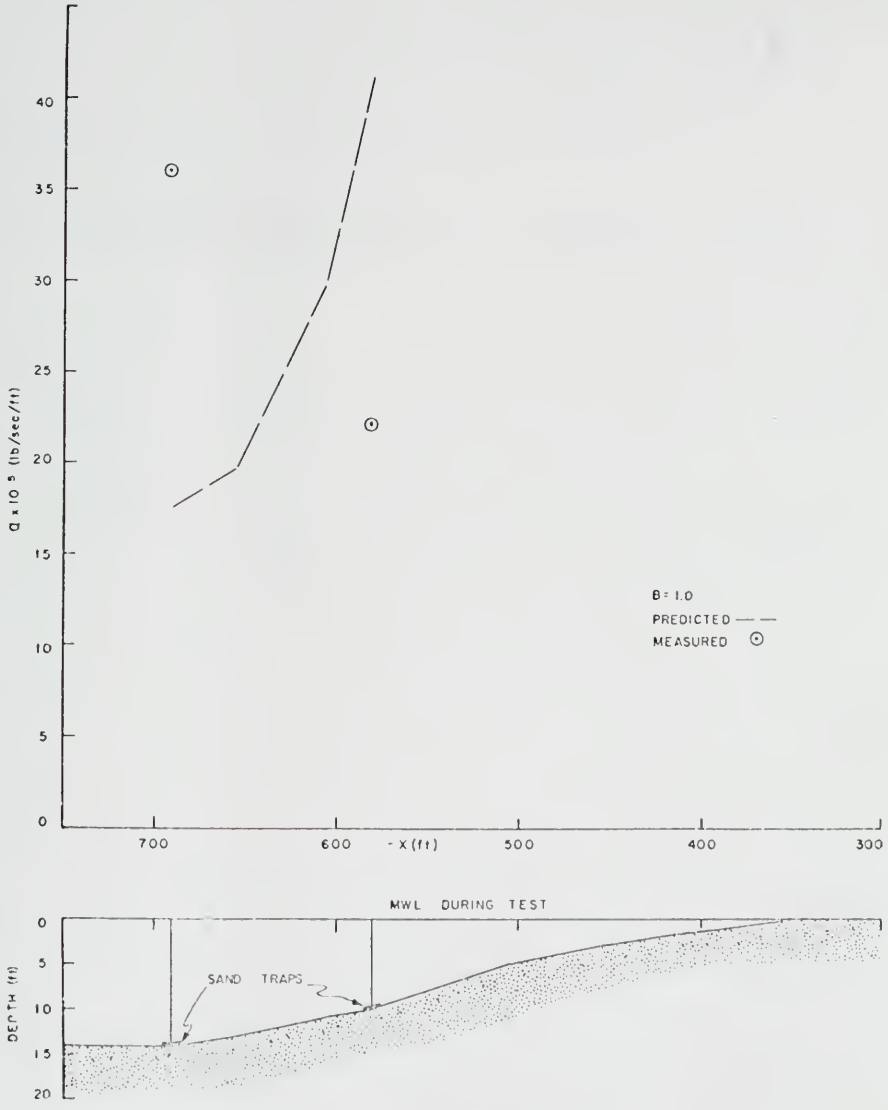

Figure 37. Distribution of Bed Load Transport, Test Number 11

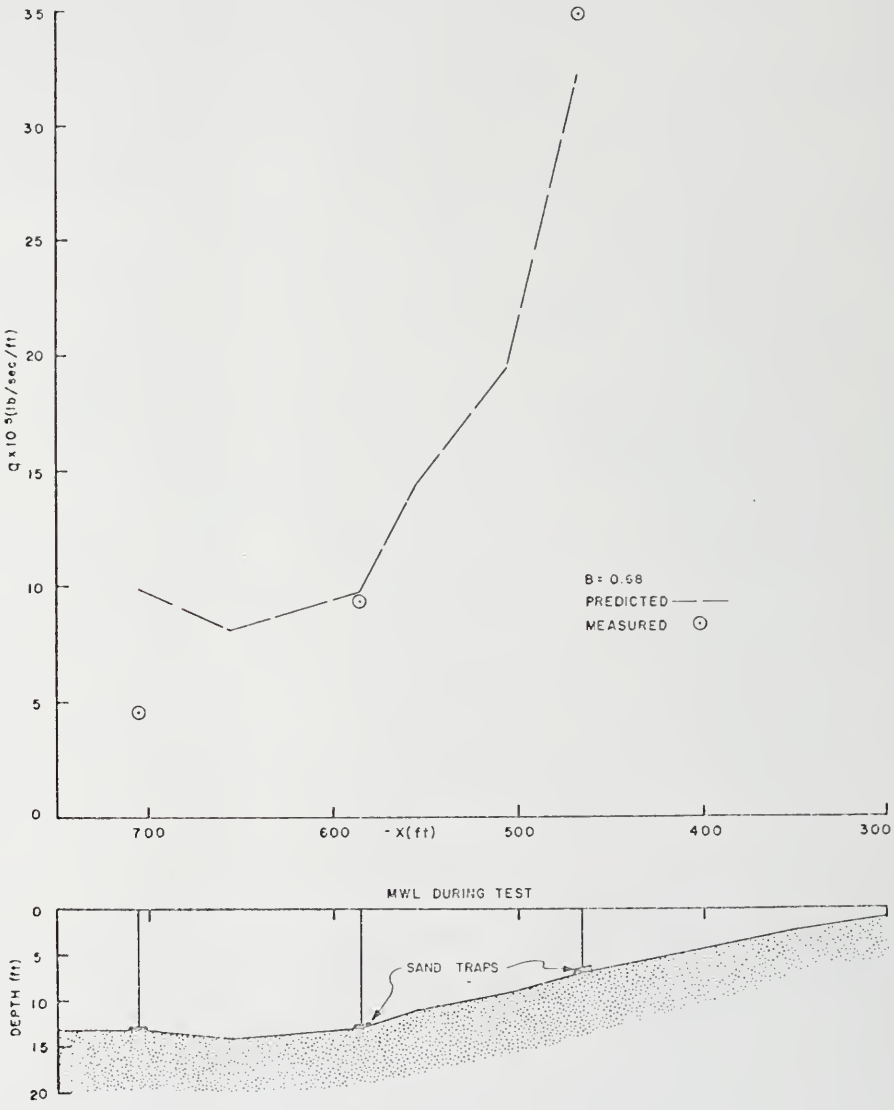

Figure 38. Distribution of Bed Load Transport, Test Number 13

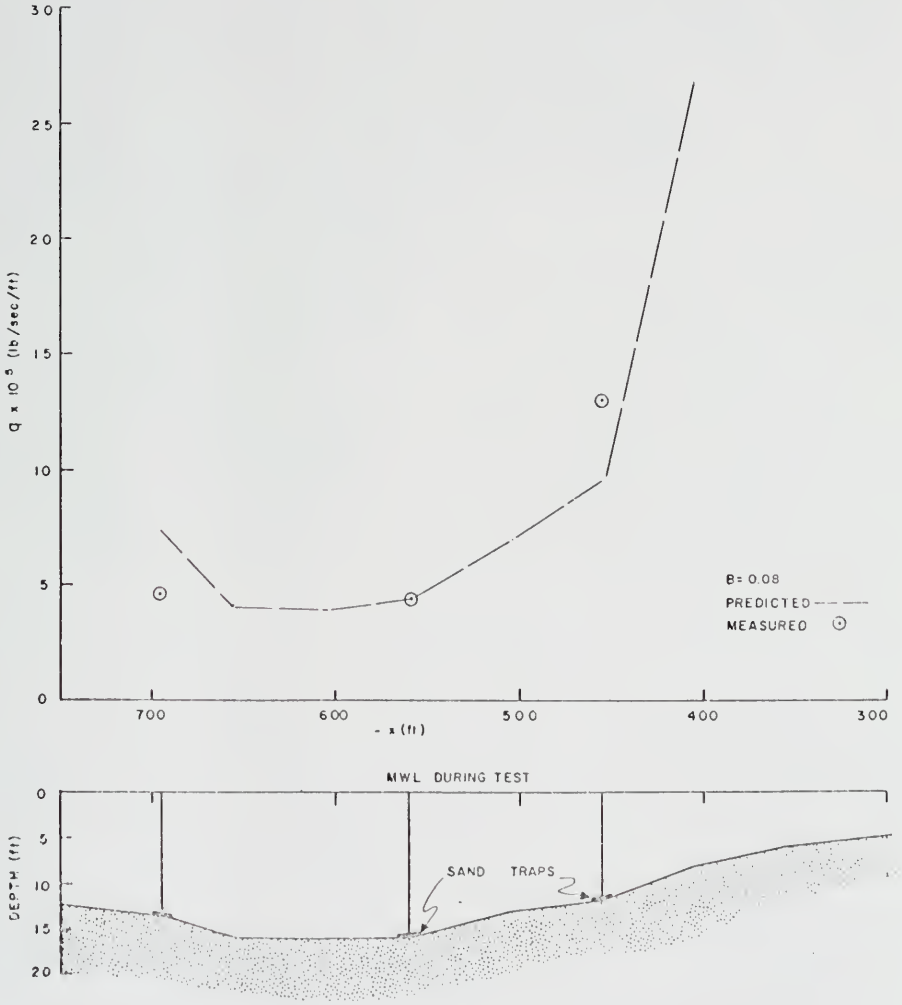

Figure 39. Distribution of Bed Load Transport, Test Number 14

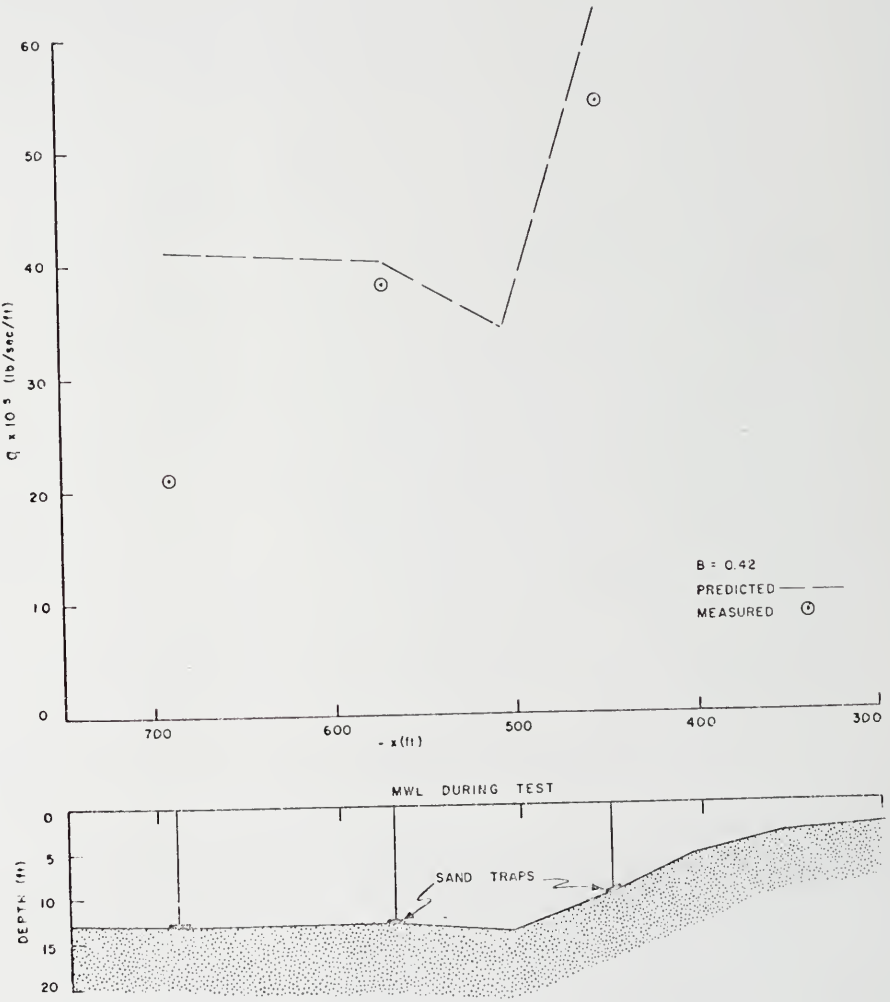

Figure 40. Distribution of Bed Load Transport, Test Number 16

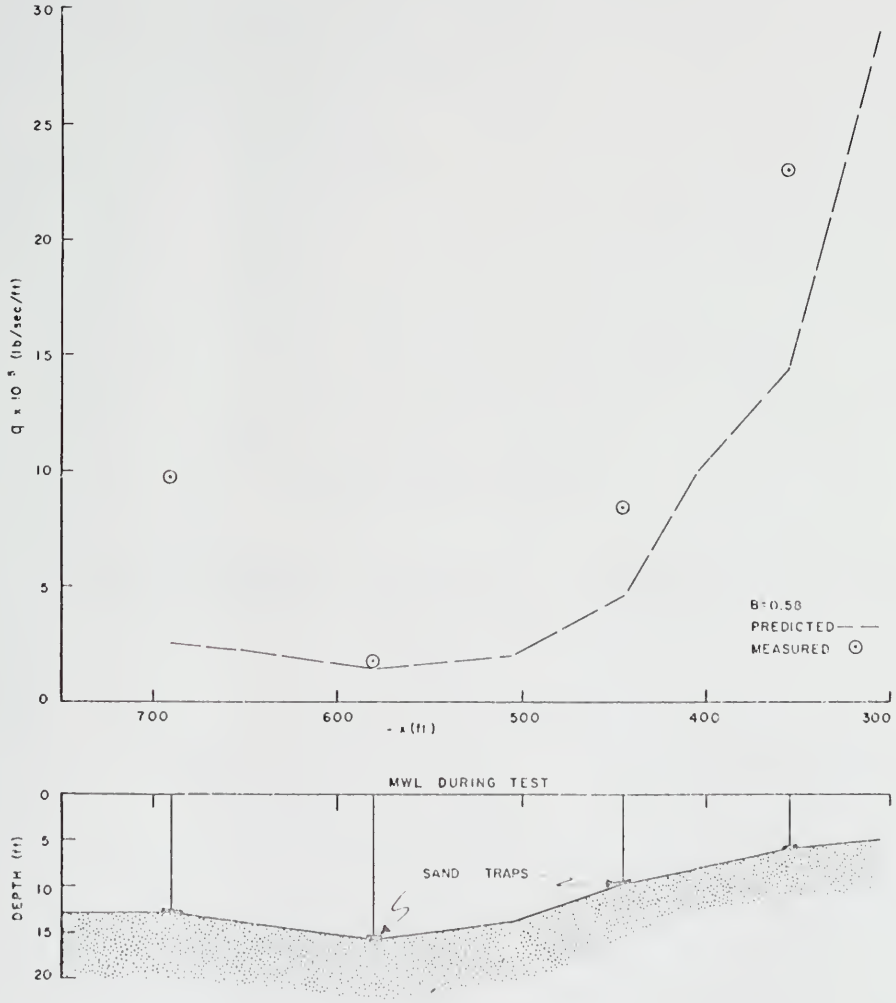

Figure 41. Distribution of Bed Load Transport, Test Number 17

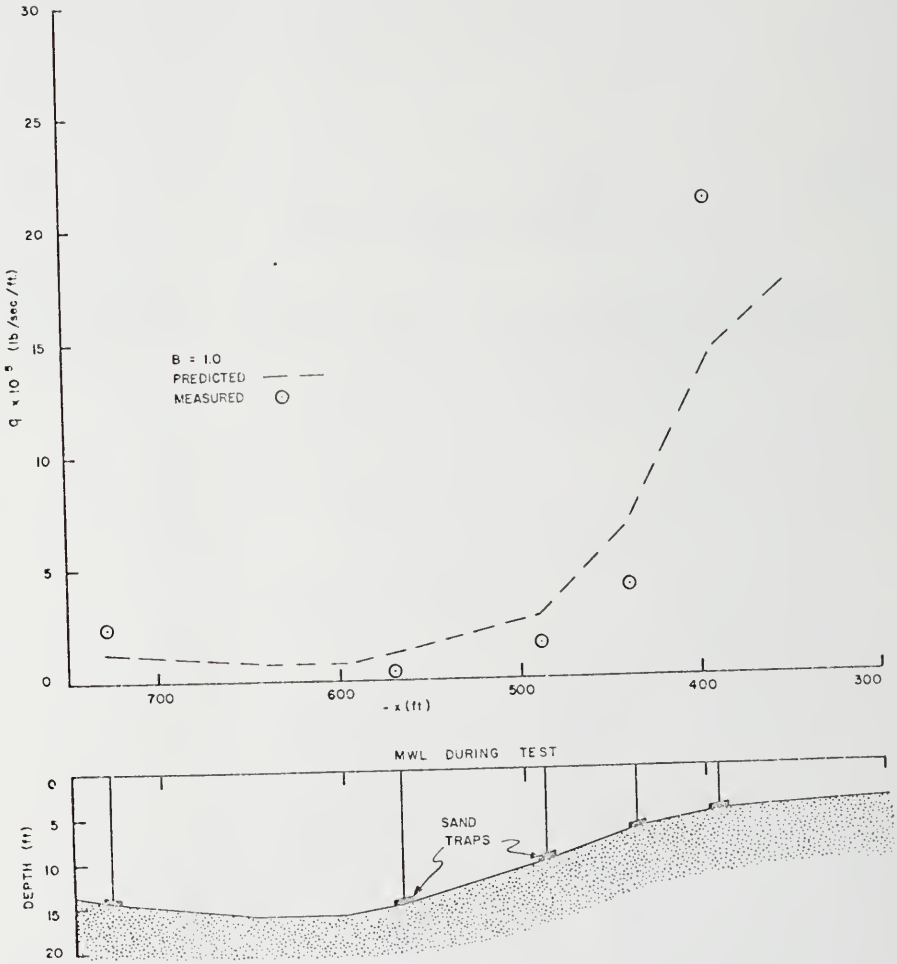

Figure 42. Distribution of Bed Load Transport, Test Number 23

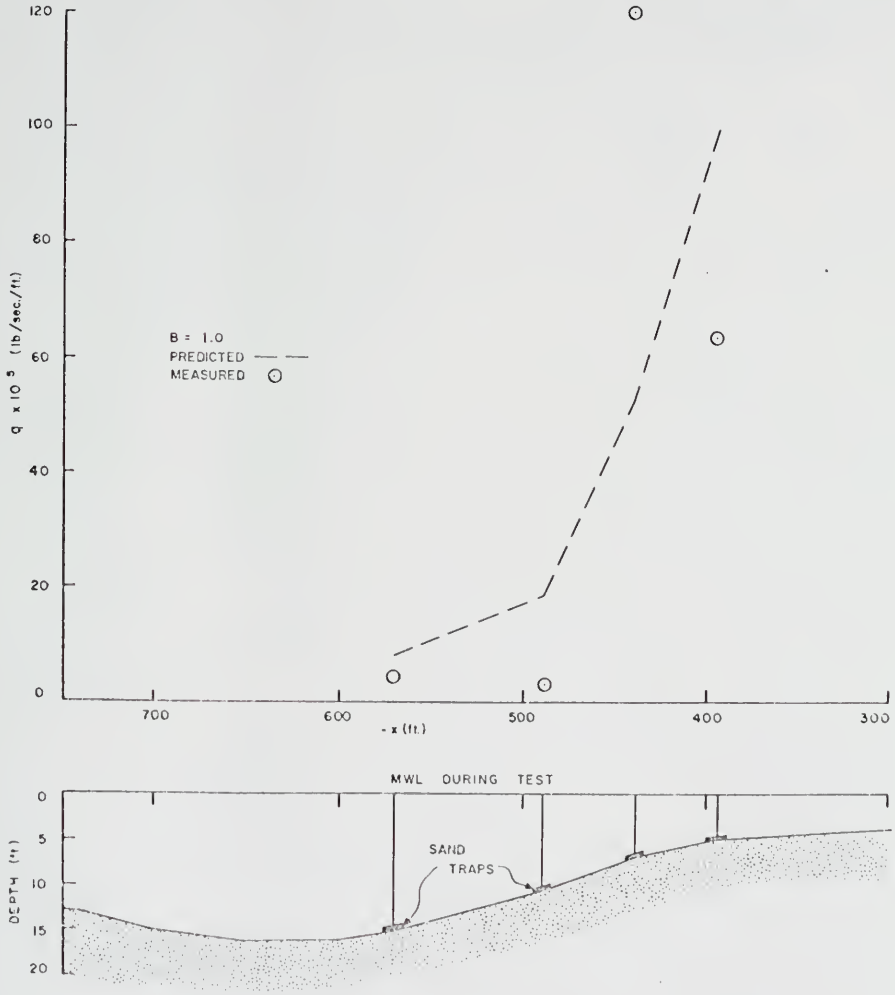

Figure 43. Distribution of Bed Load Transport, Test Number 24

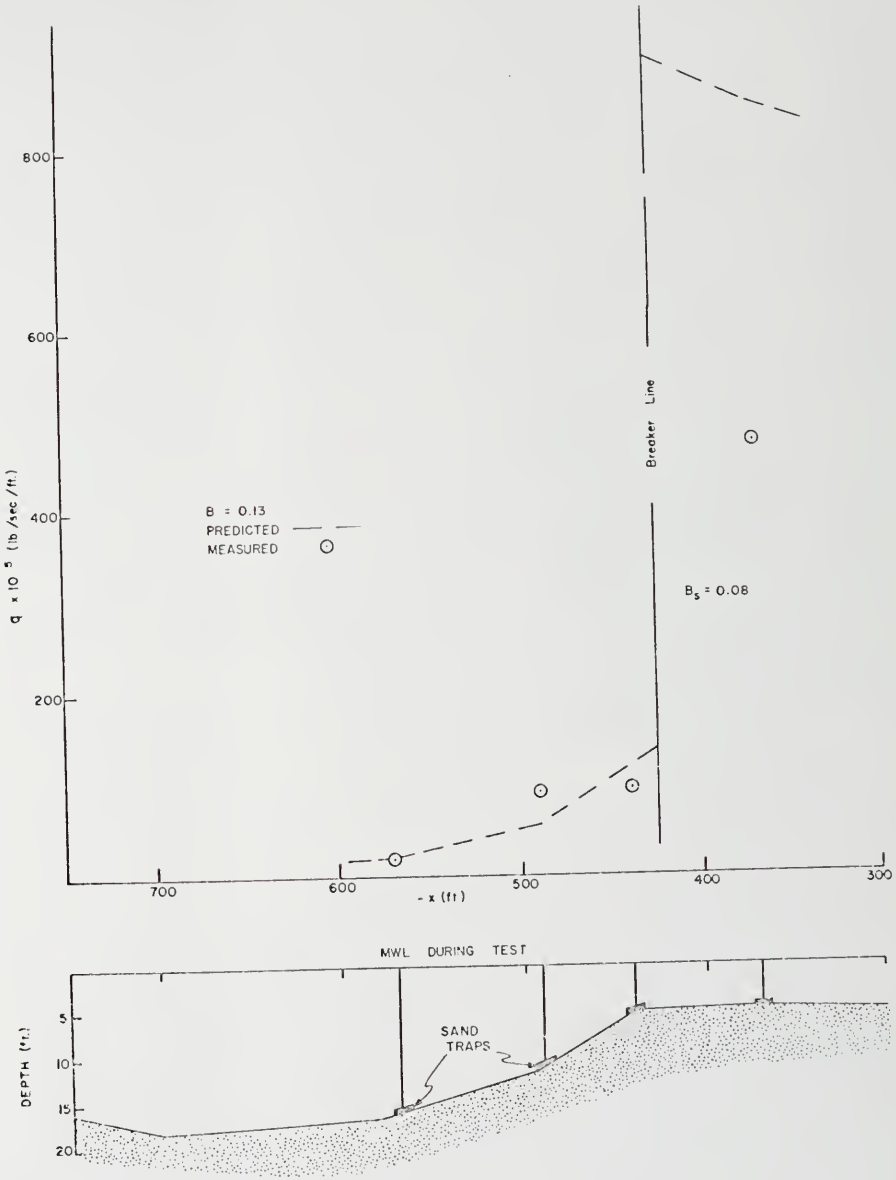

Figure 44. Distribution of Bed Load Transport, Test Number 25

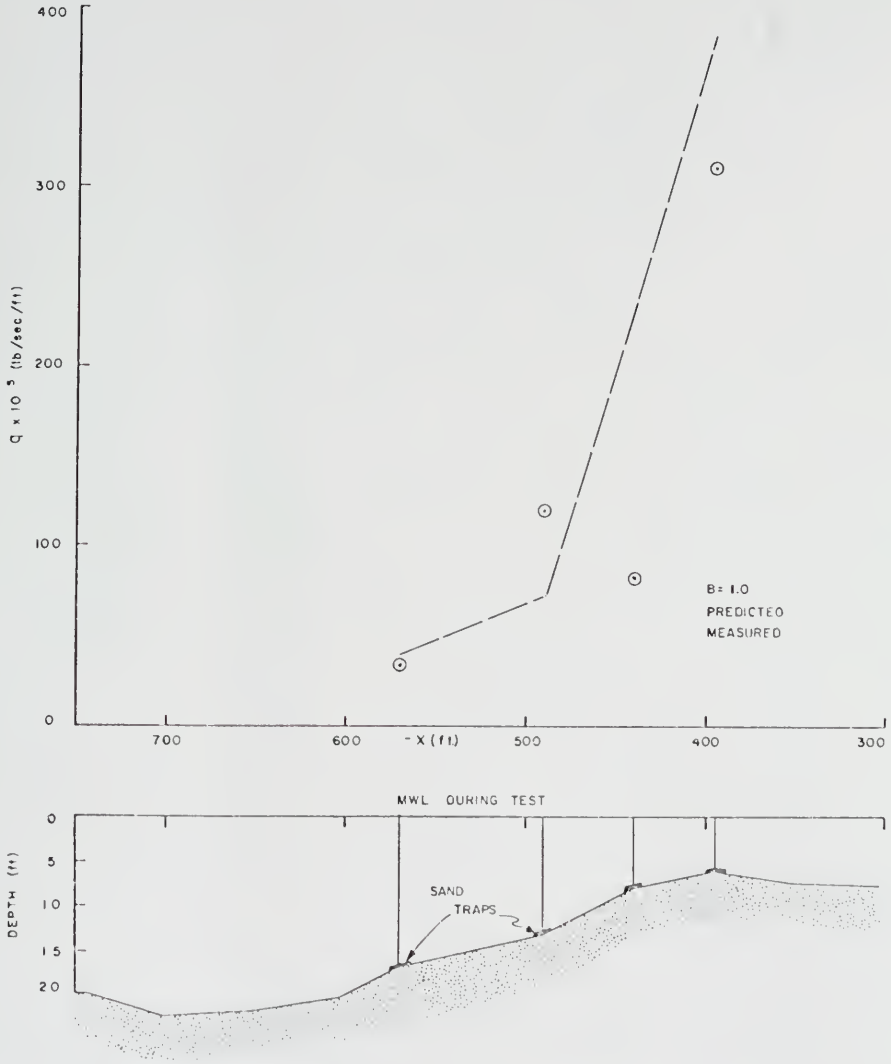

Figure 45. Distribution of Bed Load Transport, Test Number 26

REFERENCES

1. Zenkovich, V.P. Fluorescent Substances as Tracers for Studying the Movement of Sand on the Sea Bed; Experiments Conducted in the U.S.S.R. Dock and Harbour Authority, 40:280-283, 1960.

2. Munk, W.H. and Traylor, M.A. Forecasting Longshore Currents, Scripps Institution of Oceanography Wave Project No. 46, 1945.

3. Shepard, F.P. Beach Cycles in Southern California, Beach Erosion Board Tech. Memo. No. 20, U.S. Army Corps of Engrs., Washington, D.C., 1950.

4. Shepard, F.P. and Sayner, D.B. Longshore and Coastal Currents at Scripps Institution Pier, Beach Erosion Board Bulletin, U.S. Army Corps of Engrs., 7:1-9, 1953.

5. Ingle, J.O., Jr. The Movement of Beach Sand, Elsevier Publishing Co., Amsterdam, 1966.

6. Shepard, F.P. and Inman, D.L. Nearshore Water Circulation Related to Bottom Topography and Wave Refraction, Trans. Am. Geophys. Union, 31,3:196-212, 1950.

7. Bowen, A.J. Rip Currents, Doctoral Thesis, Scripps Institution of Oceanography, 1967.

8. Sonu, C.J., McCloy, J.M. and McArthur, D.S. Longshore Currents and Nearshore Topographies, Proc. Tenth Conf. Coastal Eng., ASCE, 525-549, 1967.

9. Galvin, C.J. and Savage, R.P. Longshore Currents at Nags Head, North Carolina, Coastal Eng. Res. Center Bull. 2, U.S. Army Corps of Engrs., Washington, D.C., 1966.

10. Saville, T. Model Study of Sand Transport Along an Infinitely Long Straight Beach, Trans. Am. Geophys. Union, 31,4:555-565, 1950.

11. Galvin, C.J. and Eagleson, P.S. Experimental Study of Longshore Currents on a Plane Beach, Coastal Eng. Res. Center Tech. Memo No. 10, U.S. Army Corps of Engrs., Washington, D.C., 1965.

12. Brebner, A. and Kamphuis, J.W. Model Tests on Relationship between Deep-Water Wave Characteristics and Longshore Currents, Queen's Univ. Civil Eng. Res. Rept. 31, 1963.

13. Longuet-Higgins, M.S. Mass Transport in Water Waves, Phil. Trans. Roy. Soc. A. 245:535-581, 1953.

14. Russell, R.C.H. and Osorio, J.D.C. An Experimental Investigation of Drift Profiles in a Closed Channel, Proc. Sixth Conf. Coastal Eng., Council on Wave Research, 171-183, 1958.

15. Miller, R.L. and Zeigler, J.M. The Internal Velocity Field in Breaking Waves, Proc. Ninth Conf. Coastal Eng., ASCE, 103-121, 1964.

16. Putnam, J.A., Munk, W.H. and Traylor, M.A. The Prediction of Longshore Currents, Trans. Am. Geophys. Union, 30,3:337-345, 1949.

17. Inman, D.L. and Quinn, W.H. Currents in the Surf Zone, Proc. Second Conf. Coastal Eng., Council on Wave Research, 24-36, 1952.

18. Eagleson, P.S. Theoretical Study of Longshore Currents on a Plane Beach, M.I.T. Hydrodynamics Lab. Tech. Rept. 82, 1965.

19. Bowen, A.J. The Generation of Longshore Currents on a Plane Beach, J. of Marine Research, 27,2:206-215, 1969.

20. Bruun, P. Longshore Currents and Longshore Troughs, J. of Geophys. Research, 68,1:1065-1078, 1961.

21. Inman, D.L. and Bagnold, R.A. Littoral Processes, The Sea, Interscience Publishers, New York, 3:529-549, 1963.

22. Harrison, W. and Krumbein, W.C. Interactions of the Beach-Ocean-Atmosphere System at Virginia Beach, Virginia, Coastal Eng. Res. Center Tech. Memo. No. 7, U.S. Army Corps of Engrs., Washington, D.C., 1964.

23. Harrison, W. Empirical Equation for Longshore Current Velocity, J. of Geophys. Research, 73,22:6929-6936, 1968.

24. Galvin, C.J. Longshore Current Velocity: A Review of Theory and Data, Reviews of Geophysics, 5,3:287-303, 1967.

25. Caldwell, J.M. Wave Action and Sand Movement Near Anaheim Bay, California, Beach Erosion Board Tech. Memo. No. 68, U.S. Army Corps of Engrs., Washington, D.C., 1956.

26. Watts, G.M. A Study of Sand Movement at South Lake Worth Inlet, Florida, Beach Erosion Board Tech. Memo. No. 42, U.S. Army Corps of Engrs., Washington, D.C., 1953.

27. Savage, R.P. Laboratory Study of the Effect of Groins on the Rate of Littoral Transport: Equipment Development and Initial Tests, Beach Erosion Board Tech. Memo. No. 114, U.S. Army Corps of Engrs., Washington, D.C., 1959.

28. Beach Erosion Board, Interim Report, U.S. Army Corps of Engrs., Washington, D.C., 1933.

29. Watts, G.M. Development and Field Tests of a Sampler for Suspended Sediment in Wave Action, Beach Erosion Board Tech. Memo. No. 34, U.S. Army Corps of Engrs., Washington, D.C., 1953.

30. Fukushima, H. and Mizoguchi, Y. Field Investigation of Suspended Littoral Drift, Coastal Eng. in Japan, 1:131-134, 1958.

31. Bruun, P. and Battjes, J.A. Tidal Inlets and Littoral Drift, Tenth International Assoc. Hydraulics Research Congress, London, 123-130, 1963.

32. Krumbein, W.C. Shore Currents and Sand Movement on a Model Beach, Beach Erosion Board Tech. Memo. No. 7, U.S. Army Corps of Engrs., Washington, D.C., 1944.

33. Shay, E.A. and Johnson, J.W. Model Studies on the Movement of Sand Transported by Wave Action Along a Straight Beach, Inst. of Engr. Res., University of California, Issue 7, Series 14, 1951 (unpublished).

34. Galvin, C.J. Breaker Type Classification on Three Laboratory Beaches, J. of Geophys. Research, 73,12:3651-3659, 1968.

35. Savage, R.P. Laboratory Determination of Littoral Transport-Rates, J. Waterways Harbors Div., Proc. ASCE, 88,WW2:69-92, 1962.

36. Eagleson, P.S. and Dean, R.G. Wave-Induced Motion of Bottom Sediment Particles, Trans. ASCE, 126,1:1162-1189, 1961.

37. Eagleson, P.S., Glenne, B. and Dracup, J.A. Equilibrium Characteristics of Sand Beaches, J. Hydraulics Div., Proc. ASCE, 89,HY1:35-57, 1963.

38. Kalkanis, G. Transportation of Bed Material Due to Wave Action, Coastal Eng. Res. Center Tech. Memo. 2, U.S. Army Corps of Engrs, Washington, D.C., 1964.

39. Iwagaki, Y. and Sawaragi, T. A New Method for Estimation of the Rate of Littoral Sand Drift, Coastal Eng. in Japan, 5:67-79, 1962.

40. Le Méhauté, B. and Brebner, A. An Introduction to Coastal Morphology and Littoral Processes, Queen's Univ. Civil Eng. Res. Rept. 14, 1959.

41. Bagnold, R.A. Mechanics of Marine Sedimentation, The Sea, Interscience Publishers, New York, 3:507-528, 1963.

42. Mei, C.C., Thalpa, G.A. and Eagleson, P.S. Asymptotic Theory for Water Waves on Beaches of Mild Slope, J. Geophys. Research, 73,14:4555-4560, 1968.

43. Le Méhauté, B. and Webb, L.M. Periodic Gravity Waves over a Gentle Slope at a Third Order of Approximation, Proc. Ninth Conf. Coastal Eng. ASCE, 23-40, 1964.

44. Phillips, O.M. The Dynamics of the Upper Ocean, University Press, Cambridge, 22-70, 1966.

45. Whitham, G.B. Mass, Momentum and Energy Flux in Water Waves, J. Fluid Mech., 12,2:135-147, 1962.

46. Wiegel, R.L. Oceanographic Engineering, Prentice-Hall, Englewood Cliffs, N.J., 201, 1964.

47. Reid, R.O. and Bretschneider, C.L. Surface Waves and Offshore Structures, Trans. ASCE Paper No. 3026, 1960.

48. Laitone, E.V. Limiting Conditions for Cnoidal and Stokes' Waves, J. of Geophys. Research, 67,4:1555-1564, April, 1962.

49. Dean, R.G. Breaking Wave Criteria; a Study Employing a Numerical Wave Theory, Paper presented at the Eleventh Conf. Coastal Eng., 1968 (in press).

50. Le Méhauté, B. On Non-saturated Breakers and the Wave Run-up, Proc. Eighth Conf. Coastal Eng., Council on Wave Research, 77-92, 1963.

51. Nakamura, M., Shiraishi, H. and Sasaki, Y. Wave Decaying Due to Breaking, Proc. Tenth Conf. Coastal Eng., ASCE, 234-253, 1966.

52. Munk, W.H. The Solitary Wave Theory and Its Application to Surf Problems, Ann. New York Acad. Sci., 51,3:376-424, 1949.

53. Longuet-Higgins, M.S. and Stewart, R.W. Changes in the Form of Short Gravity Waves on Long Waves and Tidal Currents, J. Fluid Mech., 8:565-583, 1960.

54. Longuet-Higgins, M.S. and Stewart, R.W. A Note on Wave Set-up, J. of Marine Res., 21:4-10, 1963.

55. Bowen, A.J., Inman, D.L. and Simmons, V.P. Wave 'Set-down' and Set-up, J. of Geophys. Research, 73,8:2559-2577, 1968.

56. Jonsson, I.G. Wave Boundary Layers and Friction Factors, Proc. Tenth Conf. Coastal Eng., ASCE, 127-148, 1966.

57. Inman, D.L. Wave-Generated Ripples in Nearshore Sands, Beach Erosion Board Tech. Memo No. 100, U.S. Army Corps of Engrs., Washington, D.C., 1957.

58. Putnam, J.A. and Johnson, J.W. The Dissipation of Wave Energy by Bottom Friction, Trans. Am. Geophys. Union, 30,1:67-74, 1949.

59. Putnam, J.A. Loss of Wave Energy Due to Percolation in a Permeable Sea Bottom, Trans. Am. Geophys. Union, 30,1:349-356, 1949.

60. Savage, P.P. Laboratory Study of Wave Energy Losses by Bottom Friction and Percolation, Beach Erosion Board Tech. Memo. No. 31, U.S. Army Corps of Engrs., Washington, D.C., 1953.

61. Bretschneider, C.L. Field Investigation of Wave Energy Loss in Shallow Water Ocean Waves, Beach Erosion Board Tech. Memo. No. 46, U.S. Army Corps of Engrs., Washington, D.C., 1954.

62. Iversen, H.W. Waves and Breakers in Shoaling Water, Proc. Third Conf. Coastal Eng., Council on Wave Research, 1-12, 1953.

63. Bruun, P. Coast Erosion and the Development of Beach Profiles, Beach Erosion Board Tech. Memo. No. 44, U.S. Army Corps of Engrs., Washington, D.C., 1954.

64. Inman, D.L. and Bowen, A.J. Flume Experiments on Sand Transport by Waves and Currents, Proc. Eighth Conf. Coastal Eng., Council on Wave Research, 137-150, 1963.

65. Bruun, P. and Purpura, J. Quantitative Research on Littoral Drift in Field and Laboratory, Proc. Ninth Conf. Coastal Eng., ASCE, 267-288, 1964.

66. Thornton, E.B. A Field Investigation of Sand Transport in the Surf Zone, Proc. Eleventh Conf. Coastal Eng., ASCE, 335-351, 1969.

BIOGRAPHICAL SKETCH

Edward Bennett Thornton was born June 20, 1939, at Alamosa, Colorado. From 1957 to 1960, he attended Willamette University, and, from 1960 to 1962, he attended Stanford University. At the end of this time, under a cooperative arrangement between the two universities, he received simultaneously a Bachelor of Arts with a major in Physics from Willamette University and a Bachelor of Science in Mechanical Engineering from Stanford University. From 1962 to 1964, he attended Oregon State University, working as a graduate assistant in the Department of Oceanography. In June, 1965, he received the degree of Master of Science. From 1964 to 1965, he worked as a consulting oceanographer for Marine Advisers, Inc. at La Jolla, California. In October of 1965, he joined the Department of Coastal and Oceanographic Engineering at the University of Florida as a research associate and, simultaneously, continued his graduate studies. In December, 1966, he received the degree, Master of Engineering in Civil Engineering. Since that time, he has pursued his work toward the degree of Doctor of Philosophy. Since May, 1969, he he has been an Assistant Professor in the Department of Oceanography at the Naval Post-Graduate School.

Edward Bennett Thornton is married to the former Sandra Jeanne Miller and is the father of two children. He is an associate member

of the American Society of Civil Engineers, the American Geophysical Union, and is a member of the Ocean Engineering Programs Committee for the American Society of Civil Engineers.

This dissertation was prepared under the direction of the chairman of the candidate's supervisory committee and has been approved by all members of that committee. It was submitted to the Dean of the College of Engineering and to the Graduate Council, and was approved as partial fulfillment of the requirements for the degree of Doctor of Philosophy.

March, 1970

Robert E. Uhrig
Dean, College of Engineering

Dean, Graduate School

Supervisory Committee:

B. H. Chenoweth
Chairman

R. G. Klein

R. G. Reuter